THE RECOVERY OF ORGANIC ACIDS BY TERNARY ANION EXCHANGE

By

Ali Reza Siahpush

A THESIS

Submitted to
Michigan State University
in partial fulfillment of the requirements
for the degree of

MASTER OF SCIENCE

Department of Chemical Engineering

1988

ABSTRACT

Experimental and modeling studies were conducted to investigate ternary ion exchange of acetate, butyrate and bicarbonate.

Axial mixing within the ion exchange column was described using the stirred tanks in series model, and the rate of exchange was described by the film model. Equilibrium experiments and batch kinetic experiments were used to evaluate the parameters needed for the model.

The following average separation factors were measured at a pH of 7.5 and 25°C, using the Rohm and Haas Amberlite IRA 904: $\alpha^{Bu}_{Ac} = 4.0$, $\alpha^{Bic}_{Bu} = 3.5$, and $\alpha^{Bic}_{Ac} = 30$. Under the same conditions, but at pH = 6.0, α^{Bu}_{Ac} increased to 6.2 and butyrate was found to be adsorbed in excess of ion exchange capacity.

The solution phase mass transfer coefficients were found to depend on liquid superficial velocity to the power of 2.2.

The model accurately predicted binary exchange but did not adequately describe ternary exchange.

TABLE OF CONTENTS

Page

I. INTRODUCTION 1

PROBLEM STATEMENT 1

OBJECTIVES 2

II. LITERATURE REVIEW 3

DEFINITION OF IMPORTANT TERMS 3

Exchanger Capacity 3

Counter Ions and Co-ions 3

Ion Exchange Equilibrium 4

Ion Exchange Selectivity 8

Separation Factor 11

ION EXCHANGE MATERIAL CHARACTERIZATION 14

Capacity Per Unit Weight or Volume 14

Functional Groups 16

Resin PK_a's 27

Matrix type 26

Degree of Cross-linking 29

Porosity 29

COLUMN OPERATIONS 30

Constant Pattern Behavior 32

Self Sharpening Behavior 32

Nonsharpening Behavior 33

Multi-component Column Operations 37

Modeling of Multicomponent Column Operations 40

III. **EXPERIMENTAL PROGRAM** 42

APPARATUS 42

CHEMICALS USED AND ANALYTICAL METHODS 46

PROCEDURES 48

EXPERIMENTS, RESULTS AND DISCUSSION 49

Equilibrium Experiments 49

Non-ionic Sorption 55

Verification of Differential Dolumn 58

Rate Experiments 59

IV. **MATHEMATICAL MODELING** 69

MATERIAL BALANCE 69

Continous Integral Model 69

Tanks in Series Model 71

RATE THEORY 74

Rate Controlling Step 78

Solution Phase Mass Transfer Controlling 79

Particle Phase Mass Transfer Controlling 81

Particle Phase and Solution Phase Controlling 83

NUMERICAL SOLUTION METHOD 85

Flow Chart of Program 87

Computer Solution of the Differential Equations 88

Runge-Kutta and the Predictor Corrector Scheme 88

Program Documentation 90

Input File 90

Cyclical Operation 92

Data Storage 93

COMPARISON OF MODEL TO EXPERIMENTAL DATA 94

Model verification for two component systems 94

Particle Phase Controlled Kinetics 94

Solution Phase and Transition regime 101

Model verification for three component systems 110

V. SUMMARY AND CONCLUSIONS 112

VI. RECOMMENDATIONS 114

VII. APPENDICES 115

DERIVATIONS AND JUSTIFICATIONS 115

SAMPLE CALCULATIONS 120

VIII. REFERENCES 145

LIST OF FIGURES

		Page
Figure 1.	Types of equilibrium isotherms	7
Figure 2.	Ratio of the areas technique	13
Figure 3.	Acid titration curves for weak base resin	15
Figure 4.	Ion exchange as redistrbution of counter ions	17
Figure 5.	Weak acid cation exchanger	18
Figure 6.	Strong acid cation exchanger	20
Figure 7,8,9.	Typical weak base anion exchangers	22-4
Figure 10.	Strong base anion exchanger	26
Figure 11.	Constant pattern breakthrough	34
Figure 12.	Self sharpening breakthrough	35
Figure 13.	Non sharpening breakthrough	36
Figure 14,15.	Zone formation for multicomponent column operations	38
Figure 16.	Differential ion exchange column	43
Figure 17.	Layout for differential column verification	44
Figure 18.	Layout for rate experiments	45
Figure 19.	Acetate/butyrate equilibrium isotherm	52
Figure 19b.	Non-ionic sorption of acetate and butyrate	57
Figure 20.	Acetate/bicarbonate equilibrium isotherm	53
Figure 21.	Butyrate/bicarbonate equilibrium isotherm	54
Figure 22.	Batch rate experiments for acetate/butyrate exchange at 20 mM.	62
Figure 23.	Calculated mass transfer coefficients for ac/bu at 20 mM.	62
Figure 24.	Batch rate experiments for ac/bu at 100 mM	63
Figure 25.	Calculated mass transfer coefficients for ac/bu at 100 mM.	63

Figure 26. Batch rate experiments for ac/bu at 300 mM 64

Figure 27. Calculated mass transfer coefficients for ac/bu at 300 mM. 64

Figure 28. Batch rate experiments for acetate/bicarbonate at 100 mM 66

Figure 29. Calculated mass transfer coefficients for ac/bic at 100 mM. 66

Figure 30. Batch rate experiments for butyrate/bicarbonate at 100 mM 67

Figure 31. Calculated mass transfer coefficients for bu/bic at 100 mM. 67

Figure 32. Analogy between stirred tanks in series and a packed column 73

Figure 33. Typical distribution of component i between the liquid and the resin phases 75

Figure 34. Concentration profile based on the film model 77

Figure 35. Flow chart of computer program 87

Figure 36. Comparison of experimental data with model under particle phase kinetics at 200 mM 97

Figure 37. Comparison of experimental data with model under particle phase kinetics at 300 mM 98

Figure 38. Comparison of experimental data with model under particle phase kinetics at 1.5 99

Figure 39. Comparison of experimental data with model under particle phase kinetics using the measured separation factor 100

Figure 40. Effect of flow rate on exchange kinetics of ac/bu at 20 mM 105

Figure 41. Effect of flow rate on exchange kinetics of ac/bu at 100 mM 106

Figure 42. Effect of flow rate on exchange kinetics of ac/bu at 300 mM 107

Figure 43. Effect of flow rate on exchange kinetics of ac/bic at 100 mM 108

Figure 44. Effect of flow rate on exchange kinetics of bu/bic 100 mM, Bu/Bic 109

Figure 45. Comparison of experimental data with model for ternary system 111

Figure 46. Example isotherm used for calculation of separation factors 124

Figure 47. Computer program code 131

LIST OF TABLES

		Page
Table 1.	pK_a of anionic resins	28
Table 2.	Concentration drop across differential column	59
Table 3.	Coefficients calculated for regression fit of particle phase mass transfer coefficents	95
Table 4.	Values of constants for the solution phase mass transfer coefficients	102
Table 5.	Equilibrium concentrations for acetate/butyrate exchange	121
Table 6.	Equilibrium equivalent fraction distribution for acetate/butyrate exchange	123
Table 7.	Concentration drop across differential column	127
Table 8.	Sample of spread for calculation of mass transfer coefficients	130

CHAPTER I

INTRODUCTION

PROBLEM STATEMENT

The Michigan Biotechnology Institute's Biomethanation Process requires the transfer of organic acids, mainly acetate and butyrate, from an acidogenic reactor to a methanogenic reactor. However, the transport of non-ionic medium components is undesirable. The "Substrate Shuttle" ion exchange unit is able to serve this purpose of substrate transfer without transferring the undesirable components.

For the purpose of automation and/or process control of the Biomethanation Process, a mathematical model capable of predicting the performance of the substrate shuttle is required. The model must be able to quickly and accurately predict the behavior of the ion exchange column in two modes of operation. The first mode, termed the "charging cycle", occurs when a stream containing the two fatty acids anions, acetate and butyrate, enters the ion exchange column and replaces bicarbonate. The second mode of operation, termed the "discharging cycle", occurs when a stream from the methanogenic reactor containing bicarbonate ions enters the column and displaces the acetate and butyrate ions. The process can be described as the cyclical modeling of ternary ion exchange with significant mixing.

OBJECTIVES

The primary purpose of this investigation was to develop a mathematical model for the numerical simulation of the substrate shuttle as an integral part of Michigan Biotechnology Institute's biomethanation process. The numerical simulation involve the prediction of unsteady-state effluent concentration profiles of the substrate shuttle anion exchange unit in the exchange of acetate and butyrate for bicarbonate.

The model must be capable of simulating significant mixing within the ion exchange column because the exchange of acetate and butyrate for bicarbonate at low pH involves the production of gaseous carbon dioxide which will disturb the flow within the unit. The model must also be implementable in microcomputers, able to predict column performance on a shorter time scale than the actual process, as well as capable of interface with microcomputer based control software.

CHAPTER II

LITERATURE REVIEW

Before any discussion of ion exchange theory can be carried out, it is necessary to define some elementary but important terms in ion exchange. The following definitions and concepts are necessary for an understanding of the ion exchange process.

DEFINITION OF IMPORTANT TERMS

Exchanger capacity

The exchanger capacity describes the number of fixed charge groups in the ion exchange material per unit volume or weight of exchanger. The capacity is the theoretical limit of the exchanger for the uptake of counter ions.

Counter ions and co-ions

The permanently bound charges of the ion exchanger together with the ions of the same charge in solution are termed "Co-ions". The term "Counter-ions" refers to the mobile ionic species that carry a charge opposite to the fixed groups of the exchanger.

Ion exchange equilibrium

The phase equilibrium for two or several transferable components between a fluid phase and an ion exchanger will often depend on both the liquid phase concentration and temperature. For the simplest case of two component ion exchange a single curve can be drawn to show the relation between the concentration of one species in the exchanger to that in the liquid phase.

The variance of the system is defined as the number of independent concentration variables at equilibrium. It is also equal to the difference between the total number of concentration variables and the number of independent relations connecting them. The variance of an ion exchange system of n components is (n-1). A two component system can then be represented on a two dimensional graph with only the solid phase-liquid phase relation of one component shown.

Generally the concentration of an ionic species within the exchanger is expressed as ion equivalents per weight or volume of exchanger, while the liquid phase concentration is expressed as mass or moles per volume of liquid. The general convention is to have the solid phase concentration measure all solute within the outer most boundaries of the individual granules of the exchanger material, regardless of solutes chemical or physical form.

For brevity, the solid and liquid phase concentrations used in equilibrium relationships or isotherms (so termed because they only apply at constant temperature) are generally given in terms of non-dimensional concentrations defined by Equations (1) and (2).

$$X_i = \frac{C_i}{C_{ref}} \qquad (1)$$

$$Y_i = \frac{q_i}{q_{ref}} \qquad (2)$$

where C_i = liquid phase concentration of species i

C_{ref} = a reference liquid phase concentration

X_i = non-dimensional liquid phase concentration of i

q_i = exchanger phase concentration of species i

q_{ref} = a reference exchanger phase concentration

Y_i = non-dimensional solid phase concentration of i

Total liquid phase and exchanger (resin) phase concentrations are often used as reference concentrations. This convention normalizes the liquid and solid phase non-dimensional concentrations to values between zero and one. The reference concentrations are defined according to Equations (3) and (4) for the exchange of n components.

$$C_{ref} = \sum_{i=1}^{n} C_i \qquad (3)$$

$$q_{ref} = \sum_{i=1}^{n} q_i = \text{exchanger capacity } (Q) \qquad (4)$$

Equations (3) and (4) then enforce the following relationships:

$$\sum_{i=1}^{n} X_i = 1 \qquad (5)$$

$$\sum_{i=1}^{n} Y_i = 1 \qquad (6)$$

Based upon the above definitions, a typical two component equilibrium isotherm can then be represented by a single curve of Y_i versus X_i.

Equilibrium isotherms that are convex upward throughout are designated as favorable to uptake of solute. The isotherms that are concave upward throughout are designated as unfavorable to uptake of solute. Isotherms that follow a rising diagonal are termed linear. It is also possible to have inflection points in the isotherm making them favorable at one range and unfavorable at another. An example of each type of isotherm is given in Figure 1.

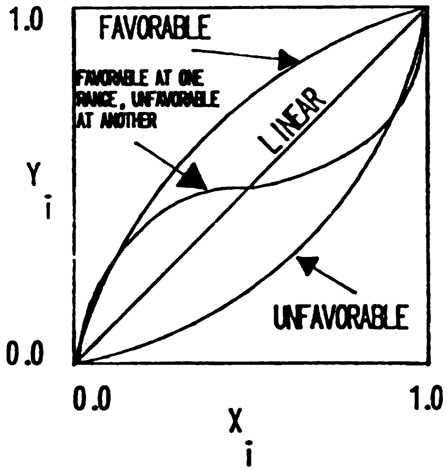

Figure 1. Different types of equilibrium isotherms plotted as resin phase dimensionless concentration versus liquid phase dimensionless concentration.

Ion Exchange Selectivity

It has long been documented that although two ions exchange with one another on an ion exchange material, they are not held by the exchanger equally strongly. Thus, at equilibrium with a liquid phase that contains equal amounts of ions A and B, the exchanger will in general not contain equal amounts of both ions, but prefer one to the other. This preference is quantified by "Selectivity". If, for example, ions A and B are in equilibrium between a liquid phase and an exchanger phase, the exchange process may be written as follows:

$$A_x + B_y \rightleftharpoons A_y + B_x \tag{7}$$

where the subscripts x and y refer to the liquid and exchanger phases respectively. The selectivity coefficient ($K'_{B/A}$) is then defined as follows:

$$K'_{B/A} = \frac{(q_B)^{Z_B}(C_A)^{Z_A}}{(C_B)^{Z_B}(q_A)^{Z_A}} \tag{8}$$

Here, Z_A and Z_B are the ionic charges of species A and B respectively, and the selectivity coefficient shows the exchanger selectivity for B over A. One can define a dimensionless selectivity coefficient ($\underline{K}'_{B/A}$) by using dimensionless concentrations.

$$\underline{K}'_{B/A} = \frac{C_o}{Q} \quad \frac{(Y_B)^{Z_B}(X_A)^{Z_A}}{(X_B)^{Z_B}(Y_A)^{Z_A}} \qquad (9)$$

Here, C_o and Q are total liquid concenetration and the resin capacity.

Any value of $\underline{K}'_{B/A}$ different from unity measures the preference of the exchanger for one species over another. These preferences can be summarized by the term activity. The higher the activity of one component in a given phase, the greater is its escaping tendency from that phase. Activities were not used in this investigation, however, all experiments were performed at or near the concentration range of interest so that any possible nonidealities would be included in the results. There also exist "Corrected Selectivity Coefficients" which account for the preferences of the exchanger only by making use of activity coefficients of the species in the liquid and resin phases. These coefficients will not be considered in this study because it is generally the combined effect of the two phases that determines the distribution of species in the phases.

Factors affecting selectivity:

Several factors affect the preference of a resin for a given ion. Typically the exchanger prefers counter ions with the following characteristics[1,2]:

1. Highest valance.
2. Smallest hydrated ionic radius.
3. Most strongly interacting with the fixed groups of the exchanger.
4. Greatest polarizability.
5. Cause the least swelling of the resin.
6. Lowest free energy of hydration in aqueous solution.

The following factors also affect the selectivity of the resin.

7. The degree of cross linking of the matrix.
8. Starting ionic form of the resin; i.e. a resin starting with Cl^- form has a lesser affinity for Cl^- than a resin predominantly saturated with HCO_3^-.
9. The non exchanging ion, if it in any way forms a complex with an exchanging ion that alters its charge or impedes its diffusion across the surface film of the resin bead.
10. The total ionic strength of the solution. The selectivity order is sometimes reversed in favor of ions that were not

preferred by the exchanger at low ionic strength as the ionic strength of the solution is increased.

Separation Factor

The separation factor is defined by Equation (10).

$$\alpha_B^A = \frac{Y_A X_B}{X_A Y_B} = \frac{X_B (1 - Y_B)}{Y_B (1 - X_B)} \qquad (10)$$

If $\alpha_B^A > 1$, the exchanger is said to prefer ion A to ion B. By virtue of its definition, the separation factor is analogous to relative volatility in distillation. Unless the equilibrium isotherm is linear, the separation factor is not constant as X changes. Generally for the purpose of brevity, average separation factors are used which apply over the entire concentration range of the isotherm. It is therefore necessary to calculate an integrated average separation factor from the experimentally measured isotherm. Figure 2 shows a typical favorable isotherm. In this study, integrated average separation factors were calculated from experimental data according to Equation (11). Please refer to the appendix or to the work of Clifford[2] for a derivation of this equation and a justification for the use of separation factors rather than selectivities.

$$\frac{\text{Area(II)}}{\text{Area(I)}} = \frac{\dfrac{(\alpha^2 - \alpha - \alpha \ln \alpha)}{(\alpha - 1)^2}}{1 - \dfrac{(\alpha^2 - \alpha - \alpha \ln \alpha)}{(\alpha - 1)^2}} \qquad (11)$$

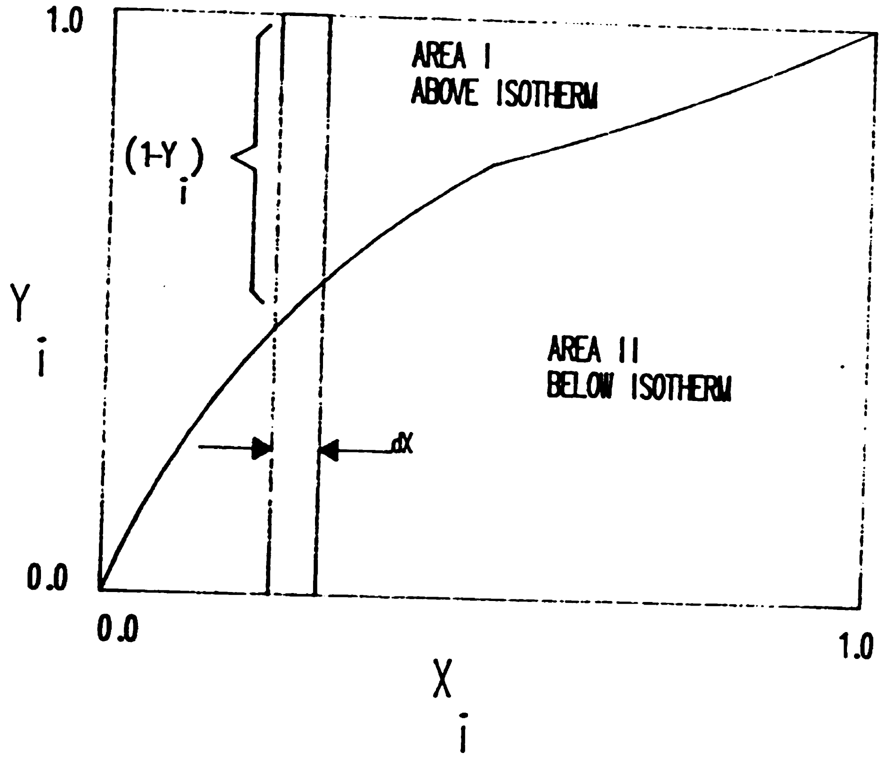
1.0
0.0
AREA I
ABOVE ISOTHERM
(1-Y_i)
Y_i
AREA II
BELOW ISOTHERM
dX
0.0
1.0
X_i

Figure 2. Typical favorable isotherm showing the reasoning used in the derivation of the average separation factor.

ION EXCHANGE MATERIAL CHARACTERIZATION

Ion exchange materials are classified by several different properties and independent variables:

I. Ion exchange capacity per weight or volume.
II. Functional groups.
III. Resin pK_a's.
IV. Matrix type.
V. Degree of cross linking.
VI. Porosity.

Capacity Per Unit Weight or Volume

For ion exchange materials that contain permanent charges, such as strong acid and strong base ion exchangers, the capacity is constant; however, for weak acid and weak base exchangers, the functional groups are charged or neutral depending on the pH of the environment, and thus the capacity of the exchanger is a function of pH. Figure 3 shows titration curves for three different acids on a weak base resin. Since the amount of acid needed to produce a given pH change is dependent on the resin capacity, the capacity is seen to be pH dependent.

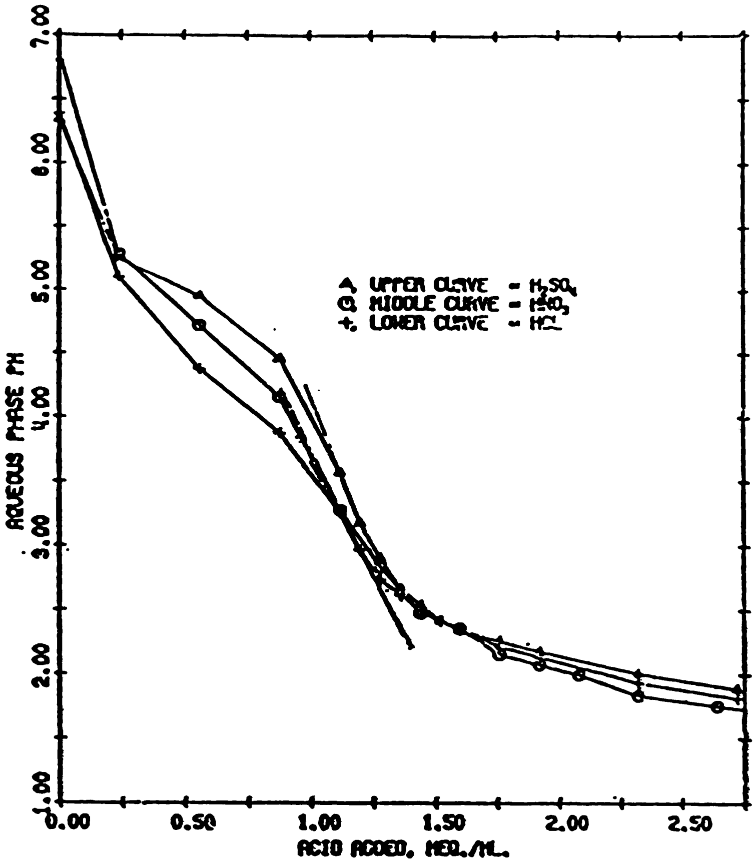

Figure 3. Acid titration curves for a weak base resin

IONAC AFP 329, MACROPOROUS RESIN
STYRENE-DVB MATRIX
TERTIARY-AMINE FUNCTIONALITY
TOTAL CAPACITY = 1.25 MEQ./ML.

[From Clifford (2)].

Functional Groups

The two main categories of functional groups are Cation and Anion exchangers. Cationic ion exchangers are so named because they participate in the exchange of cations. The functional groups in this type of material are negatively charged and depending on the type of the exchanger (Strong Acid, or Weak Acid), they may posses either permanent or pH dependent charges. Figure 4 shows the crosslinked polymeric matrix containing the fixed charges together with the mobile exchanging counterions.

Cationic ion exchangers are themselves classified in two categories: weak acid and strong acid exchangers.

Weak acid cation exchangers consist of functional groups that are weakly acidic. Functional groups such as carboxylic acids demonstrate a good example of a weak acid functionality. It is clear that such weak acids only exhibit negatively charged behavior at a pH range above their respective pK_a. The molecular structure of a typical weak acid exchanger is shown in Figure 5.

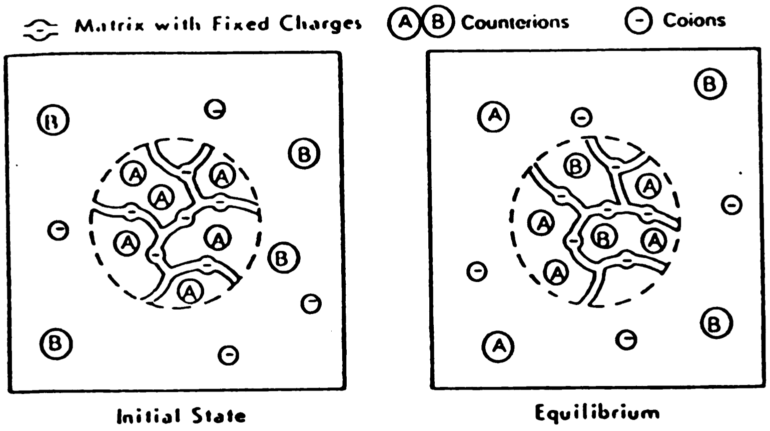
Matrix with Fixed Charges
A B Counterions
- Coions
Initial State
Equilibrium

Figure 4. Mechanism of ion exchange, a redistribution of counterions between particle and solution. [From Marinski (1), Chap. 2].

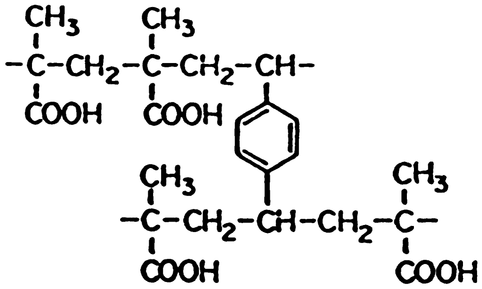

Figure 5. Weak acid cation exchange resin

Methacrylic acid-divinylbenzene copolymer

Functional group: COOH
Acidity: pK_a = 4 to 6, ionized at pH > 5
Swelling: +65% going from H^+ to Na^+ form
Capacity: 10 meq/gm, 4.3 meq/gm

$\overline{\text{RCOOH}} + Na^+ \rightleftarrows \overline{\text{RCOON}}_a + H^+$

$\overline{R}$ denotes the resin matrix
[From Clifford (2)].

Strong acid cation exchangers posess rongly acidic functional groups. The molecular structure of a typical strong acid cation exchanger, Duolite C-20, is shown in Figure 6 together with its physical properties. All of the major strongly acidic cation exchangers involved in industrial water treatment applications have a chemical matrix consisting of Styrene-divinyl benzene (STY-DVB) with sulfonic acid radical functional groups. These resins differ mainly in DVB content and pore structure[32](Rohm & Haas catalog).

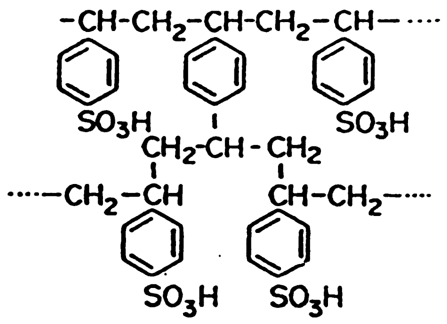

Figure 6. Typical strong acid cation exchange resin
Sulfonated polystyrene-divinylbenzene copolymer

Typical degree of crosslinking: 8%
Physical form: Translucent spheres
Specific gravity: 1.23, hydrogen form
Moisture retention capacity: 50%, hydrogen form
Effective size: 0.45 to 0.55 mm
Swelling: -7% when going from H^+ to Na^+ form
Ion-exchange capacity: 4.8 meq/gm, 2.0 meq/ml
Uniformity coefficient: 1.4 to 1.8
Functional group: $R\text{-}SO_3H$
Acidity: $pK_a < 1$, ionized at $pH > 1$

$$\overline{R\text{-}SO_3H} + Na^+ \rightleftarrows \overline{RSO_3Na} + H^+$$

Anion exchangers have positively charged functional groups and anionic counter ions. Anion exchangers can be classified as either weak base or as strong base.

Weakly basic anion exchange resins, similar to weak acid resins are ionized at a specific pH and therefore are primarily used to remove strong acids such as hydrochloric, and sulfuric. Unlike strongly basic anion exchange resins, weak base resins do not have the capability to remove bicarbonates, silica, or weak organic acids. The main advantage of weak base resins is that they can be regenerated with relative ease and with stoichiometric amounts of regenerant. They are therefore more efficient than strong base resins. Typical structures of weak base resins are shown in Figures 7, 8 and 9.

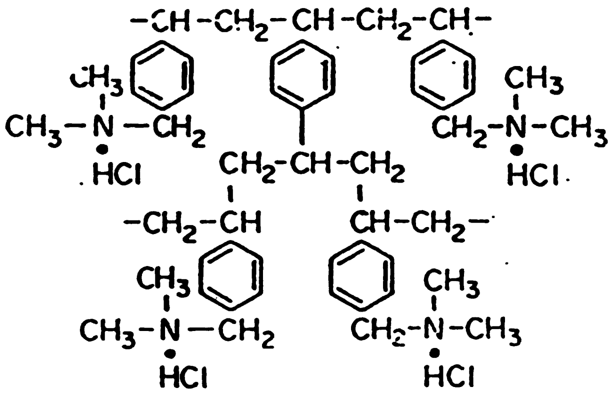

Figure 7. Typical weak base anion exchange resin Styrene-divinylbenzene copolymer with tertiary-amine functionality

Typical examples: Amberlite IRA-93, Duolite ES-368
Physical from: tan, spherical particles
Moisture retention: 50%, free base form
Capacity: 3.8 meq/gm, 1.3 meq/ml
Swelling: +23% free base to salt form
Basicity: pK_a = 7 to 9, ionized at pH < 8

$$\overline{RN(CH_3)_2} + HNO_3 \rightleftarrows \overline{RN(CH_3)_2 \cdot HNO_3}$$

[From Clifford (2)].

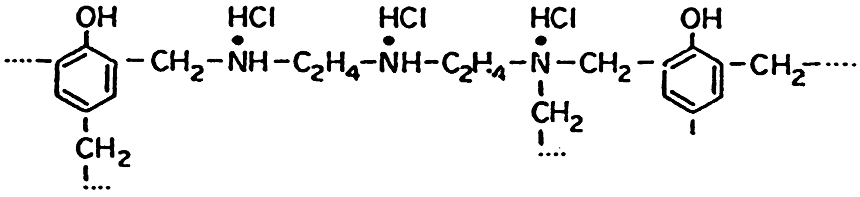

Figure 8. Typical weak base anion exchange resin

Phenol-formaldehyde polyamine, condensation polymer with secondary amine functionality

Typical example: Duolite A-7
Physical form: cream colored granules
Specific gravity: 1.12, free base form
Particle size: 0.3 to 1.2 mm
Moisture retention: 60%
Total capacity: 9.1 meq/gm, 2.4 meq/ml
Swelling: +18% going from free base to salt form
Basicity: pK_a = 7 to 9, ionized at pH < 8

$\overline{R_2NH} + HCl \rightleftarrows \overline{R_2NH \cdot HCl}$

[From Clifford (2)].

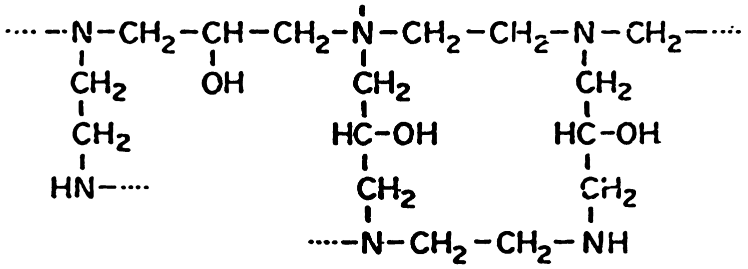

Epoxy-polyamine condensation polymer

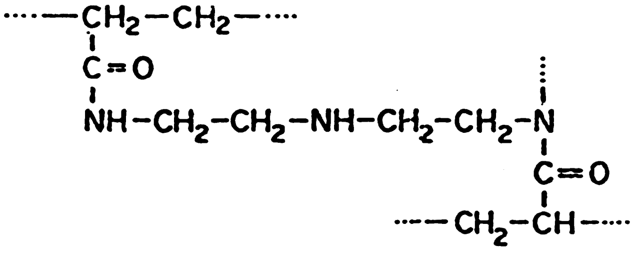

Polyacrylic-polyamine copolymer

Figure 9. Other common weak base anion exchange resins. [From Clifford (2)].

Strongly basic anion exchange resins can be divided into two major categories called Type I and Type II. Type I resins have the highest overall basicity and will therefore more completely adsorb weakly acidic ions such as weak organic acids. Type II resins will also remove weak acids, but are not as basic as Type I and do not require as much regenerant. They are therefore more efficient than Type I resins. Based on oral and written communication with a technical representative of The Rohm and Haas Company [33], type II strongly basic resins were chosen for the recovery of weak organic acids such as butyric and acetic acids. Some typical structures of strong base resins are shown in Figure 10.

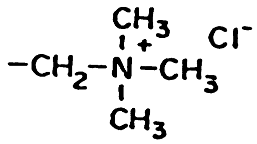

$$-CH_2-\overset{CH_3}{\underset{CH_3}{\overset{|+}{\underset{|}{N}}}}-CH_3 \quad Cl^-$$

Type 1

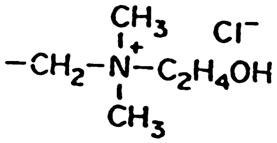

$$-CH_2-\overset{CH_3}{\underset{CH_3}{\overset{|+}{\underset{|}{N}}}}-C_2H_4OH \quad Cl^-$$

Type 2

Figure 10. Two typical strong base anion exchange resins. Other strong base resins include a matrix of ST-DVB back bone.
Physical form: moist, cream-colored beads, opaque
Moisture retention capactiy: 50%, chloride form
Specific gravity: 1.07 chloride form
Capacity: 4.0 meq/gm, 1.3 meq/ml
Swelling: -12% going from OH^- to Cl^- form

$$\overline{RN(CH_3)_3Cl} + NO_3^- \rightleftarrows \overline{RN(CH_3)_3NO_3} + Cl^-$$

Resin pK_a's

The pK_a of the functional group indicates the pH range in which the resin can effectively operate. Ion exchangers are classified into four different categories based on pK_a's.

1. Strong acid cation exchangers with an operating pH range of (0-14) and a pK_a value less than 1.
2. Weak acid cation exchangers with operating pH range of (5-14) and a pK_a value of approximately 4.5.
3. Strong base anion exchangers with operating pH range of (0-14) and a pK_a value greater than 13.
4. Weak base anion exchangers with operating pH range of (0-9) and a pK_a's value between 7 and 9.

The resin pK_a is not necessarily equal to pK_a of its individual functional groups, because this value is dependent on the environment of the functional groups. The functional groups in an aqueous environment may exhibit different pK_a than functional groups in the interior of the resin matrix. Table 1 shows some anion exchange functional groups and their apparent pK_a.

Table 1. pK_a of anion resins [From Marinski (1), and Clifford (2)].

ION EXCHANGER	STRUCTURE	APPARENT pK_a
Type I, Strong Base	$-N^+(CH_3)_3{}^-OH$	> 13
Type II, Strong Base	$-N^+(C_2H_4OH)(CH_3)_2{}^-OH$	>13
Secondary amine Weak base	$-N(CH_3)H$	7-9
Tertiary amine Weak base	$-N(CH_2)_2$	7-9
Primary amine Weak base	$-NH_2$	7-9
Phenylamine Weak base	- $-NH_2$	5-6

Matrix Type

Several types of polymeric matrices are used in commercial ion exchange resins. Some of the most common polymeric backbones are listed below:

1. Polystyrene crosslinked with divinyl benzene (STY-DVB).
2. Polyacrylic acid-polyamine condensation polymers (Acrylic-Amine).
3. Phenol-Formaldehyde-Polyamine polymers (Phenol-HCHO-PA).
4. Epichlorohydrin-Polyamine condensation polymers (Epoxy-Amine).
5. Acetone-Formaldehyde-Polyamine condensation polymers (Aliphatic-Amine).

Degree of Cross Linking

This is the product of the chemical cross-bridging between linear polymeric chains in the resin matrix. Crosslinking produces a three dimensional polymeric network with an effective "pore" diameter. High degrees of crosslinking (>12%) produce tight structures that favor small ions and are kinetically slow, but chemically stable. Low degrees of cross linking (≤ 4%) produce a relatively open structure that is kinetically quick and permits easier penetration of large ions such as organic acids.

For styrene-DVB resins, generally the amount of DVB in the backbone is a direct indication of the degree of crosslinking.

Porosity

Porosity is a measure of openness of the polymer matrix and is related to type and degree of the matrix crosslinking. Three basic classifications exist in this type of physical categorization.

1. Gel resins are microporous with apparent pore diameters of atomic dimensions (10-20 Å). Gel resins resins containing DVB are generally 6-8% crosslinked. The matrix is usually transparent and continuous with little true porosity.

2. Macroporous resins, also known as macroreticular resins, have internal pores whose diameters far exceed atomic dimensions (≥100 Å). These type of resins generally have a high degree

of crosslinking, are opaque, have large surface area per unit volume, and have great physical stability when compared to gelular resins.

3. Isoporous resins have higher porosity than gel resins, but are not as porous as macroreticular resins. This type of matrix generally has a low degree of DVB crosslinking (0.5-2%). The product is transparent.

COLUMN OPERATIONS

Effluent concentration profiles from packed-bed ion exchange columns are dependent upon several variables, including the liquid flow rate, number of ionic species, and phase equilibria. Favorable, unfavorable and linear isotherms produce different effluent concentration profiles as described below.

Mobile ions are transported through the column by the carrier solvent, (water in most cases). The velocity of each ionic species is only equal to the solvent velocity if the ion exchange material behaves only as a nonporous packing, and does not interact with the dissolved species in any way. However, the counter ions penetrate the porous matrix of the exchanger material and engage in the process of ion exchange, thus reducing the velocity with which each individual specie travels through the column. The velocity of the concentration front is generally much less than that of the solvent and its shape is dependent on the equilibrium isotherm and the rate of mass transfer. In the following discussion it is assumed that the column is initially

presaturated with the counter ion (B^-) and the influent solution contains (A^-) at a certain concentration. For the purpose of brevity A^- and B^- will be referred to as A and B.

Constant Pattern Behavior

This type of behavior occurs when the equilibrium isotherm is "linear". It is referred to as constant pattern because the velocity of the transition region is independent of concentration. In the absence of axial mixing, the shape of the concentration front remains constant throughout the column. This behavior is shown schematically in Figure 11.

Self Sharpening Behavior

Self sharpening refers to a concentration gradient that continuously increases in magnitude in the axial direction across the concentration wave that is decreasing in the direction of flow. This type of behavior occurs when the equilibrium between the exchanger and the liquid phase is favorable to uptake of counterion in the feed. The velocity of A through the column is concentration dependent. Because the isotherm is favorable to uptake of A the largest relative driving force for the uptake of A occurs at lowest equivalent fractions of A. Therefore the regions of low A composition are adsorbed more readily than regions of high A composition. The result is that the regions of the front containing lower equivalent fractions of A move at a lower velocity than regions of high A composition. This behavior is schematically shown in Figure 12.

Non Sharpening Behavior

Non sharpening behavior occurs when the equilibrium is unfavorable to uptake of A. An inspection of the unfavorable equilibrium isotherm shows that large equivalent fractions of A in the exchanger will only exist at high liquid phase equivalent fractions of A. This results in a concentration dependent solute velocity that will cause the concentration front to stretch out. Thus, regions of the concentration front with small concentration of A will move more rapidly than the regions with a high concentration of A. This type of behavior is schematically shown in Figure 13 for comparison with the self sharpening behavior.

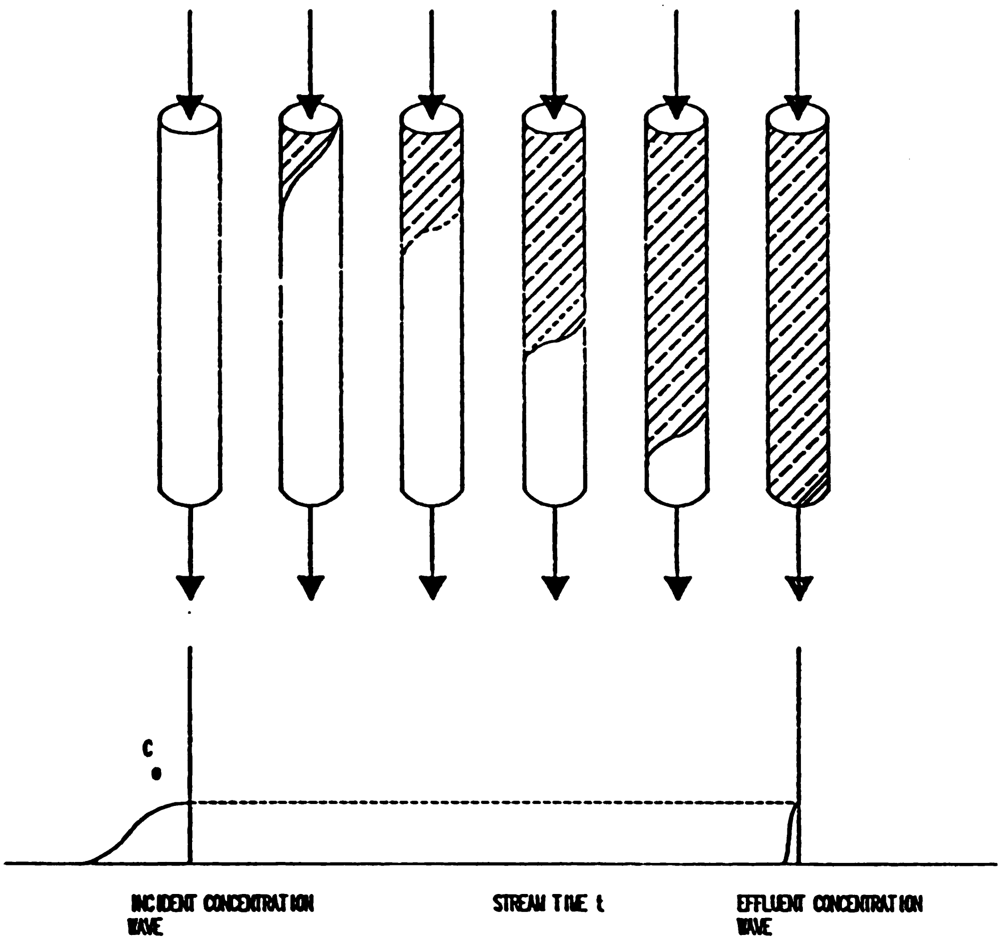
C_o
INCIDENT CONCENTRATION WAVE
STREAM TIME t
EFFLUENT CONCENTRATION WAVE

FIGURE 11. SELF SHARPENING BREAKTHROUGH CURVES PRODUCED BY FAVORABLE ISOTHERMS. THE SOLUTE VELOCITY IS DEPENDENT ON SOLUTE CONCENTRATION. HIGH EQUIVALENT FRACTIONS OF THE HIGH AFFINITY SOLUTE MOVE THROUGH THE BED AT HIGHER VELOCITY THAN LOW EQUIVALENT FRACTION REGIONS.

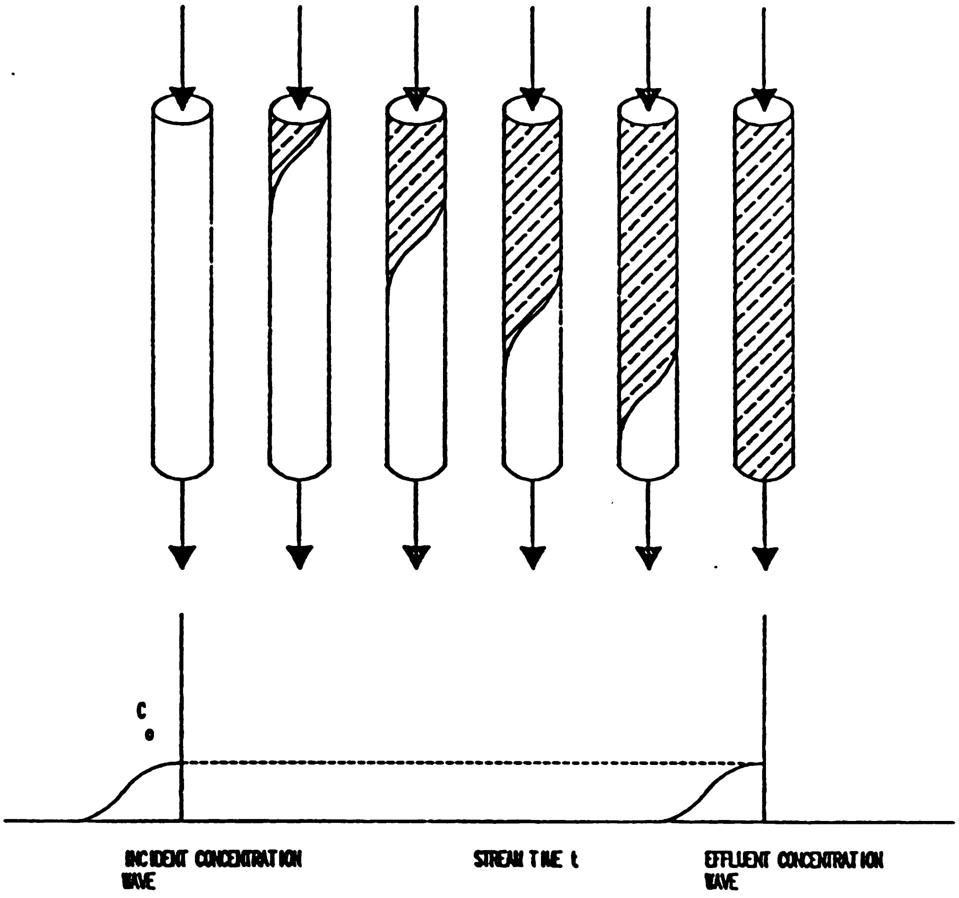
C
o
INCIDENT CONCENTRATION WAVE
STREAM TIME t
EFFLUENT CONCENTRATION WAVE

FIGURE 12 CONSTANT PATTERN BREAKTHROUGH CURVES PRODUCED BY LINEAR ISOTHERMS AND MAINTAIN THEIR SHAPE THROUGHOUT THE COLUMN. THE SOLUTE VELOCITY IS INDEPENDENT OF SOLUTE CONCENTRATION.

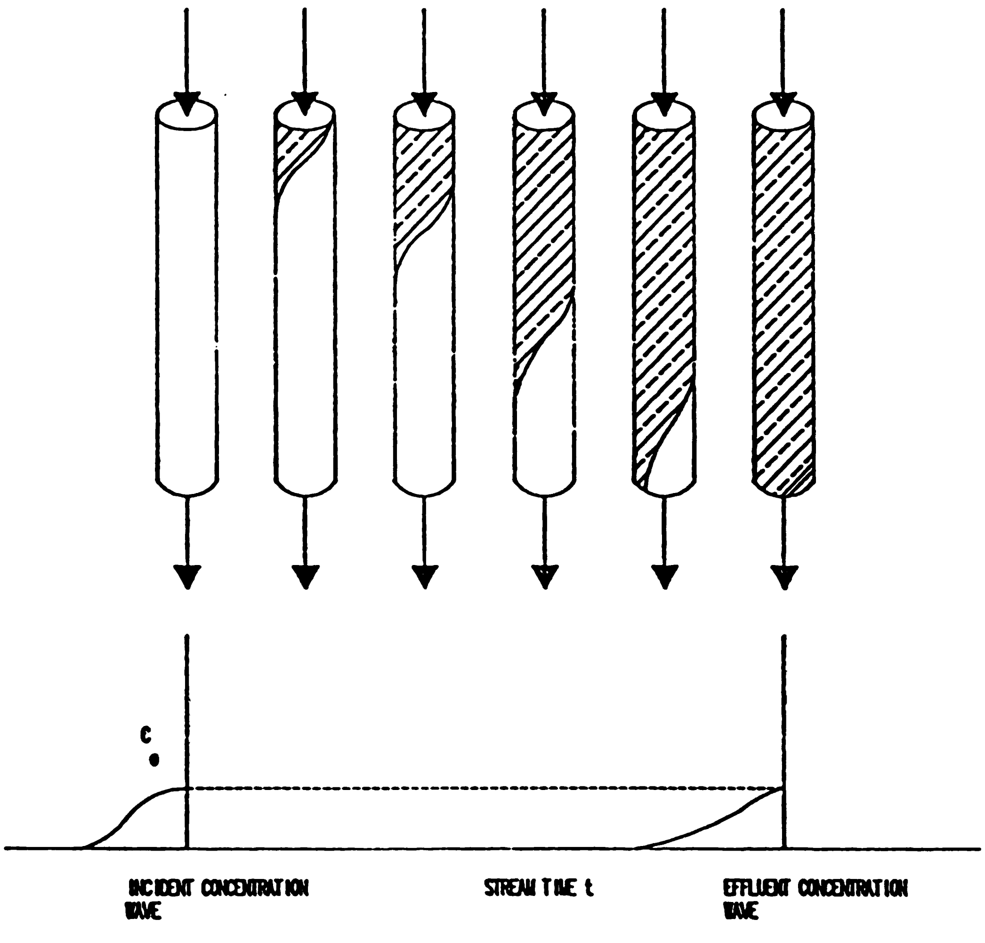
C
o
INCIDENT CONCENTRATION WAVE
STREAM TIME t
EFFLUENT CONCENTRATION WAVE

FIGURE 13 NON SHARPENING OR "GRADUAL" BREAKTHROUGH CURVES PRODUCED BY UNFAVORABLE ISOTHERMS. THE SOLUTE VELOCITY IS DEPENDENT ON SOLUTE CONCENTRATION. HIGH EQUIVALENT FRACTIONS OF THE HIGH AFFINITY SOLUTE MOVE THROUGH THE BED AT LOWER VELOCITY THAN LOW EQUIVALENT FRACTION REGIONS.

Multi Component Column Operations

Consider the three component system of butyrate, acetate and bicarbonate denoted as B, A, and C. Assuming that the resin is more selective for B than for A, (α^{Bu}_{Ac} >1).

The feed contains only B and A and the resin bed (or column) is initially saturated with C. As the feed passes through the column a fraction of the more prefered ion B, greater than its equivalent fraction in the feed, is preferentially removed in the first differential bed segment, while a smaller amounts of the less prefered ion A is removed in this segment. In this way, B is removed from the liquid phase before component A, and A is subsequently removed in deeper segments of the bed. As the bed becomes saturated, the least preferred ion A shows up first in the column effluent.

Once flow has commenced, zones will form that are predominantly rich with one species, as shown in Figure 15. Zone one is B rich with small amounts of A and C. Since B is the most preferred specie, it is completely removed in zone 1 so that the fluid passing through zone 2 only contains A and C. In zone 2 the more preferred ion A is preferentially removed, so that zone 2 is A rich in the resin phase. Zone 3 still contains the presaturant.

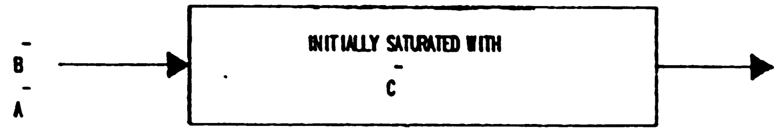
$\bar{B}$
$\bar{A}$
INITIALLY SATURATED WITH
$\bar{C}$

FIGURE 14. INITIAL CONDITION OF THE COLUMN.

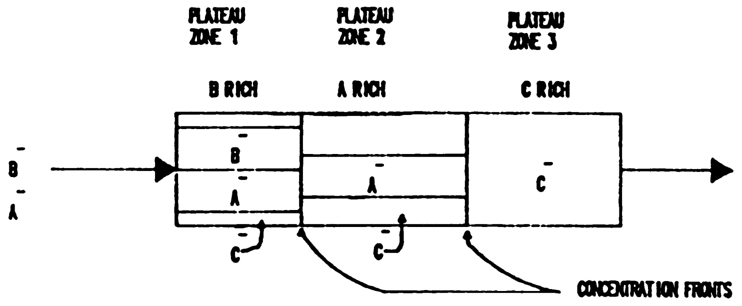
PLATEAU ZONE 1
PLATEAU ZONE 2
PLATEAU ZONE 3
B RICH
A RICH
C RICH
$\bar{B}$
$\bar{A}$
$\bar{B}$
$\bar{A}$
$\bar{A}$
$\bar{C}$
$\bar{C}$
$\bar{C}$
CONCENTRATION FRONTS

FIGURE 15 MULTICOMPONENT COLUMN OPERATION SHOWING THE PLATEAU ZONES AND THE CONCENTRAION FRONTS IN THE COLUMN

With time, the resin will become saturated with B, and zone 1 will extend through the entire length of the column. Figure 15 shows two concentration fronts. One exists between zones 1 and 2 across which B disappears, and the other exists between zones 2 and 3, across which A disappears.

In Figure 15, it is assumed that no axial mixing takes place in the column. Mixing would distort the wave fronts, and depending on the degree of mixing, the zones may not be observed at all.

Prediction of column behavior for a multicomponent ion exchange system is exceedingly more difficult than that of a binary (two component) system. For an n component system (here n refers only to the counter ions), it has been shown by Helfferich and Klein[27] and by Tondeur, Klein and Vermeulen[18] that n plateau zones will occur in the exchanger and the effluent concentration profile. There will also necessarily exist n-1 transition regions between the n plateau zones. The prediction of the effluent concentration profile necessitates the prediction of the shape and location of these transition regions as a function of time and axial position in the column.

Modeling of Multicomponent Column Operations

The numerical simulation of multicomponent ion exchange has received considerable attention recently. However, the modeling of multicomponent ion exchange with finite rates of mass transfer and significant mixing has received little attention.

Dranoff and Lapidus[16,29] applied Thomas' second order kinetic model[5] to ternary exchange and numerically solved the resulting equations. The ion exchange process was treated as a chemical reaction and the resulting reaction rate constants were correlated to flowrate. This was an incorrect picture of the process because ion exchange is controlled by rates of mass transfer, which are affected by the flow dynamics as well as the diffusivities of the different components as shown by Boyd et. al.[23]. Visawanthan et. al.[26] reported a non equilibrium analysis of multicomponent ion exchange based on irreversible thermodynamics in a single bead. Klein et. al. [18], Helfferich and Klein [27], and Rhee et. al.[28] reported methods of predicting effluent profiles if local resin-liquid equilibrium is maintained. Sanders et. al.[30] modeled the separation of animo acids by ion exchange chromatography by calculating equilibrium liquid and resin phase concentrations of different species by various prediction methods and treating the remainder of the problem as standard chromatography modeling with the restriction of charge neutrality. Although it is generally assumed that the compositions of the resin and the liquid phases are in equilibrium at the interface, the bulk liquid and resin concentrations are usually not in equilibrium. This equilibrium assumption is especially poor for dilute solutions with finite rates of mass transfer and high flowrate operations. in this latter case, the bulk concentrations of the ions in the liquid feed remains relatively constant while the liquid phase concentration of the presaturating ions vary.

Bradley and Sweed [9] used the same type of driving forces as Vermeulen and Clazie [31] to predict the multicomponent effluent profiles assuming finite rates of mass transfer and axial dispersion. However, for cases with high degrees of axial mixing, other models, such as the stirred tanks in series model, may be preferable. Barba, Del Re, and Foscolo [17] used the Nernst-Planck model for the diffusion coefficients and orthogonal collocation to solve the solid phase diffusional equations. This treatment allows the particle side flux to be directly calculated from concentration gradients.

Omatete [24] successfully predicted effluent profiles for ternary ion exchange for the limiting cases of solution phase mass transfer controlling and particle phase mass transfer controlling. However, this study did not treat the range of concentrations in which both phases control the rate of mass transfer and did not include liquid phase mixing. The present study extends the film model used by Omatete to all concentration ranges by using the resistances in series model and describes different degrees of mixing by using the stirred tanks in series model.

b

c

o

be

to

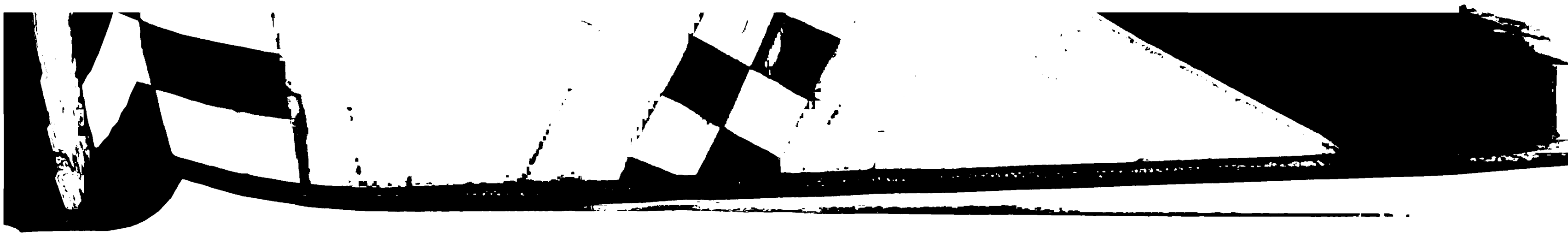

CHAPTER III

EXPERIMENTAL PROGRAM

APPARATUS .

The experimental apparatus used for the various experiments is shown in Figures 16, 17, and 18. The Cole-Parmer Master Flex peristaltic pump (model 7520-25) was calibrated and used in all experiments. The pump was found to deliver a relatively constant flow rate over the range of interest.

Differential Column

The differential column is shown schematically in Figure 16. The column consisted of three plexiglass parts held together by stainless steel screws. The middle part consisted of a hollow cylindrical chamber that contained the ion exchange resin. Two different middle sections were available; a 2.9 cm long section or a 5.0 cm long section were used depending on the desired amount of resin. The resin bed was held in place by stainless steel screens at the top and bottom of the middle section. Rubber o-rings were used at the top and bottom of the middle section to prevent leakage.

Glass beads of the same diameter as the resin were used above and below the packed resin bed to uniformly distribute the liquid feed and to allow for the used of different quantities of resin.

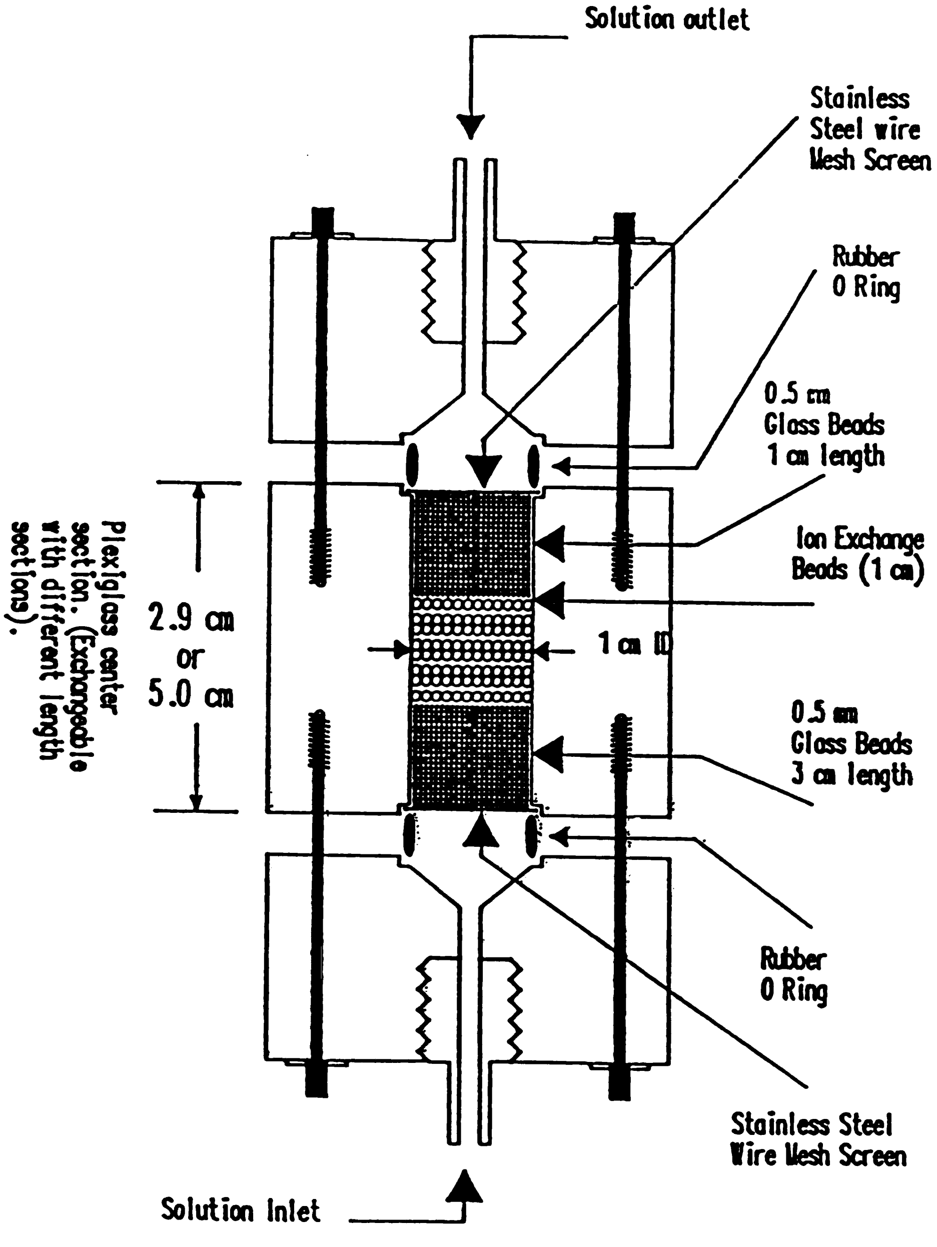
Solution outlet
Stainless Steel wire Mesh Screen
Rubber O Ring
0.5 cm Glass Beads 1 cm length
Ion Exchange Beads (1 cm)
1 cm ID
0.5 mm Glass Beads 3 cm length
Rubber O Ring
Stainless Steel Wire Mesh Screen
Solution Inlet
2.9 cm or 5.0 cm
Plexiglass center section. (Exchangeable with different length sections).

FIGURE 16. SCHEMATIC OF DIFFERENTIAL COLUMN

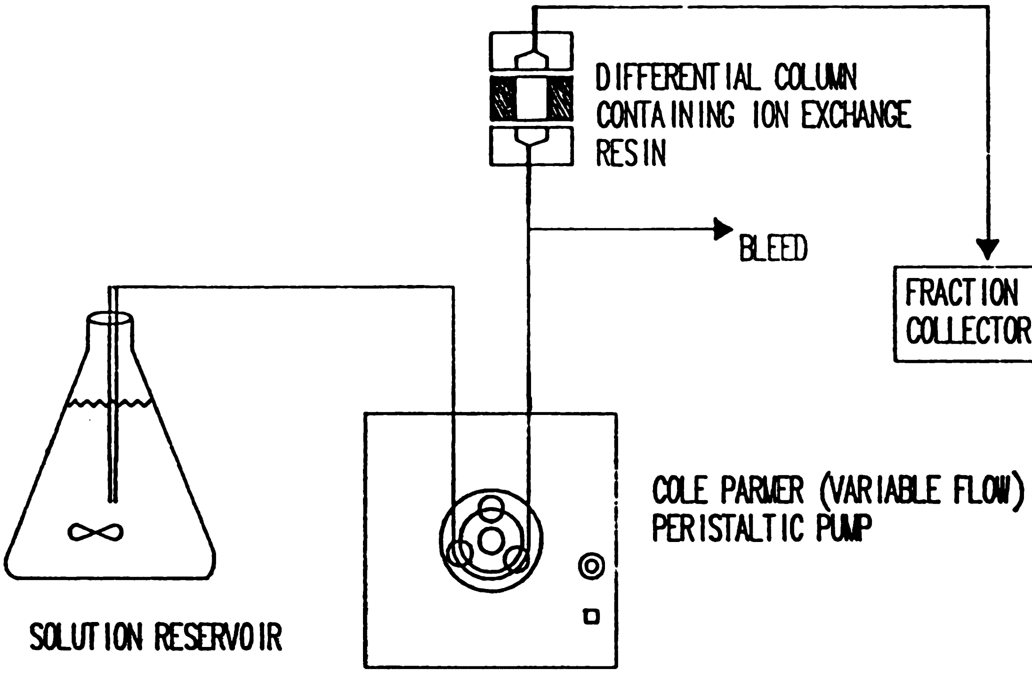
DIFFERENTIAL COLUMN
CONTAINING ION EXCHANGE
RESIN
BLEED
FRACTION
COLLECTOR
COLE PARMER (VARIABLE FLOW)
PERISTALTIC PUMP
SOLUTION RESERVOIR

FIGURE 17. SCHEMATIC DIAGRAM OF THE DIFFERENTIAL COLUMN VERIFICATION EXPERIMENT. THE BLEED STREAM IS USED TO PURGE SYSTEM OF WATER BEFORE THE STEP INPUT RISE IN CONCENTRATION IS MADE.

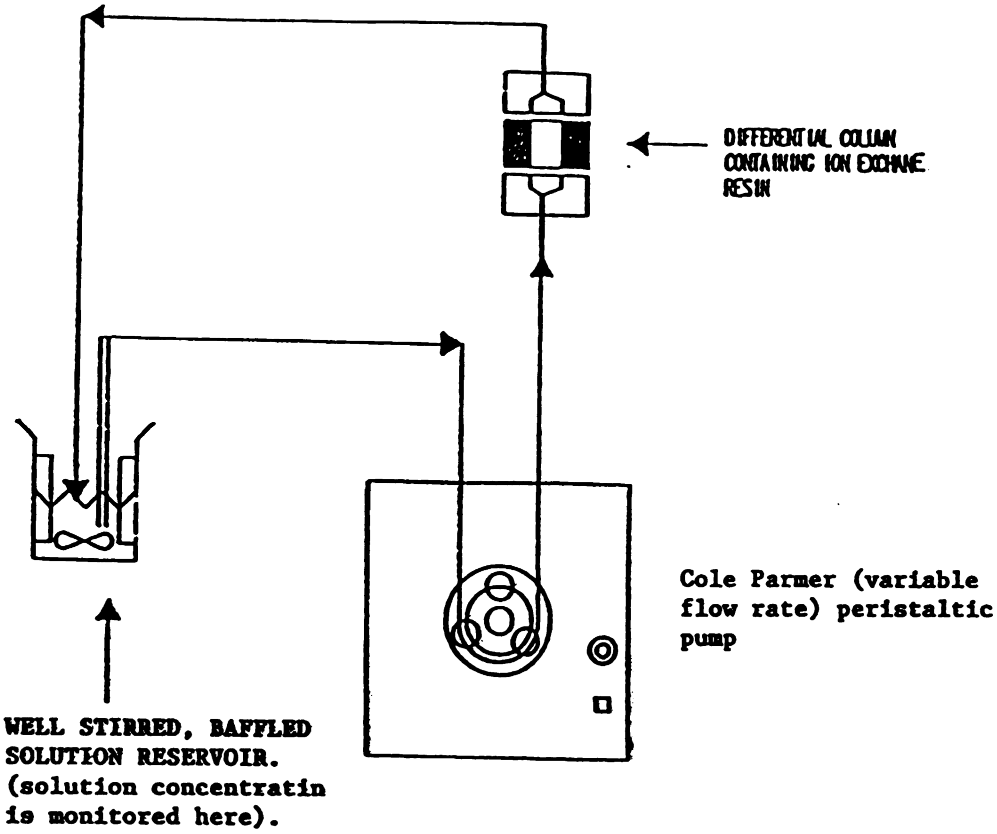
DIFFERENTIAL COLUMN CONTAINING ION EXCHANGE RESIN
Cole Parmer (variable flow rate) peristaltic pump
WELL STIRRED, BAFFLED SOLUTION RESERVOIR. (solution concentratin is monitored here).

Figure 18. Schematic diagram of the equipment setup for the rate experiments. System liquid holdup (pump, column, all connections, and tubing) = 3.8 ml.

CHEMICALS USED AND ANALYTICAL METHODS

Analytical grade anhydrous sodium acetate, hygroscopic sodium butyrate and sodium bicarbonate were used in all solutions. Glacial acetic acid and analytical grade butyric acid were used to adjust the pH of acetate and butyrate solutions. The pH of the sodium bicarbonate solutions was adjusted by addition of acetic or butyric acids and 0.1 N sodium hydroxide.

The effluent concentration of the organic acids was determined by a Hewlett Packard 5890A gas chromatograph equipped with an auto-sampler and integrator. A 4 foot glass column was packed with 80-100 mesh Chromosorb 101 and operated under the following conditions:

Carrier flowrate: 22.9 mL/min (N_2)

Oven temperature: 180 ^oC

Injector temperature: 220^oC

Detector temperature: 250^oC

Under these conditions, the maximum chromatograph error observed was 4%.

The bicarbonate concentration was determined by alkilametric pH titration with 0.1 M NaOH, and the maximum error observed was 2%. The main contributor to the scatter of experimental data was thought to be experimental and dilution error.

The resin used in all experiments was the Rohm & Haas Amberlite IRA-904 strongly basic type II resin. It belongs to the class of resins specified as macroporous and has the following general properties:

Capacity: 2.4 meq/gm (dry basis)

Average Particle Diameter: 0.45-0.5 mm

Moisture Content as Shipped: 57%

Density : 670 g/l (as shipped)

For further information please refer to the Rohm & Haas Catalog[32].

The resin used in this study was chosen on the basis of efficiency of regeneration, ability to recover weak organic acids, low cost, and resistance to fouling.

PROCEDURES

Procedure For Drying Resin

The resin was thoroughly dried, as described below, and weighed prior to all experiments. The rinsed, saturated resin was vacuum filtered using a Buchner funnel and air dried for several hours. The moist resin was then dried in a vacuum oven at 25 inches of Hg vacuum at 45°C to a constant weight. The resin was then stored in a vacuum desiccator until needed. The dryness of the resin was verified by comparing the measured capacity of the dried resin to manufacturer's data.

Procedure For Resin Saturation

Resin was initially soaked in double-distilled and deionized water for 24 hours to achieve its hydrated diameter; a vacuum was then placed upon the vessel containing the submerged resin to remove any air from the pores of the resin. The aspiration was continued until no visible bubble formation was observed and resin particles no longer floated when subjected to low pressure. The resin/water slurry was then poured into a standard 1.2 foot glass chromatography column with an inner diameter of one inch.

The ion with which the resin was to be saturated was then slowly pumped through the top of the column (dilution rate $\leq 0.01\ hr^{-1}$) and the column effluent was checked for the ion initially contained in the

resin. This exchange was continued until the presaturating ion could no longer be detected in the effluent. Double distilled deionized water was then pumped through the column until the column effluent contained no detectable concentration of ions.

EXPERIMENTS, RESULTS AND DISCUSSION

Equilibrium Experiments

Equilibrium isotherms were experimentally measured as outlined by Clifford[2]. The binary isotherm for acetate and butyrate was constructed at pH values of 7.5 and 6.0 to establish the effect of pH. However, the isotherms for the other binary systems containing bicarbonate were only constructed at a pH value of 7.5 because the bicarbonate concentration is pH dependent. Thus, a constant total concentration cannot be maintained if the pH changes.

The following procedure was used to measure the equilibrium isotherm for acetate (A) and butyrate (B). The same approach was also used on the other binary systems.

Starting with the resin presaturated with B, the weights of resin needed to give desired equilibrium liquid phase equivalent fractions of A ($X_A = 0.1, 0.3, 0.5, 0.7, 0.9$) were estimated using the Equation (12)given by Clifford[2]:

$$\beta = \frac{(1-\alpha)\, X_A^2 + (\alpha-2)\, X_A^2 + 1}{\alpha\, (\bar{B}_o/\bar{A}_o)\, X_A} \qquad (12)$$

Where,

β - resin weight required per liter of solution to achieve X_A

α - α_B^A - separation factor - $(Y_A X_B)/(X_A Y_B)$

A_o,B_o - initial concentration of A and B in liquid phase (mM/L)

$\bar{A}_o$,$\bar{B}_o$ - concentration of A and B initially in resin (meq/g)

X_A - equivalent fraction of A in solution at equilibrium

The separation factor is not known initially and must be estimated. The initial estimates were not accurate, but subsequent guesses made use of data already acquired and were thus more accurate.

The calculated amounts of resin were added to 100 mL aliquots of solution in 200 mL vials, sealed and shaken at approximately 60 RPM for 36 hours at 25°C in a New Brunswick gyrotory water bath shaker (model G76). The liquid phase was periodically assayed until the liquid phase concentration became constant. The liquid phase was then assumed to be in equilibrium with the resin. The experimentally measured resin capacity was used together with the resin weight and a material balance to calculate the resin phase concentration of each component. The average separation factor was then calculated using the "Ratio of the areas" technique described in the appendix.

The equilibrium isotherms for butyrate/acetate, butyrate/bicarbonate and acetate/bicarbonate are shown in Figures 19, 20, and 21. The average separation factors were as follows:

α_{AC}^{BU}(pH - 7.5) - 4.0

α_{AC}^{BU}(pH - 6.0) - 6.2

$$\alpha^{BU}_{HCO_3}(pH = 7.5) = 0.303$$

$$\alpha^{AC}_{HCO_3}(pH = 7.5) = 0.031$$

Thus, the order of selectivity, or preference by the resin, is as follows:

$$HCO_3 > \text{BUTYRATE} > \text{ACETATE}$$

The increase in the resin selectivity for butyrate at the lower pH is thought to be related to the dissociation chemistry of the weak acid. At the lower pH, there is a higher concentration of the undissociated acids, and non-ionic interactions between the acids and the resin would be increased. Evidence of significant non-ionic sorption of butyrate to the resin was obtained, and is discussed in the section titled "Non-ionic Sorption".

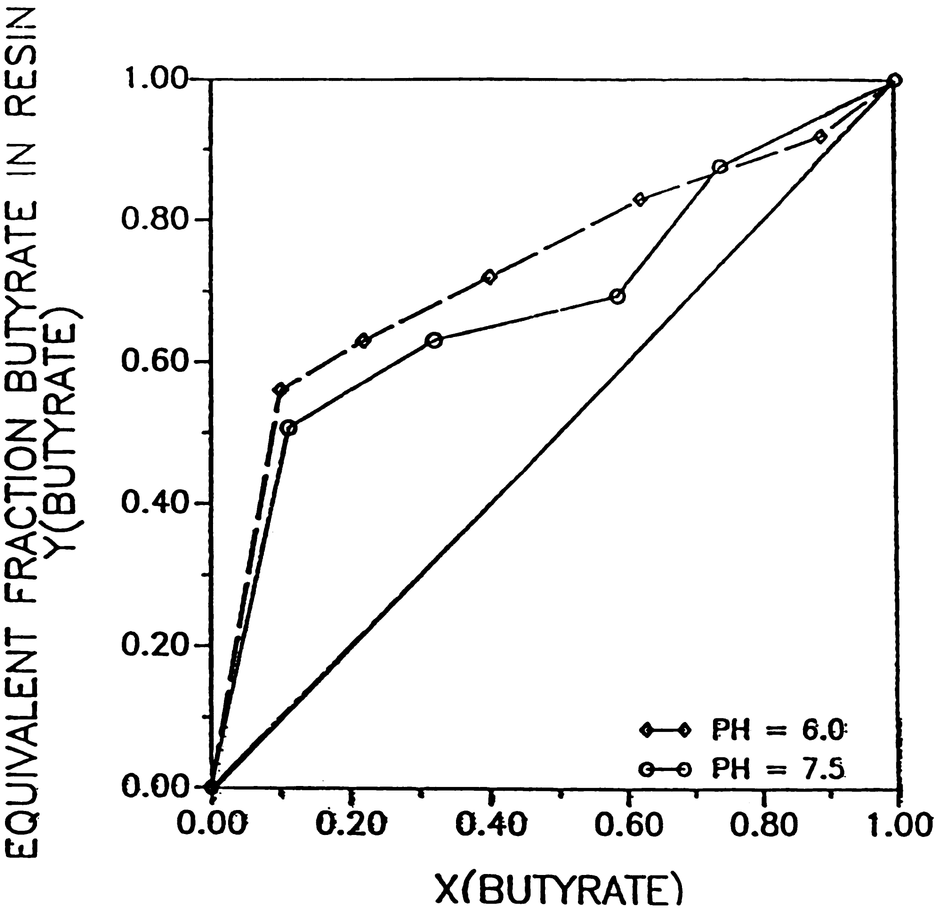

Figure 19. Equilibrium isotherm for butyrate/acetate exchange. Equivalent fraction of butyrate in resin versus equivalent fraction of brtyrate in the liquid phase at a total concentration C_T = 270 mM, T = 25 °C.

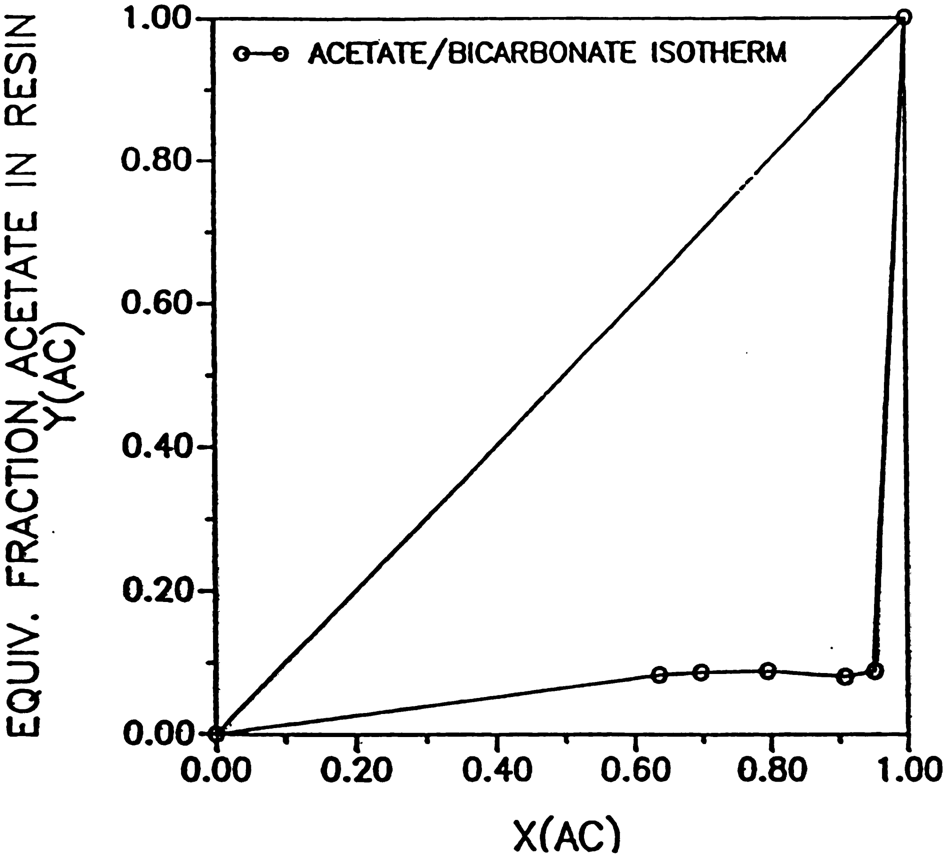

Figure 20. Equilibrium isotherm for acetate/bicarbonate exchange. Equivalent fraction of acetate in resin versus equivalent fraction of acetate in the liquid phase at a total concentration C_T = 100 mM, pH = 7.5, T = 25° C.

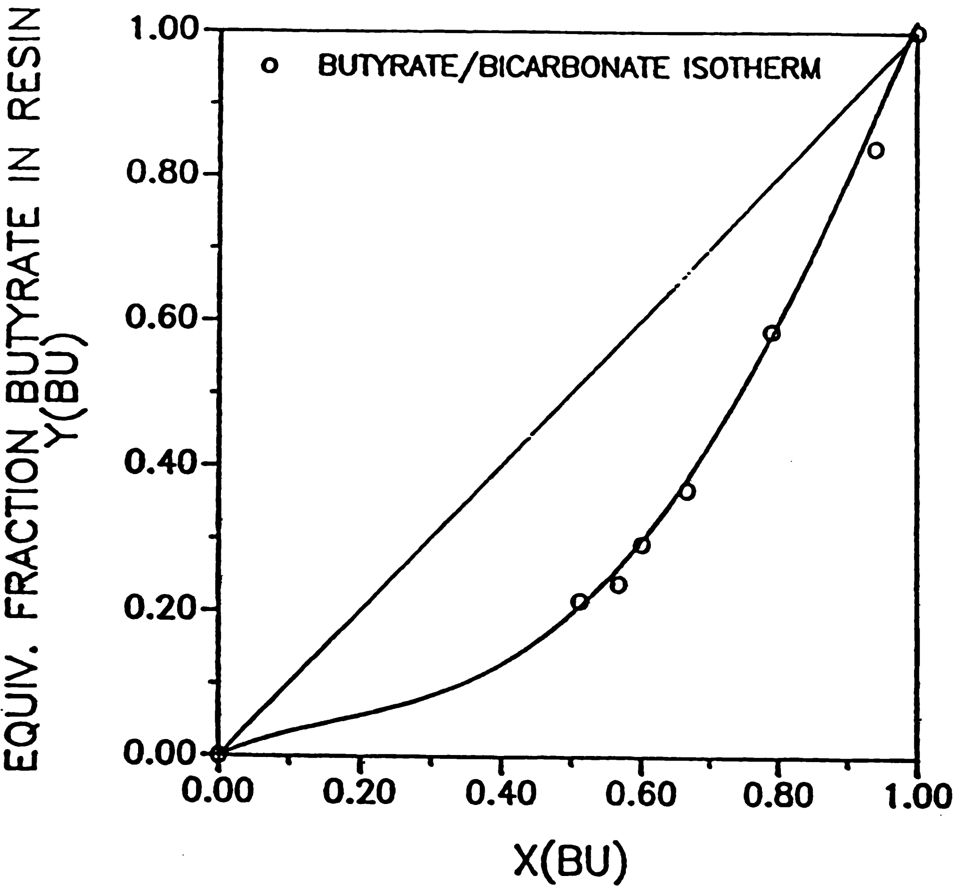

Figure 21. Equilibrium isotherm for butyrate/bicarbonate exchange. Equivalent fraction of butyrate in resin versus equivalent fraction of butyrate in the liquid phase at a total concentration C_T = 100 mM, pH = 7.5, T = 25°C.

Non-Ionic Sorption Experiment

An experiment was performed to determine if the resin would adsorb the ions of interest, mainly acetate and butyrate, by mechanisms other than ion exchange interactions. (e.g., hydrophobic interactions).

Six different solutions were prepared at three different concentrations, three solutions of sodium acetate and three solutions of sodium butyrate. The solutions of sodium acetate and sodium butyrate were prepared at a pH = 6.0 and at concentrations of 200, 300 and 500 mM. Next 100 mL portions of each solution were placed into 125 mL vials together with 10 g samples of dry resin saturated with the same ion as it was being placed in. Thus, resin in butyrate form was sealed with solution of butyrate at three different concentrations, and resin in acetate form was sealed with solutions of acetate at three different concentrations. The vials were shaken for 36 hours at 25°C and the liquid phase concentration was once again checked. The quantity of ion adsorbed was calculated by a material balance. Sorption of acetate and butyrate in excess of resin capacity was attributed to non-ionic interactions.

The results of this experiment are shown in Figure 19b. Butyrate was adsorbed to a greater extent than acetate by non ionic interactions, it is therefore logical that these interactions would account for a larger relative amount of butyrate adsorbed at lower pH. It is also possible that butyrate polymerizes similar to lactic acid in highly concentrated solutions; and the resin phase concentration of butyrate may be sufficient for such polymerization. It should also be noted that no experiments were performed to confirm the mechanism by which these non-ionic interactions occur.

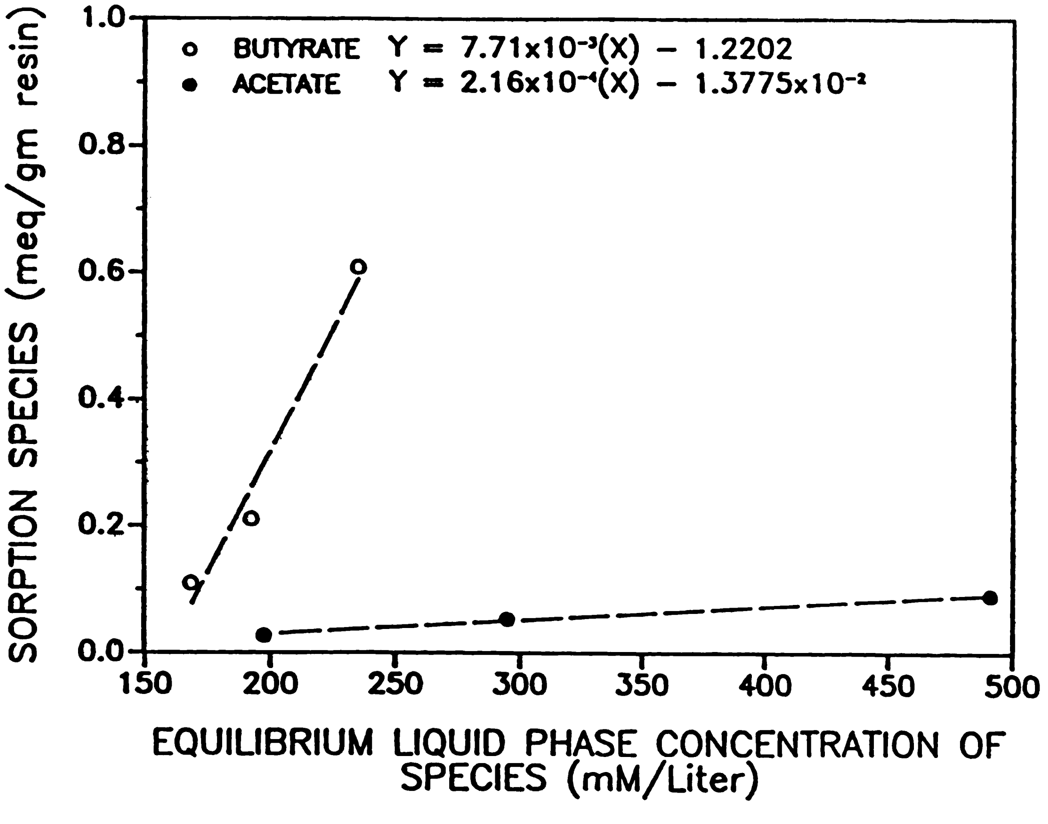

Figure 19b. Adsorption of acetate and butyrate by IRA 904 to excess of ion exchange capacity of the resin by non ionic interactions. Quantity of ion adsorbed versus equilibrium liquid phase concentration. pH = 6.0, T = 25°C.

Verification Of The Differential Column

The measurement of kinetic parameters in a packed ion exchange column is much easier if it can be assumed that the liquid phase concentration remains constant throughout the packed bed. This desirable effect is approximated in a differential column. It must therefore be verified that the small column used is in fact a differential column. The experiments discussed here were carried out in the layout shown in Figure 17. The following procedure was used to verify the assumption of a differential column and to determine the minimum flow rate at which this assumption would break down.

The differential column was packed with 0.227 g of resin in the acetate form, then soaked and aspirated according to the procedures outlined in the previous sections. Five hundred mL of deionized water were then pumped through the column to ensure a clean column. Butyrate solutions of different concentrations and a pH of 6 were pumped through the column, and the effluent was collected via a fraction collector every 10 seconds. Only selected samples were analyzed. The samples were analyzed for presence of acetate, and the rate of release of acetate was calculated versus time. This information was then used to determine average concentration drops across the length of the column. The largest value of acetate flux was used to calculate the concentration drop of butyrate across the column.

Typical experimental data for adsorption of butyrate are shown in Table 2. Experimental conditions were as follows:

Flow rate: 37 mL/min
Total Concentration: 102 mM
pH : 6.0
Resin weight: 0.50 g
Resin presaturant: Acetate

Table 2. Concentration drop across the differential column versus time shown as percent of total concentration.

Time (s)	Δ C %
5	11.8
15	6.60
25	5.00
35	5.01
45	3.30

Here ΔC refers to the difference between the inlet and outlet concentrations of butyrate per centimeter of packed bed as calculated in the appendix.

Rate Experiments

To measure the mass transfer coefficient a series of experiments were carried out at high dilution rates in the differential column such that the largest percentage drop in liquid phase concentration across the column was 6%. The experimental setup is shown in the previous section titled Apparatus in Figure 18. The column was packed with 0.227 g of resin, and 0.5 mm glass beads were place above and below the resin to achieve uniform liquid velocity profiles passing through the resin bed. The resin was then aspirated to remove trapped air and allowed to soak for 24 hours by pumping water through the column. Next, the resin was saturated with acetate using 1 liter of 50 mM sodium acetate solution at a pH of 6 and dilution rate of one min $^{-1}$. The effluent was periodically checked to ensure resin saturation. Once saturated, the resin was rinsed with deionized water until no acetate was detected in the effluent. One hundred or 50 mL of a solution of sodium butyrate at a pH of 6 was placed in a baffled, well stirred, reservoir and then pumped through the column in recycle fashion as shown in Figure 18. The acetate concentration was monitored in the stirred reservoir by assaying 0.5 mL samples taken at specific intervals. This procedure was repeated at several different flow rates and concentrations and was also repeated with butyrate-saturated resin exchanging with acetate as well as with bicarbonate. The results of these experiments are presented in Figures 22-31. Figures 22, 24, and 26 show rates of exchange between acetate and butyrate at different total concentrations and flow rates. In each case the resin was initially saturated with acetate and exchanged with a liquid phase containing butyrate. Figures 23, 25, and 27 show corresponding values of overall particle phase mass transfer coefficients calculated from the rate data according to the procedure in the appendix (sample calculation D). The calculated overall mass transfer coefficients are plotted versus the concentration of butyrate in the resin, which corresponds to a progression in the ion exchange process, because the resin initially contains no butyrate. The overall mass transfer coefficients increased with increasing flow rate. This result is thought to be due to improvements in the solution phase mass transfer rate, or explained in terms of the film model, thinner liquid side film. The overall mass transfer coefficients were also observed to increase as the liquid phase concentration increased. This increase is due to larger driving forces in the liquid phase improving the liquid side rates of mass transfer and forcing the process closer to particle phase controlled kinetics, and the larger mass transfer coefficients measured are due to elimination of the liquid phase resistances.

A reduction in the magnitude of the overall mass transfer coefficients was observed as a function of time. Initially the resin beads contain only acetate, and butyrate ions can easily access and exchange with acetate ions near the surface of the beads. However, as time passes, the butyrate ions must penetrate deeper into the beads to access sites in the interior of the resin and the rate of mass transfer reflects this slower diffusion through the solid resin.

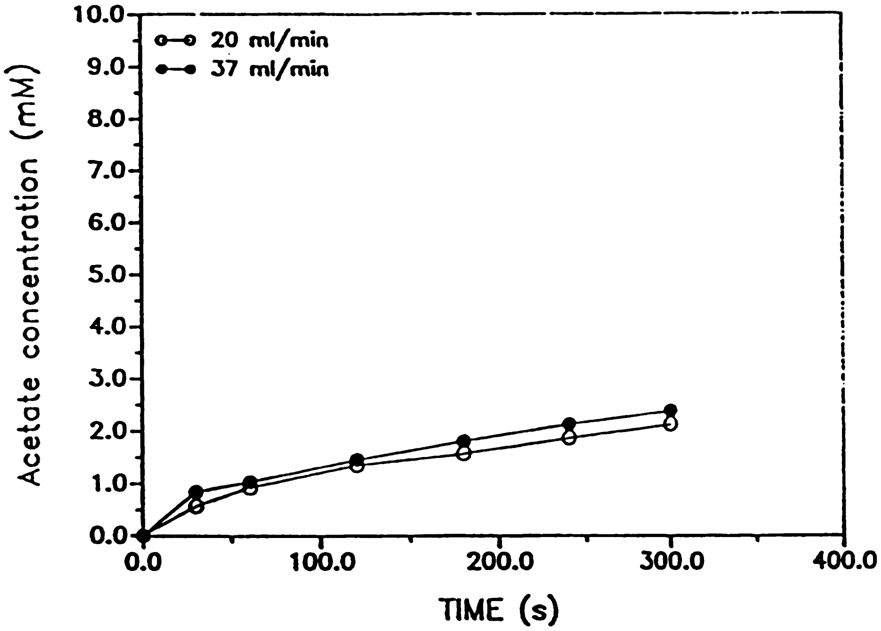

Figure 22. Kinetic experiment run using a differential column packed with 0.227 g of IRA-904 initially saturated with acetate and exchanged with butyrate at C_T = 20 mM and pH = 6.0. Column volume = 0.7854 ml with void fraction = 0.35, total liquid volume = 100 ml.

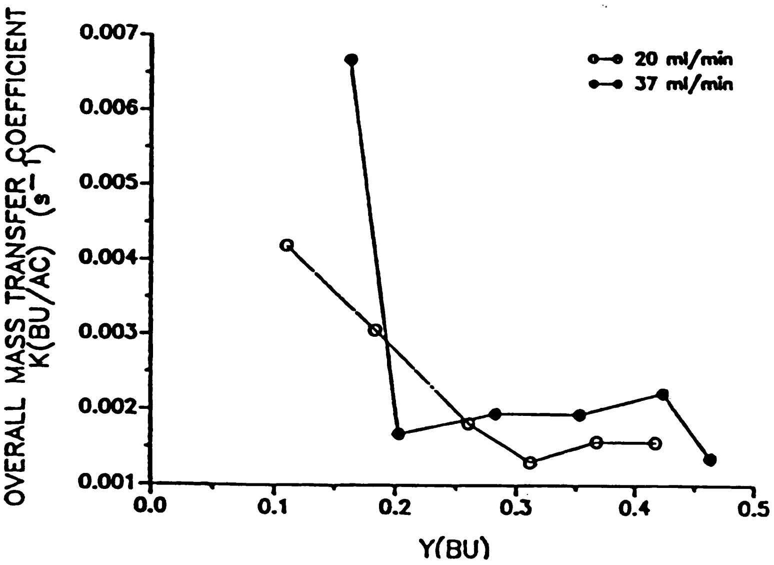

Figure 23. Experimentally calculated values of overall mass-transfer coefficients versus the solid phase concentration of butyrate in the exchange of acetate for butyrate shown in figure 22.

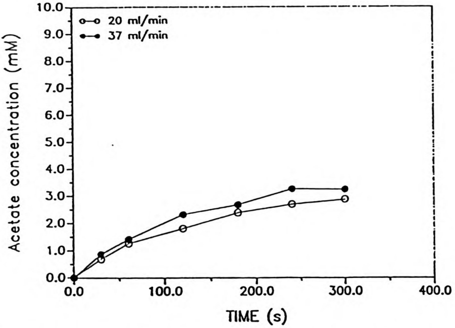

Figure 24. Kinetic experiment run using a differential column packed with 0.227 g of IRA 904 initially saturated with acetate and exchanged with butyrate at C_T = 100 mM and pH = 6.0. Column volume = 0.7854 ml with void fraction = 0.35. Total liquid volume = 100 ml.

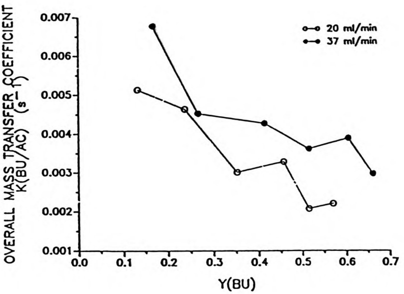

Figure 25. Experimentally calculated values of overall mass-transfer coefficients versus the solid phase concentration of butyrate in the exchange of acetate for butyrate shown in figure 24.

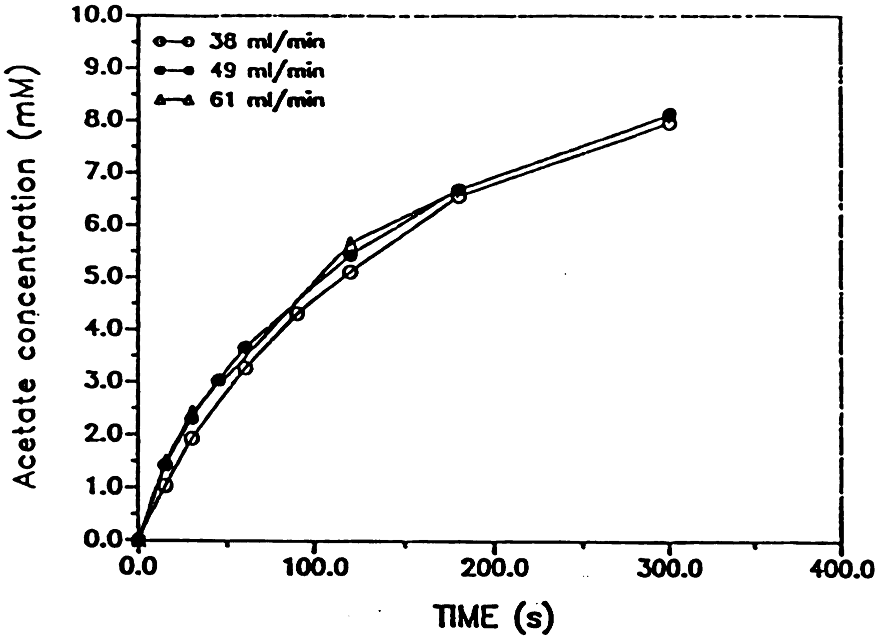

Figure 26. Kinetic experiment run using a differential column packed with 0.227 g of IRA 904 initially saturated with acetate and exchanged with butyrate at C_T = 300 mM and pH = 6.0. Column volume = 0.7854 ml with void fraction = 0.35. Total liquid volume = 50 ml.

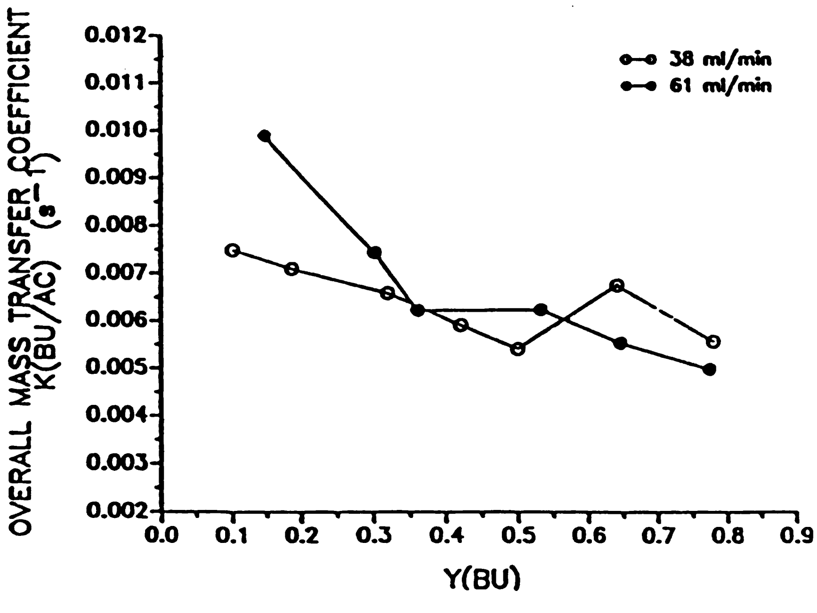

Figure 27. Experimentally calculated values of overall mass-transfer coefficients versus the solid phase concentration of butyrate in the exchange of acetate for buryrate shown in figure 26.

Figures (28) and (30) show rate experiments performed with the acetate/bicarbonate, and butyrate/bicarbonate binary systems. In each case the ion exchange resin was saturated with the organic acid anion and then exchanged with bicarbonate at a pH of 7.5. As in Figure 26, the rate of mass transfer was observed to increase as the flow rate was increased up to a certain point; beyond this point, the rate of mass transfer was independent of flow rate. The calculated values of overall mass transfer coefficients at this point were assumed to be particle phase controlled mass transfer coefficients, and therefore, an intrinsic property of the resin and the exchanging ions. These overall mass transfer coefficients are plotted as a function of the resin phase concentration of the species initially in the liquid phase in Figures (29) and (31).

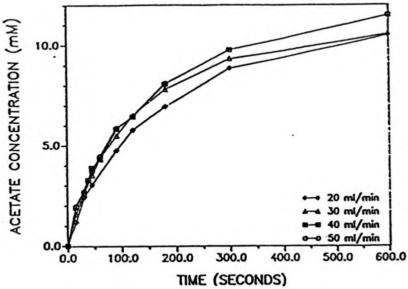

Figure 28. Kinetic experiment run using a differential column packed with 0.227 g of IRA 904 initially saturated with acetate and exchanged with bicarbonate at C_T = 100 mM and ph = 7.5. Column volume = 0.7854 ml with void fraction = 0.35. Total liquid volume = 50 ml.

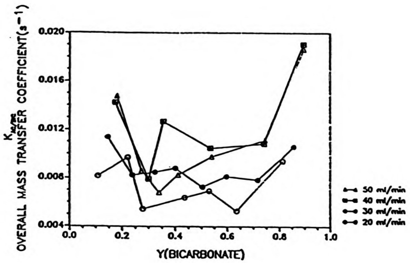

Figure 29. Experimentally calculated values of overall mass-transfer coefficients versus the solid phase concentration of bicarbonate, in exchange of acetate for bicarbonae shown in figure 28.

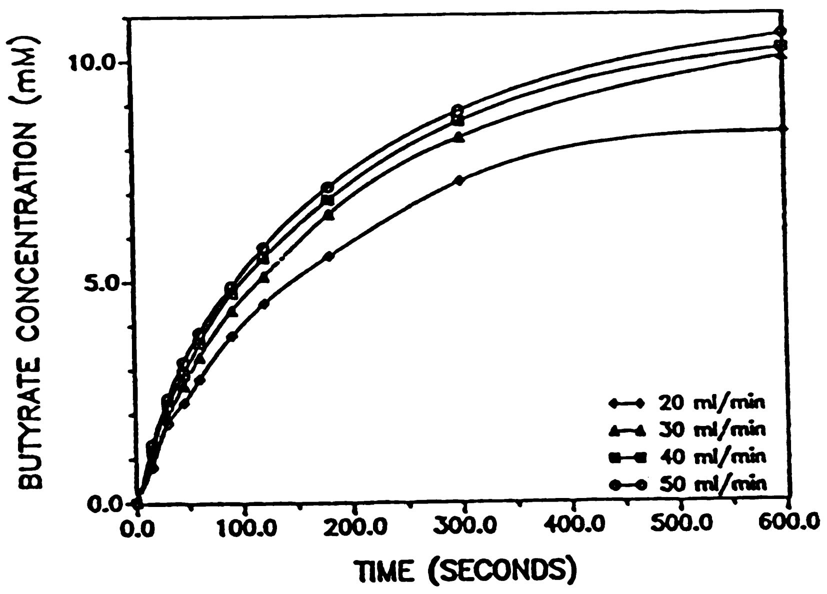

Figure 30. Kinetic experiment run using a differential column packed with 0.227 g of IRA, 904 initially saturated with butyrate and exchanged with bicarbonate at C_T = 100 mM and pH = 7.5. Column volume = 0.7854 ml with void fraction = 0.35. Total liquid volume = 50 ml.

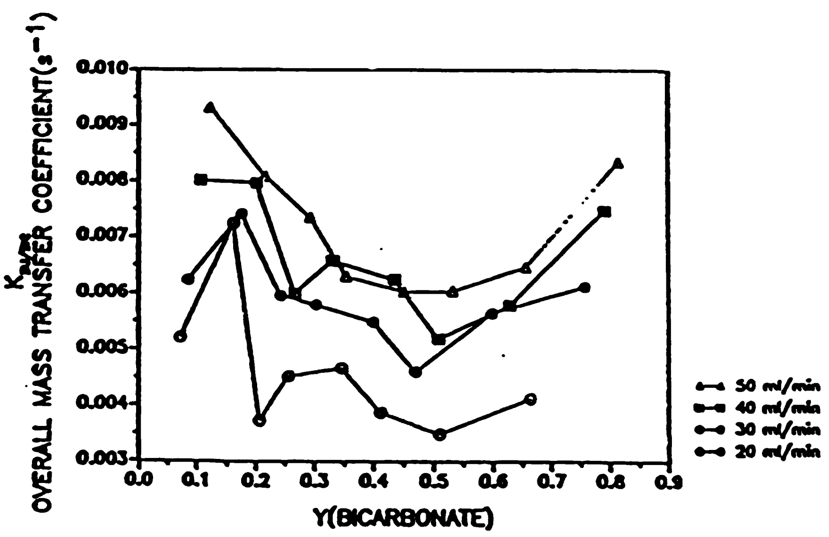

Figure 31. Experimentally calculated values of overall mass-transfer coefficients versus the solid phase concentration of vicarbonate in the exchange of butyrate for bicarbonate shown in figure 30.

The magnitude of the calculated mass transfer coefficients in Figures (29) and (31) were observed to decrease initially as ion exchange progressed and then increased. The decrease in the mass transfer coefficients can be explained by similar reasoning as the acetate/butyrate exchange. However, the increases at large resin phase concentrations of bicarbonate are thought to be artifacts caused by numerical errors. As shown in the appendix, these values are calculated from the experimental data by several numerical differentiations and calculations. Small errors in the data introduce significant errors in these calculations. There are also larger errors introduced at high values of Y(bicarbonate), because this value is closer to the equilibrium value of Y^*(bicarbonate); as the two values approach one another small errors in either Y or Y^* contributes to a larger error in the inverse of their difference ($1/Y^*-Y$), and hence in the value of the mass transfer coefficient (see appendix).

CHAPTER IV

MATHEMATICAL MODELING

MATERIAL BALANCE EQUATIONS

Continuous Integral Model

The liquid phase material balance for each of the species in a three component, packed bed ion exchange column can be written over a differential section of the column as follows[24]:

$$(F/S)(\partial C_i/\partial z) + \epsilon(\partial C_i/\partial t) = -\rho_b(\partial q_i/\partial t) \qquad (13)$$

where,

C_i = concentration of species i (mole/L)

F = volumetric flowrate of feed (L/s)

t = time (s)

ϵ = bed void fraction

ρ_b = packed bed density (g/L)

q_i = resin phase concentration of species i (meq/g)

z = axial position (dm)

C_{io} = feed concentration of species i (mole/L)

q_{io} = presaturation condition of the column for species i (meq/g)

With the following boundary and initial conditions:

$$q_i(z,0) = q_{io} \qquad @\ t=0,\ z\geq 0 \qquad (14)$$

Or uniform presaturation of the resin, and

$$C_i(0,t) = C_{io} \qquad @\ z=0,\ t\geq 0 \qquad (15)$$

or constant feed concentration.

The following assumptions are made in arriving at Equation (13):

1. No axial Dispersion.
2. No radial concentration gradients.
3. Plug flow velocity profile.

The rate of exchange of species i represented by $(\partial q_i/\partial t)$, must then be represented by a rate equation to solve the material balance equations and predict the effluent concentration profiles. There will exist as many material balance equations as there are exchanging ions and an equal number of rate expressions. Thus, six simultaneous partial differential equations must be solved for the prediction of the effluent concentration profile for a ternary system. The total number of simultaneous partial differential equations to be solved for an n component system is 2n. In addition, effects such as axial mixing and the possible effect of co-ions and counter ions on one another and on the overall exchange process would further increase the complexity of the model.

Tanks In Series Model

Material balance equations can be written for the ion exchange column based on the tanks in series model. This model assumes that no radial concentration gradients exist in the column being modeled; Fujine, Saito and Shiba[22] have shown this to be a valid assumption. Different degrees of backmixing are modeled via different number of stirred tanks in series. Since each tank in the model is perfectly mixed, modeling the column with a small number of tanks represents a great degree of mixing in the column, while modeling the column with a larger number of tanks represents less axial mixing and an approach to plug flow conditions. The analogy between a packed bed and N tanks in series is shown schematically in Figure (32).

The material balance for each component can then be written for the Nth stirred tank as follows:

$$V_T dC_i(N,t)/dt = F(C_i(N-1,t)-C_i(N,t)) - W_r dq_i(N,t)/dt \qquad (16)$$

where:

V_T = liquid volume in each stirred tank (L)

t = time (s)

N = axial position index indicating the number of stirred tanks from the inlet.

F = solution volumetric flow rate (L/s)

$C_i(N,t)$ - time dependent liquid phase concentration of species i in tank N (mole/L solution).

$q_i(N,t)$ - time dependent resin phase concentration of species i in tank N (meq/g of dry resin).

$C_i(N-1,t)$- time dependent liquid phase concentration of species i in tank N-1 (mole/L solution).

W_r - resin weight contained in tank N (g dry).

There will be three such equations in each tank for a three component system which must then be solved together with the rate equations. It should be noted that each partial differential Equation in (13) has been replaced by N ordinary differential equations; since each tank represents a fixed axial position, the composition in each tank is a function of time only. Thus, the six simultaneous partial differential equations are converted into a (6XN) system of ordinary differential equations.

Generally, for rapid ion exchange processes such as this, the liquid and solid phase compositions will not be in equilibrium, and sole knowledge of the equilibrium theory of multicomponent ion exchange will produce results that will be inaccurate. It is therefore necessary to model the kinetics of the exchange process.

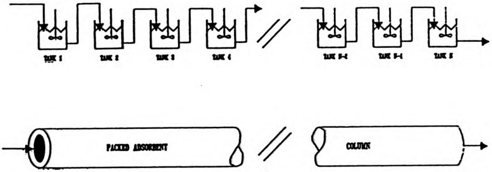
TANK 1
TANK 2
TANK 3
TANK 4
TANK N-2
TANK N-1
TANK N
PACKED ABSORBENT
COLUMN

Figure 32. The analogy between stirred tanks in series and a packed column.

RATE THEORY

The rate of transfer of species between phases is a traditional chemical engineering problem that has been extensively studied. Assuming that the rate of ion exchange at the resin active sites is rapid relative to diffusion of ions to the active sites, a typical concentration profile for species i would be expected, as shown in Figure 33. The liquid phase concentration of species i, which is being adsorbed onto the resin, drops from a bulk value of C_i(bulk) to C_i(int) at the interface. The resin phase concentration drops from an interfacial value of q_i(int) to its lowest value at the center of the particle.

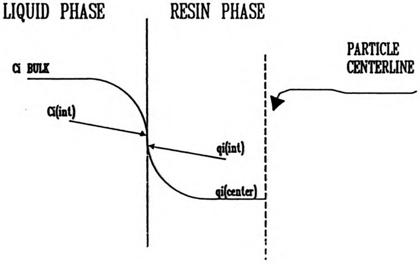
LIQUID PHASE
RESIN PHASE
PARTICLE CENTERLINE
Ci BULK
Ci(int)
qi(int)
qi(center)

Figure 33. Distribution of species (i) between the resin and the liquid in contact with the resin. Species (i) is being transfered from the liquid phase to the resin phase.

C_i(int) and q_i(int) are taken to be in equilibrium and are related by the equilibrium partition coefficient. If the electrical potential due to the separation of charges between liquid phase and the resin may be disregarded, the rate of mass transfer in each phase can be represented by the product of a mass transfer coefficient and a driving force. A local mass transfer coefficient (k) can be defined based upon the assumption of an imaginary film of thickness (δ) across which the concentration drop or rise occurs. This film is schematically represented in Figure (34), and the defining equations for the liquid-phase and resin-phase local mass transfer coefficients are given as Equation (17) and (18).

$$N_i = k_c(C_i(\text{bulk})-C_i(\text{int})) \qquad (17)$$

Since no chemical reaction takes place at the interface and there is no accumulation of mass, the liquid phase flux must equal to the flux of species into the resin:

$$N_i = k_q(q_i(\text{int})-q_i(\text{avg})) \qquad (18)$$

In Equation (18), flux of component i across the interface (N_i) is expressed in terms of local mass transfer coefficient (k_q) and driving force (q_i(int) - q_i(avg)).

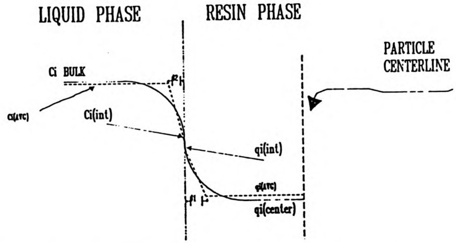
LIQUID PHASE
RESIN PHASE
PARTICLE CENTERLINE
Ci BULK
Ci(ATC)
Ci(int)
qi(int)
qi(ATC)
qi(center)
δ2
δ1

Figure 34. Distribution of species (i) between the resin and the liquid in contact with the resin represented together with the film model.

In general, interfacial compositions are difficult to measure; the use is therefore made of an overall mass transfer coefficent (K_c) and a corresponding overall driving force. This driving force is defined as the difference between the bulk liquid concentration of the exchanging species and the liquid phase concentration that would be in equilibrium with the average resin phase concentration (C_i^*):

$$N_i = K_c(C_i(\text{bulk})-C_i^*) \tag{19}$$

Rate Controlling Step:

The transfer of species i between the liquid and the resin phases can be thought of as a series of consecutive steps, each with an inherent resistance to mass transfer. This is known as the resistances in series model. These steps are listed below:

1. Diffusion of ions from the bulk liquid phase to the outer boundary of the liquid side film.
2. Diffusion of ions through the liquid film to the resin surface.
   (For porous particles one must also include the diffusion of ions into the pores of the resin).
3. Diffusion of ions into the solid or gel resin matrix across a particle side film to the ionic exchange groups of the resin.

4. The exchange of ions for counter ions.
5. Steps 1-3 in reverse order for the counter ions diffusing back out of the resin particle and into the liquid phase.

The rate controlling step is defined as the slowest step, such that the rate of mass transfer in this step adequately represents that of the entire process. Boyd et. al.[23] first showed the rate controlling step to be diffusion either within the particle or in the stagnant liquid film; in some cases, both mechanisms may affect the rate. Ion exchange is said to be solution phase mass transfer controlled when diffusion across the liquid film is rate limiting, and particle phase mass transfer controlled when the diffusion of ions within the particles is rate limiting.

Solution Phase Mass Transfer Controlling

Omatete[24], has shown that for solution phase mass transfer controlled case in a ternary system, the rate of mass transfer is well represented by the following equation:

$$(d\underline{Y}_i/dt)_z = (C_o/Q\ W_t)\sum_{\substack{j=1 \\ j \neq i}}^{n} \kappa_{ij}(X_j^{*} - X_j) \qquad (20)$$

Where $\underline{Y}_i$ = solid phase average concentration expressed in terms of equivalent fractions ($Y_i = q_i/Q$).

Q - total capacity of the resin (meq/g dry resin)

C_o - inlet feed total concentration $= (\Sigma\ C_i)_{z=0}$ (Mole/L)

W_t - total resin weight (g dry)

κ_{ij} - liquid phase ternary overall mass transfer coefficient predicted from binary coefficients (s^{-1}).

X_j - average liquid phase composition of species j, in equivalent fractions. $X_j = C_j/C_o$ for constant total concentration

$X_j = C_j/C_T$ for variable total concentration

C_T - local total concentration $= (\Sigma\ C_i)_z$

X_j^* - liquid phase concentration in equilibrium with the resin phase of composition $\underline{Y}_j$.

$$X_j^* = \frac{\alpha_j^{ref}\underline{Y}_j}{\sum_{k=1}^{n} \alpha_k^{ref}\ \underline{Y}_k} \tag{21}$$

n - number of species

α_j^{ref} - separation factor between a reference component and j

$$\alpha_j^{ref} = \frac{\underline{Y}_j\ X_{ref}}{\underline{Y}_{ref}\ X_j} \tag{22}$$

The ternary overall mass transfer coefficients can be calculated from binary coefficients by applying the multicomponent theory of Bird,

Stewart, and Lightfoot[25] to diffusion of ions in the liquid phase. The result is shown in Equation (23)[24]:

$$\kappa_{ij} = \frac{K_{ij}[(X_j+X_k)X_{ik} + X_i K_{ik}]}{X_i K_{jk} + X_j K_{ik} + X_k K_{ij}} \tag{23}$$

Since the resin particles are spherical and a radial concentration gradient exists within them, an average Y will be defined as follows:

$$\underline{Y}_i = (3/R^3)\int_0^R Y_i(r)\, r^2\, dr \tag{24}$$

Particle Phase Mass Transfer Controlling

For the particle phase mass transfer controlling step, Omatete has shown that

$$(d\underline{Y}_i/dt)_z = \sum_{\substack{j=1 \\ j\neq i}}^{n} \underline{\kappa}_{ij}(\underline{Y}_j - \underline{Y}_j^{*}) \tag{25}$$

adequately represents the rate of mass transfer.

$\underline{\kappa}_{ij}$ = solid phase overall ternary mass transfer coefficient predicted from binary coefficients.

$$X_j^* = \frac{\alpha_j^{ref} X_j}{\sum_{k=1}^{n} \alpha_k^{ref} X_k} \tag{26}$$

The ternary overall mass transfer coefficients for the particle phase can be calculated analogously to the liquid phase ternary coefficients by Equation (27):

$$\underline{\kappa}_{ij} = \frac{\underline{K}_{ij}[(\underline{Y}_j+\underline{Y}_k)\underline{K}_{ik} + \underline{Y}_i\underline{K}_{ik}]}{\underline{Y}_i\underline{K}_{jk} + \underline{Y}_j\underline{K}_{ik} + \underline{Y}_k\underline{K}_{ij}} \tag{27}$$

The study of the pore mass transfer controlling case is ignored, and the particle phase is taken as a whole, including the pores. The corresponding particle phase mass transfer coefficient used is then the effective particle phase mass transfer coefficient. Vermeulen[20], and Vermeulen and Quilici[21] have shown that for the pore mass transfer controlling case a driving force using particle side concentrations is a valid approximation. It is therefore possible to model the pore phase mass transfer controlling case by the product of a particle phase driving force and a pore phase mass transfer coefficient. The pore mass transfer equation and the particle phase mass transfer equation can then be combined as the product of the particle phase driving force and an effective particle side mass transfer coefficient.

Particle Phase and Solution Phase Controlling

For the case where both the liquid and the particle phase control the rate of mass transfer, the so called transition regime, the overall mass transfer coefficient is calculated by a sum of the resistances model [34].

$$1/\underline{K}_{ij} = m/k_{ij} + 1/\underline{k}_{ij} \qquad (28)$$

Where:

$\underline{K}_{ij}$ = overall particle side binary mass transfer coefficient

$\underline{k}_{ij}$ = local particle side binary mass transfer coefficient

k_{ij} = local solution side binary mass transfer coefficient

m = slope of the equilibrium isotherm

Converting the material balance Equation (16) to equivalent fraction form and assuming constant total concentration yields:

$$V_T C_o \frac{dX_i(N,t)}{dt} = FC_o(X_i(N-1,t)-X_i(n,t)) - W_r Q \frac{dY_i(N,t)}{dt} \qquad (29)$$

with the boundary conditions:

$X_i = X_i(0)$ $\qquad N = 0,\ t \geq 0$

$X_j = X_j(0)$ $\qquad N = 0,\ t \geq 0$

$$X_k = 1 - X_i(0) - X_j(0) \qquad\qquad N = 0,\ t \geq 0$$

N = 0 represents the inlet to the column, or axial position (z=0) where all concentrations are that of the feed.

and the following initial conditions:

$$\underline{Y}_i = \underline{Y}_i(0) \qquad\qquad t = 0,\ N \geq 1$$

$$\underline{Y}_j = \underline{Y}_j(0) \qquad\qquad t = 0,\ N \geq 1$$

$$\underline{Y}_k = 1 - \underline{Y}_i(0) - \underline{Y}_j(0) \qquad\qquad t = 0,\ N \geq 1$$

Component material balances of Equation (29) must then be written for all counter ions and solved simultaneously with the rate equations shown in Equation (30):

$$\frac{d\underline{Y}_i(N,t)}{dt} = \sum_{\substack{j=1 \\ j \neq i}}^{n} \underline{\kappa}_{ij}(\underline{Y}_j - \underline{Y}_j^{*}) \qquad (30)$$

NUMERICAL SOLUTION METHOD

Because of the complexity of the equations defined by Equations (29) and (30), the system was solved numerically. A third-order Runge-Kutta algorithm using a predictor corrector scheme was written to solve the equations. This scheme was then combined with a fortran simulation program to model the unsteady-state performance of the substrate shuttle unit.

The substrate shuttle program was designed for ease of operation and is controlled by four basic parameters that control the following:

1. The manner in which the needed constants are entered into the program, (i.e. interactively or via an input file).
2. The concentrations that need to be monitored, (i.e. liquid phase or resin phase concentrations).
3. The independent variable,(i.e. time or bed volumes).
4. Process periodicity, (i.e. whether the adsorption/desorption event is a single operation or a cyclical multiple adsorption/desorption process).

A logical flow chart of the program is shown in Figure 35.

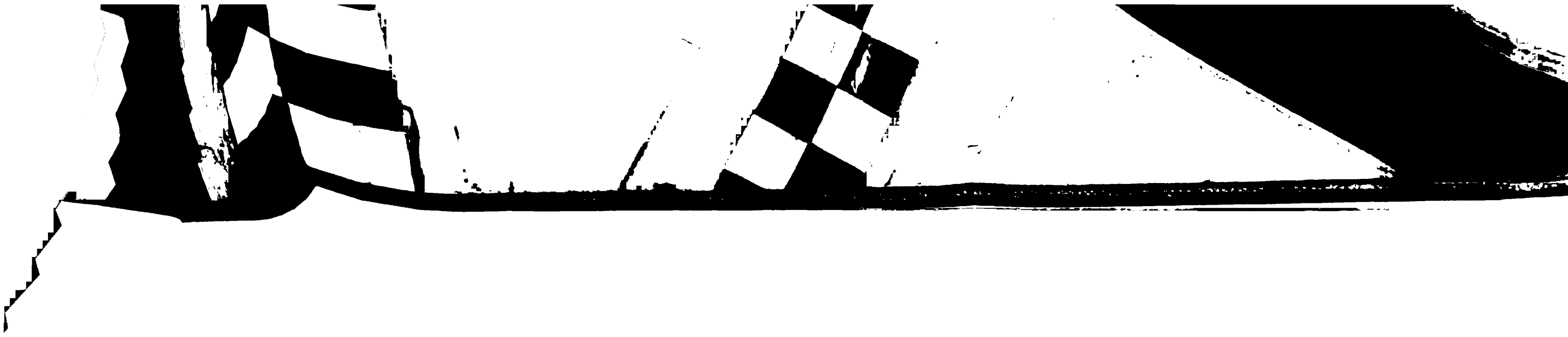

Figure 35. Computer flow chart showing the logic flow for the Fortran program written to simulate the Substrate Shuttle. Please refer to the appendix for a copy of the Fortran code.

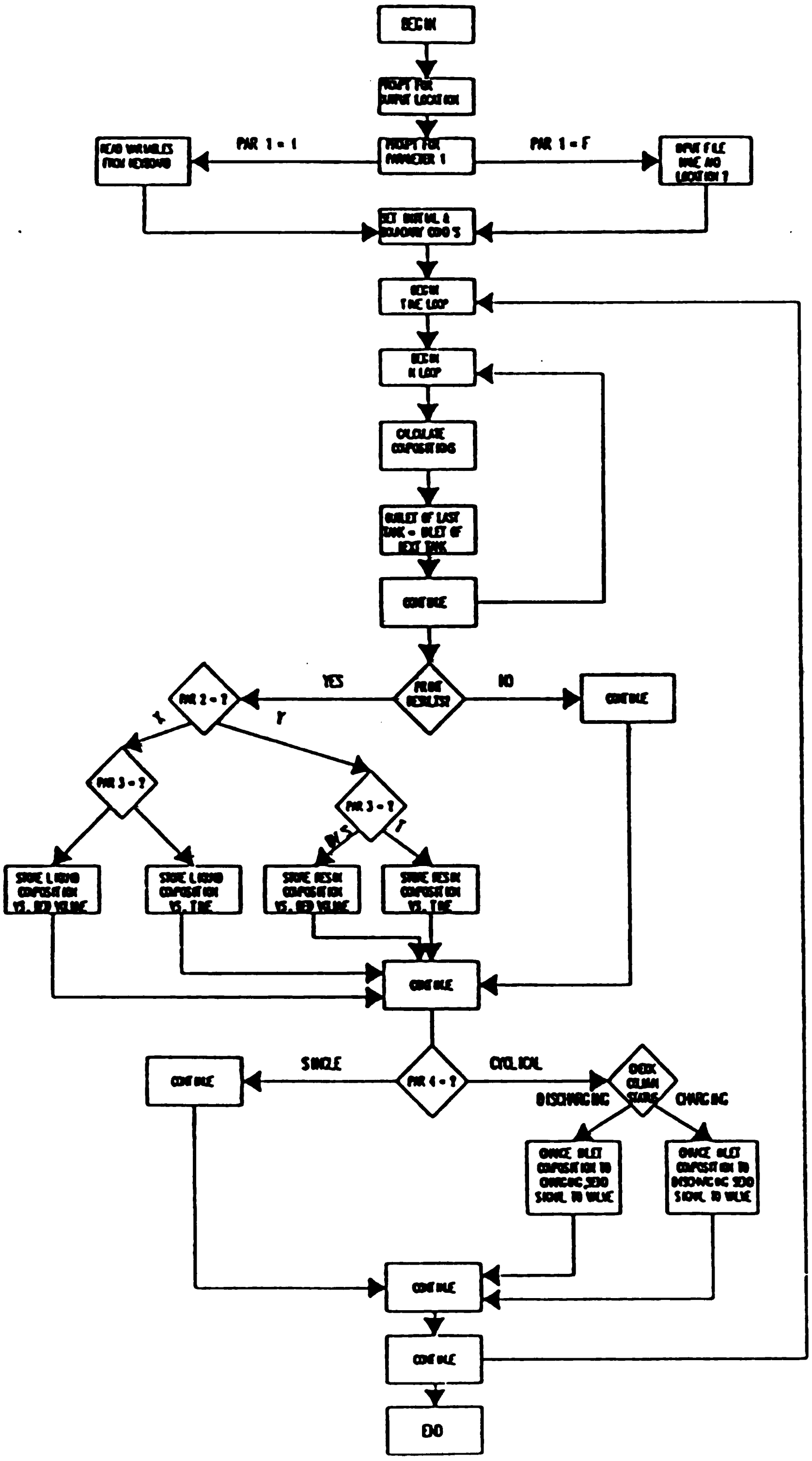
BEGIN
PROMPT FOR OUTPUT LOCATION
PROMPT FOR PARAMETER 1
PAR 1 = I
PAR 1 = F
READ VARIABLES FROM KEYBOARD
INPUT FILE NAME AND LOCATION ?
SET INITIAL & BOUNDARY COND'S
BEGIN TIME LOOP
BEGIN N LOOP
CALCULATE COMPOSITIONS
OUTLET OF LAST TANK = INLET OF NEXT TANK
CONTINUE
PRINT RESULTS?
YES
NO
CONTINUE
PAR 2 = ?
X
Y
PAR 3 = ?
PAR 3 = ?
BV'S
T
STORE LIQUID COMPOSITION VS. BED VOLUME
STORE LIQUID COMPOSITION VS. TIME
STORE RESIN COMPOSITION VS. BED VOLUME
STORE RESIN COMPOSITION VS. TIME
CONTINUE
SINGLE
CYCLICAL
PAR 4 = ?
CONTINUE
CHECK COLUMN STATUS
DISCHARGING
CHARGING
CHANGE INLET COMPOSITION TO CHARGING, SEND SIGNAL TO VALVE
CHANGE INLET COMPOSITION TO DISCHARGING, SEND SIGNAL TO VALVE
CONTINUE
CONTINUE
END

Figure 35.

Computer Solution of the Differential Equations

The computer model of this process solves the material balances equations together with the rate equations by using the method of characteristics together with a third order Runge-Kutta technique with a predictor corrector scheme. The method works as follows: given the initial conditions of known composition in the resin and the boundary conditions at the inlet to the column, (i.e. inlet to the first tank), all concentrations in the first tank are calculated for a small time step. The concentrations of tank (2) can then be calculated at constant time using the liquid phase concentration of tank (1) as inlet to tank (2) and so on up to tank (N). The composition of the liquid phase in tank (N) corresponds to the effluent of the column. Another time step is then taken, and the same steps are repeated until a desired length of time is reached.

Runge-Kutta and the Predictor Corrector Scheme

The predictor corrector Runge-Kutta technique works as follows:

1. All needed mass transfer coefficients and equilibrium values are calculated from the initial conditions of tank (1).
2. At constant N, assuming $d\underline{Y}_i/dt = 0$, an estimate of $X_i(N-1,t+\Delta t)$ is calculated.
3. Based on an average X value of $X_{avg} = \dfrac{X_i(N,t+\Delta t) + X_i(N,t)}{2}$, a first estimate of $\underline{Y}_i(N-1,t+\Delta t)$ is calculated.

4. $X_i(N-1,t+\Delta t)$ is recalculated based on the new value of $\underline{Y}_i(N-1,t+\Delta t)$ and again averaged.
5. The final value of $\underline{Y}_i(N-1,t+\Delta t)$ is calculated from the corrected value of $X_i(N-1,t+\Delta t)$.
6. If the value of $X_i(N-1,t+\Delta t)$ is different from that in step (4), it is recorrected by using $\underline{Y}_i(N-1,t+\Delta t)$ from step (5).
7. The $X_i(N-1,t+\Delta t)$ is used as the inlet to tank (2) and the same steps are then repeated on tank (2) and so on up to tank (N).
8. The liquid and resin concentrations in each tank are stored as initial conditions for the next time step.
9. Starting at tank (1) the operation is repeated with new initial conditions in each tank.

The time step for the solution of the differential equations must be chosen (by trial and error) to minimize computer run time while maintaining accuracy. Generally time steps between (0.5 to 5 seconds) provided stable solutions. Low liquid phase concentrations produce gentle slopes in effluent profiles and can be stable at larger time steps $\approx$ 5 seconds, while high solution concentrations produce steep breakthrough curves and must be run with smaller time steps ($\leq$ 0.5 seconds). It would be desirable in future work to optimize this time step size as a function of total solution concentration and total number of tanks to achieve results in shortest possible time and to program this variation into the model. In this way, depending on process conditions, an optimal step size could be calculated by the program.

Program Documentation

Input File:

It is necessary to have an input file to enter the needed parameters into the program if (PAR 1 = F), or the data is not being entered interactively. The values of the following parameters must be contained in the input file, with each value entered on a separate line.

1. Total resin weight (g).
2. Weight percent water in resin (%)
3. Inlet concentration of acetate (mM).
4. Inlet concentration of butyrate (mM).
5. Inlet concentration of bicarbonate (mM).
6. Presaturation condition of resin with acetate (equivalent fraction).
7. Presaturation condition of resin with butyrate (equivalent fraction).
8. Total process duration (s).
9. Time step size for solution of differential equations (s).
10. Resin capacity (meq/g).
11. Number of tanks in series.
12. Volumetric flow rate (mL/s).
13. Column diameter (cm).
14. Resin bed volume (mL).

15. Average separation factor for (Bu/HCO_3^-).

16. Average separation factor for (Ac/HCO_3^-).

17. Data storage or printing frequency (number of time steps per data output).

18. Parameter 2 (X or Y).

19. Parameter 3 (B or T).

20. Parameter 4 (S or C).

The remaining variables (21 through 27) need to be entered for cyclical operation; if the operation is single pass, then a value of (0) can be entered for the remaining variables.

21. Maximum acetate concentration allowed in effluent (mM).

22. Minimum acetate concentration allowed in effluent (mM).

23. Maximum butyrate concentration allowed in effluent (mM).

24. Minimum butyrate concentration allowed in effluent (mM).

25. Acetate concentration in the discharging stream (mM).

26. Butyrate concentration in the discharging stream (mM).

27. Bicarbonate concentration in the discharging stream (mM).

Where, the discharging stream refers to the stream that would be used to exchange with the column saturated with the fatty acid anions and to release these ions into the methanogenic reactor during the "discharging cycle".

If (PAR 1 = I) then all of the above variables are prompted for by the program and must be entered interactively.

Cyclical Operation:

Because the operation of the substrate shuttle is cyclical in nature, the program was designed to simulate continuous charging and discharging of the column as follows. The resin in the column is initially saturated with bicarbonate or mostly with bicarbonate. A stream rich in volatile fatty acid anions (from the acidogenic reactor) is passed through the ion exchange column. The volatile fatty acids are exchanged for bicarbonate and slowly, as the column begins to saturate with these acids, they begin to leak out. Since these acids are to be captured and later converted to methane, the leakage concentrations, (as indicated by the critical breakthrough concentrations), must be controlled.

Once the concentration of either one of the desired products reaches the critical concentration, the program can signal a solenoid valve to divert the inlet solution into a second column and to divert another stream, rich in bicarbonate (from the methanogenic reactor) into the column. The effluent of the column can now be easily sent to the methanogenic reactor by an appropriate signal to a second solenoid valve. This discharging process continues until the effluent concentration of these acids drops below other critical values. At this time the program signals all appropriate valves to return to their initial settings and begins to "charge" the column with the acids once again.

Data Storage:

Since the program has not yet been connected to an actual process, its output is stored in data files in the form of nondimensional concentration versus time or bed volumes. These data files have been defined within the program with the command, "status-'OLD'" and therefore must already exist before the program can be run. Initially they will ofcoarse contain no data. For the purpose of run time optimization the output is not stored at every time step at a specific interval. This data storage interval must also be optimized as a function of step size, process length, number of tanks in series and any other variable that affects the run time. This variable was found to strongly affect the computer time required to solve a process simulation. It is estimated that once the program logic has been optimized, this variable alone will most strongly affect run time. This parameter (SPC) is entered as an integer showing the number of time steps between data entries.

COMPARISON OF MODEL TO EXPERIMENTAL DATA

Model Verification For Two Component Systems

Particle Phase Controlled Kinetics:

The values of the mass transfer coefficients measured at high flow rates were assumed to be particle phase controlled mass transfer coefficients. The calculated values of the particle phase mass transfer coefficients were then correlated with the particle phase concentration of the species initially having the lowest concentration in the resin by means of curve fitting techniques. Thus, in acetate/butyrate exchange using resin that was initially saturated with acetate, the particle phase concentration of butyrate was used as the independent variable showing the progress of ion exchange. The mathematical form of these correlations was not chosen based on theory but rather based on good fit.

The acetate/butyrate particle phase controlled mass transfer coefficients were fit using Equation (31):

$$\underline{K}_{BU/AC} = B(1)\ \exp(B(2)*\underline{Y}(BU)) + B(3) \qquad (31)$$

Table 3 shows the calculated values of the coefficients B(1), B(2), and B(3) as a function of total liquid phase concentration.

Table 3. Statistically calculated values of constants for the regression fit of particle phase controlled mass transfer coefficients used in equation (31).

Constant	20mM	100mM	200mM	300mM	1.5M
B(1)	0.006694	0.009511	0.01301	0.01297	0.01299
B(2)	-7.39877	-4.89570	-1.4707	-1.1012	-0.9573
B(3)	0.001267	0.002548	-0.00016	-0.00025	-0.00012

The values of B(1), B(2), and B(3) were found to change with total concentration up to 200 mM, however, at all concentration above 200 mM these values appeared to remain constant. A total concentration of 200 mM appears to be the lowest concentration for the attainment of particle phase controlled kinetics, because the value of the particle phase controlled mass transfer coefficient must be independent of the liquid phase concentration. No further experiments were performed to verify the variations in the particle phase mass transfer coefficients at concentrations below 200 mM. In this investigation, the particle phase mass transfer coefficients at lower concentrations than 200 mM were calculated by the constants given in Table 3 and were assumed to vary as measured.

The particle phase controlled mass transfer coefficients for the exchange of bicarbonate with butyrate and the exchange of bicarbonate with acetate shown in Figures (28) and (30) were curve fit using equation (32):

$$K_{ij} = B(1) + B(2)*Y(HCO_3) + B(3)*Y(HCO_3)^2 \qquad (32)$$

where i = bicarbonate

j = acetate or butyrate

For j = acetate

B(1) = 0.022035
B(2) = -0.061160
B(3) = 0.0639270

For j = butyrate

B(1) = 0.0120195
B(2) = -0.024088
B(3) = 0.0240139

Figures 36-39 show the fit of the model to experimental data for the system of acetate and butyrate in the particle phase controlled regime. The values of B(1), B(2), and B(3) used for acetate butyrate exchange were those of the experiment performed at 1.5 M shown in Table 3.

The total concentrations are 200 mM, 300 mM, and 1500 mM for Figures (36), (37), and (38) respectively, while the liquid flow rate, pH, and amount of resin are held constant. In Figure (39), both charging and discharging cycles of the acetate/butyrate system are shown using the experimentally measured acetate/butyrate separation factor.

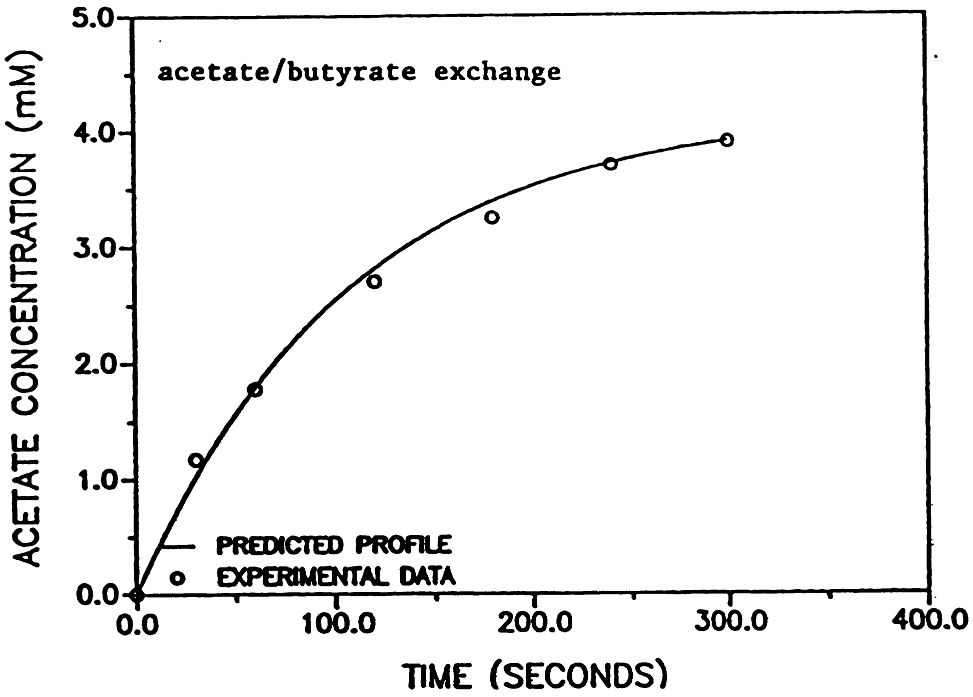

Figure 36. Comparison of model prediction with experimental data in the exchange of acetate with butyrate. Total concentration = 200 mM, pH = 6.0. Experiment performed in the differential column with 0.227 g of IRA 904 under particle phase controlled kinetics, i.e. flow rate = 50 ml/min. Total liquid volume = 100 ml.

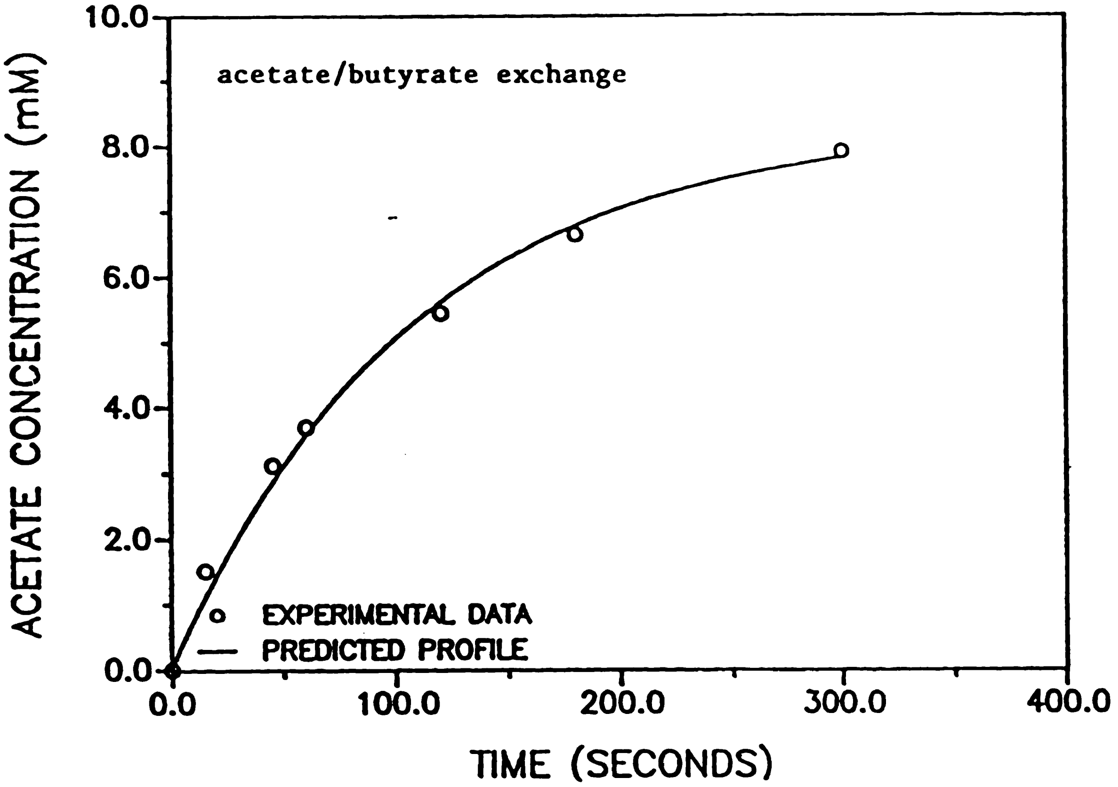

Figure 37. Comparison of model prediction with experimental data in the exchange of acetate with butyrate. Total concentration of liquid = 300 mM, pH = 6.0. Experiment performed in the differential column with 0.227 g of IRA 904 under particle phase controlled kinetics, i.e. flow rate = 50 ml/min. Total liquid volume = 50 ml.

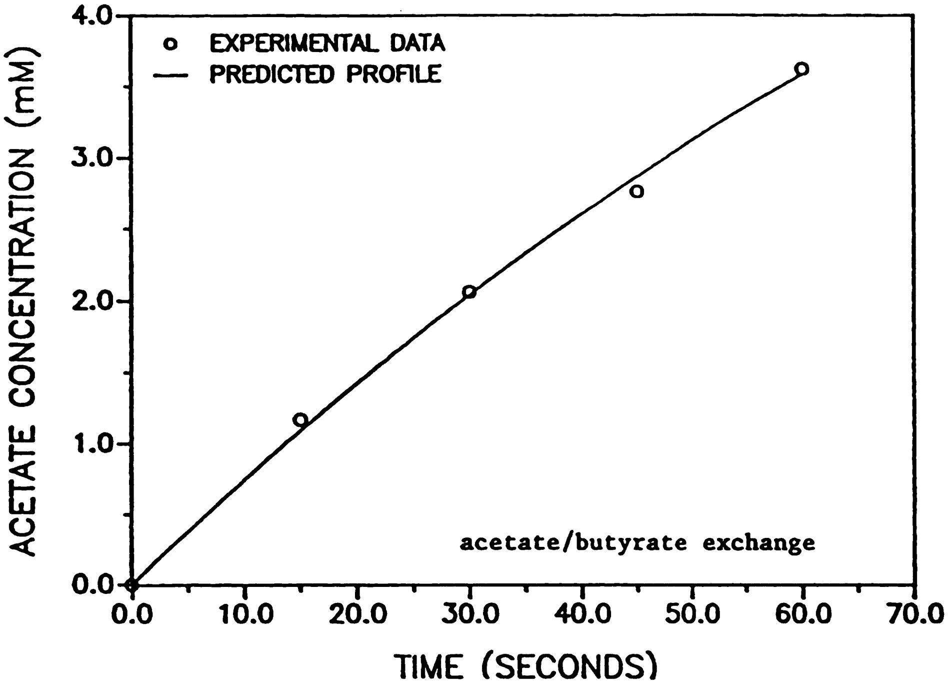

Figure 38. Comparison of model prediction with experimental data in the exchange of acetate with butyrate. Total concentration of liquid = 1.5 M, pH = 6.0. Experiment performed in the differential column with 0.227 g of IRA 904 under particle phase controlled kinetics, i.e. flow rate = 50 ml/min. Total liquid volume = 50 ml.

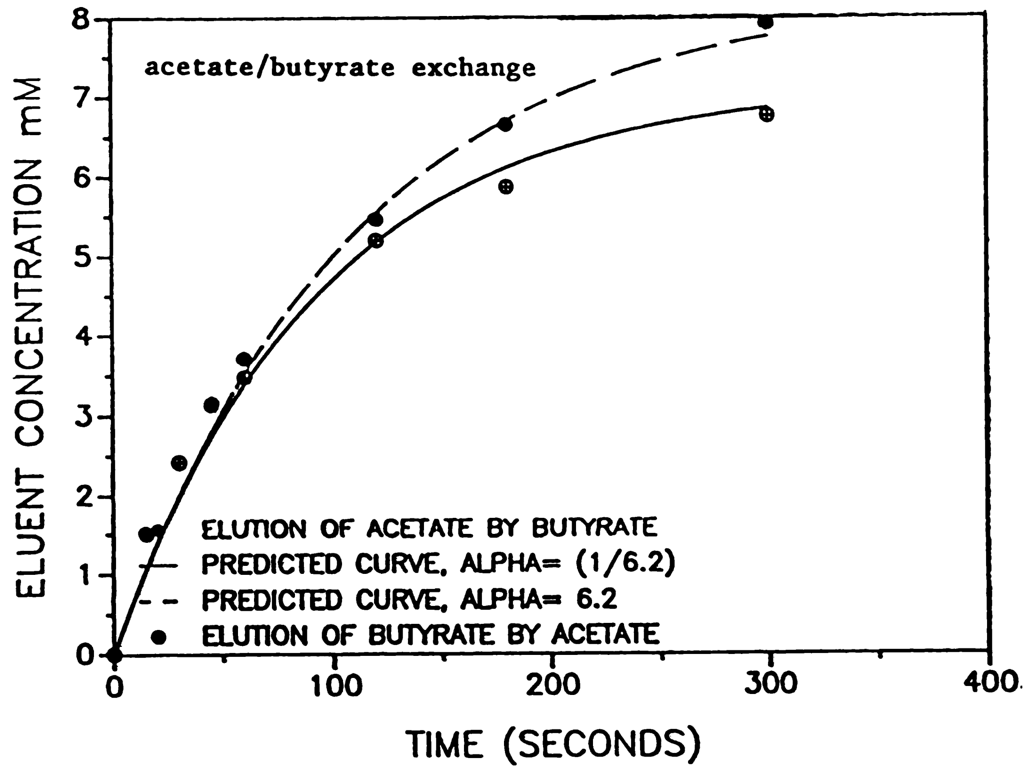

Figure 39. Comparison of model prediction with experimental data in the exchange of acetate by butyrate and the exchange of butyrate by acetate using the measured separation factor = 6.2. total concentration = 270 mM, pH = 6.0. Experiment performed in the differential column with 0.227 g of IRA 904 under particle phase controlled kinetics, i.e. flow rate = 50 ml/min. Total liquid volume = 50 ml.

As shown in Figures (36) through (39), the model predictions of experimental data at different concentrations and total volumes are very accurate. Since the particle phase controlled mass transfer coefficients are not varied between Figures (36), (37), (38), and (39), the experimentally evaluated rates of mass transfer are thought to accurately describe particle phase controlled kinetics.

Solution Phase Controlled and Transition Regime:

At relatively low flow rates, changes in the liquid superficial velocity were found to affect the rate of ion exchange. These effects were modeled via a solution side mass transfer coefficient. Vermeulen et. al.[20] list the following equation for the solution phase mass transfer coefficient in a column packed with spherical particles and for the case of liquid-solid contact:

$$k_s = \frac{k1\ D_f}{d_p^{1.5}} (F/A)^{k2} \qquad (33)$$

where k_s = solution phase mass transfer coefficient (s^{-1})

D_f = liquid phase diffusion coefficient (cm^2/s)

d_p = particle diameter (cm)

F = volumetric flow rate (cm^3/s)

A = column cross sectional area (cm^2)

k1,k2 = empirically fitted constants.

(k1 = 2.62 and k2 = 0.5)

In this investigation the solution phase mass transfer coefficient was modeled by the same form of equation; however, different values of kl and k2 were found to better describe the data. Equation (34) was used to model variations in the solution phase mass transfer coefficient.

$$k_s = kl' \ (F/A)^{k2} \qquad (34)$$

The value of the constant k2 was found to be the same in all cases.

$$k2 = 2.2$$

However, the value of the constant kl' was found to vary, depending on the binary system studied. These constants are listed in Table 4.

Table 4. Values of the first constant in the solution phase mass transfer coefficient, Equation (34).

System	kl'
acetate/butyrate	0.11090
acetate/bicarbonate	0.16820
butyrate/bicarbonate	0.14710

The values of the constant kl' contain liquid phase diffusivities and particle phase diffusivities and therefore cannot be directly compared to the value of kl suggested by Vermeulen et. al [20]. The magnitudes of these constants are consistent with estimates of liquid phase diffusivities. These diffusivities are $2.0 \times 10^{-5} cm^2/s$ for bicarbonate [35], $1.6 \times 10^{-5} cm^2/s$ for acetate [35], $1.0 \times 10^{-5} cm^2/s$ for butyrate [36]. The binary diffusion coefficients can then be calculated by the method of Omatete[24]; these binary diffusion coefficients will have a magnitude comparable to a mole fraction average of the individual diffusivities. It can therefore be predicted that the binary system of acetate and bicarbonate should have the largest kl' and that the smallest value of kl' will belong to the system of acetate and butyrate.

Vermeulen et. al.[20] suggest that the solution phase mass transfer coefficient is weakly dependent on the superficial velocity (square root dependence). However, the solution phase mass transfer coefficient was found to have a much stronger dependence on the superficial velocity as shown by a value of 2.2 for k2. This stronger dependence was thought to be the product of the high resin porosity, (listed as $\epsilon_p = 0.5$ mL pores/mL). Increases in the liquid superficial velocity are thought to affect the liquid concentration within the pores and affect the rate of mass transfer to a greater degree than for a nonporous resin.

For prediction of effluent concentration profiles, overall mass transfer coefficients were calculated from the particle phase mass transfer coefficient and the solution phase mass transfer coefficient according to Equation (28). These overall mass transfer coefficients were then used with appropriate driving forces to model the effect of changes in the liquid superficial velocity on the binary exchange of acetate with butyrate. The results are shown in Figures (40) through (42). Model predictions and experimental data are in good agreement.

Figure (43) compares experimental data to model predictions for the exchange of butyrate with bicarbonate, and Figure (44) shows the same results for the exchange of acetate with bicarbonate. In each case the resin was initially saturated with the organic acid and then exchanged with an aqueous bicarbonate solution of 100 mM concentration at pH = 7.5. It is readily evident that the model's fit for the binary exchange of acetate/bicarbonate and butyrate/bicarbonate to experimental data is not as good as the model's fit to experimental data for the acetate/butyrate exchange.

Figures (43) and (44) show that the model only predicts exchange behavior accurately for short times, but as ion exchange progresses the model overpredicts the effluent concentrations. This overprediction of effluent concentration is another indication that the increases calculated in the overall mass transfer coefficients in Figures 29 and 31 are results of numerical and/or experimental errors. These errors are explained on page 68 and also in sample calculation D of the appendix.

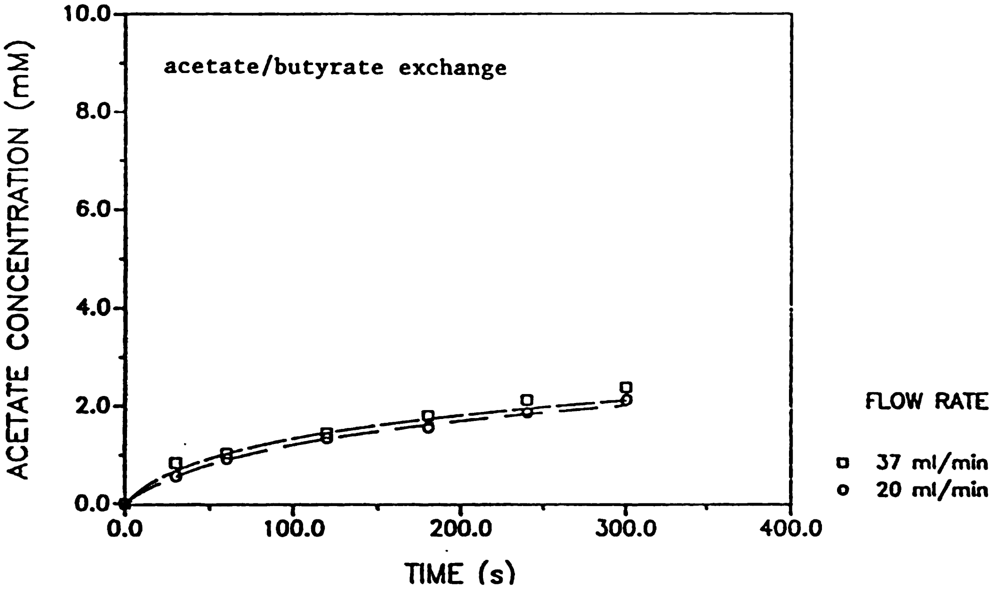

Figure 40. Comparison of model prediction with experimental data for the effect of changes in the liquid superficial velocity in the exchange of acetate with butyrate. Total concentration = 20 mM, pH = 6.0, liquid volume = 100 ml. Experiment performed in the differential column using 0.227 g of IRA 904.

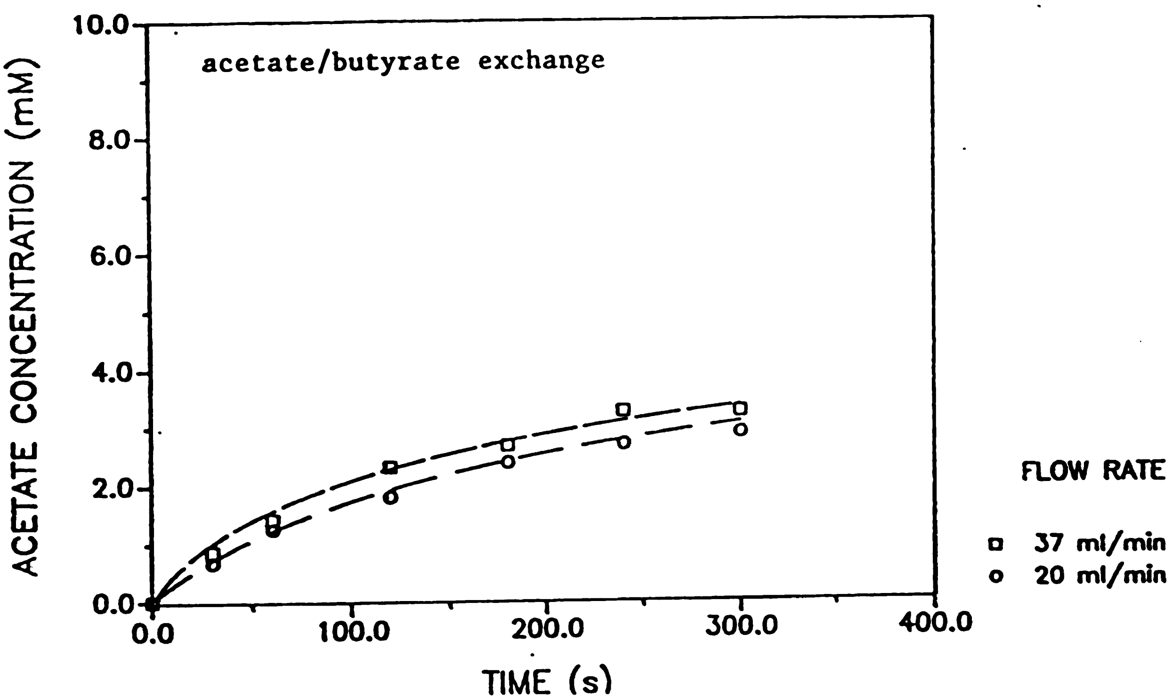

Figure 41. Comparison of model prediction with experimental data for the effect of changes in the liquid superficial velocity in the exchange of acetate with butyrate. Total concentration = 100 mM, pH = 6.0, liquid volume = 100 ml. Experiment performed in the differential column using 0.227 g of IRA 904.

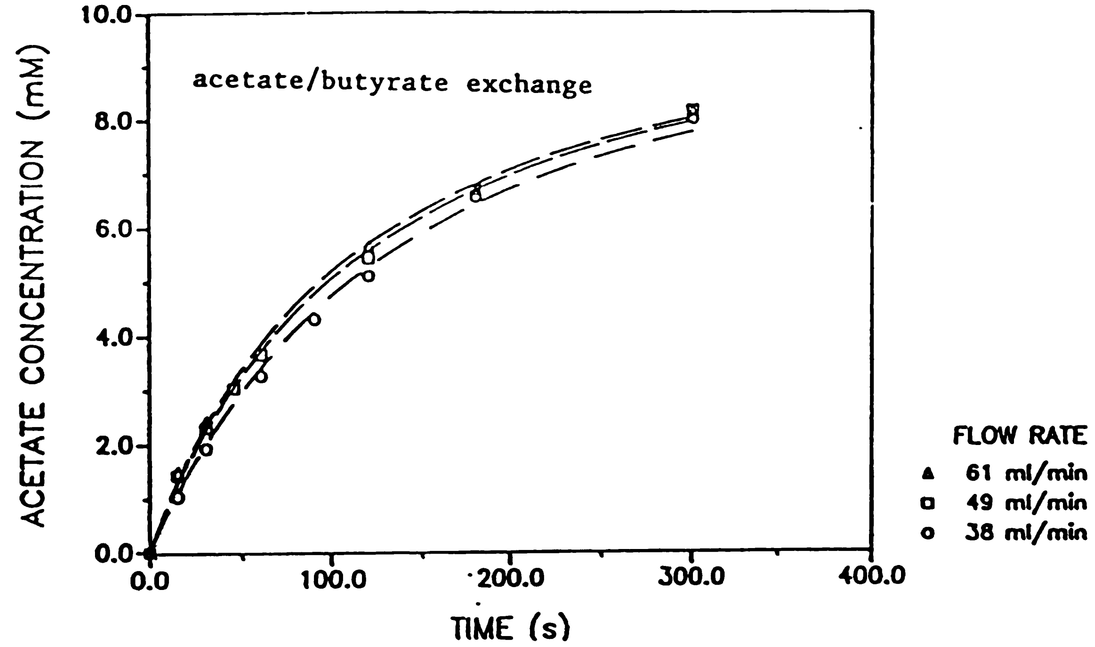

Figure 42. Comparison of model prediction with experimental data for the effect of changes in the liquid superficial velocity in the exchange of acetate with butyrate. Total concentration = 300 mM pH = 6.0, liquid volume = 50 ml. Experiment performed in the differential column using 0.227 g of IRA 904.

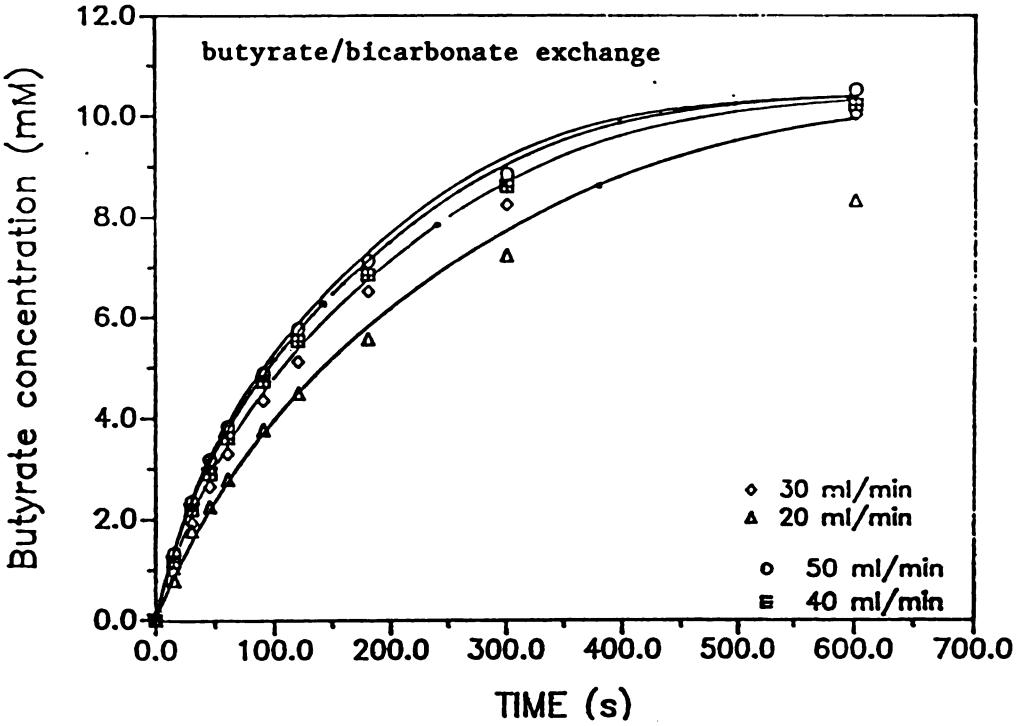

Figure 43. Comparison of model prediction with experimental data for the effect of changes in the liquid superficial velocity in the exchange of butyrate with bicarbonate. Total concentration =100mM pH = 7.5, liquid volume = 50 ml. Experiment performed in the differential column using 0.227 g of IRA 904.

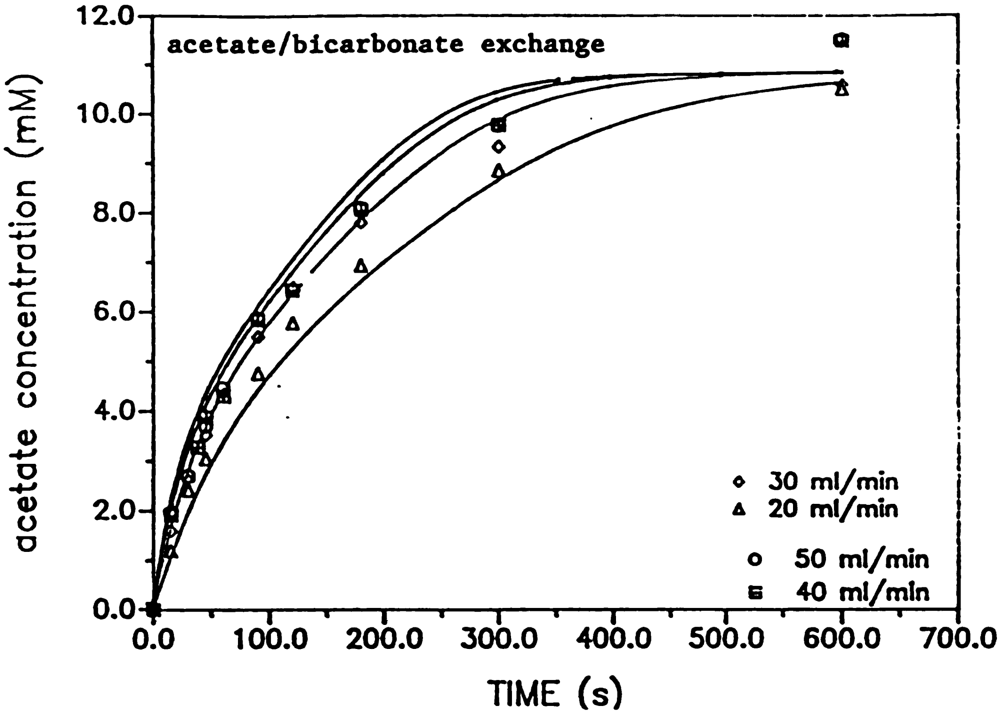

Figure 44. Comparison of model prediction with experimental data for the effect of changes in the liquid superficial velocity in the exchange of acetate with bicarbonate. Total concentration=100 mM pH = 7.5, liquid volume = 50 ml. Experiment performed in the differential column using 0.227 g of IRA 904.

Model Verification For Three Component Systems

Ternary overall particle phase mass transfer coefficients were calculated from binary ones by Equation (27) and used to predict ternary column behavior. One such prediction is shown in Figure (45). The resin was initially saturated with 100 mM sodium bicarbonate and then exchanged with an aqueous solution of 50 mM sodium acetate and 50 mM sodium butyrate at pH = 6.0. The total solution concentration was therefore 100 mM. This would place the rate of mass transfer in the transition regime where the rate is controlled by both phases. A larger quantity of resin (1.58 g) was used in the column, which occupied a volume of 4.8 mL.

The concentration profiles predicted by the model rise more steeply than the experimental results shown in Figure (45). The liquid phase has a low bicarbonate solubility at a pH of 6. Once the solubility limit is reached, additional bicarbonate is converted to gaseous carbon dioxide and lost from the system. This mechanism maintains a low liquid phase bicarbonate concentration, and hence, a large driving force for ion exchange. Thus, acetate and butyrate are more effectively adsorbed at a pH of 6 than at 7.5, where the bicarbonate solubility is higher. This reasoning explains why the observed experimental concentrations were smaller than those predicted by the model.

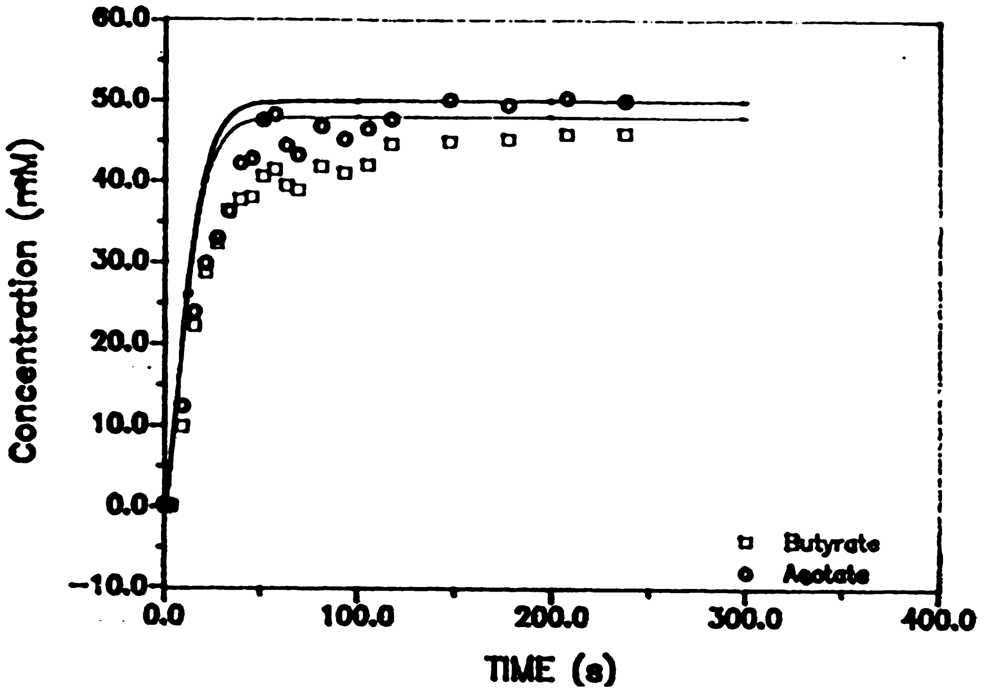

Figure 45. Comparison of model predictions with experimental data in the three component exchange of acetate, butyrate and bicarbonate ions. Column inlet concentration = 50 mM acetate, 50 mM butyrate, pH = 6.0. Flow rate = 20 ml/min.

CHAPTER V

SUMMARY AND CONCLUSIONS

Experimental and modeling studies of a three component anion exchange process for the system of acetate, butyrate and bicarbonate were performed. Conclusions based on the results of this work are as follows:

1. Investigation of equilibrium behavior for the exchange of acetate with butyrate showed that the resin (Amberlite IRA 904) became more selective for butyrate ions at lower pH. This effect resulted, in part, because the resin adsorbed butyrate to excess of its ion exchange capacity. The mechanism for this non-ionic sorption was not determined.
2. Under all concentrations studied the resin prefered butyrate to acetate. The average separation factor at 25 °C and a pH of 7.5 was $\alpha_{Ac}^{Bu} = 4.0$, and at a pH of 6.0 and the same temperature the average separation factor increased to $\alpha_{Ac}^{Bu} = 6.2$.
3. At a pH of 7.5 and a temperature of 25°C the resin prefered bicarbonate to both acetate and butyrate. The average separation factors calculated were ($\alpha_{Bu}^{Bic} = 3.5$) and ($\alpha_{Ac}^{Bic} = 30$).

4. At relatively low flow rates the overall rates of ion exchange were found to increase as a function of liquid superficial velocity.
5. The liquid phase mass transfer coefficient was found to depend on superficial velocity of the liquid by a power of 2.2 in all cases. This was a stronger dependence than suggested by Vermeulen et. al.[20] for columns packed with spherical particles.
6. Particle phase mass transfer coefficients were found to decrease as the ion exchange progressed for all systems.
7. Binary exchange behavior was predicted adequately using the film model for all systems studied.
8. Ternary model predictions did not fit experimental data adequately. The discrepancies were thought to be due to variations in the liquid phase concentration of bicarbonate as a function of pH, variations in equilibrium behavior as a function of pH, and also gas formation in the ion exchange column.

CHAPTER VI

RECOMMENDATIONS

From the results of this exploratory work, the following recommendations are given for future research:

1. Investigate the mechanism of butyrate adsorption to excess of resin capacity.
2. Incorporation of bicarbonate chemistry to the model in predict variations in the concentration of bicarbonate as a function of pH.
3. Investigate effect of pH on equilibrium isotherms for the systems containing bicarbonate.
4. Investigation of the effect of resin fouling on ion exchange properties such as operating resin capacity and rate of mass transfer.
5. Comparison of model predictions to experimental data obtained from non-differential ion exchange columns.

APPENDICES

CHAPTER VII

APPENDICES

DERIVATIONS AND JUSTIFICATIONS

Derivation of Separation Factor

Using the definition of the separation factor, Equation (10), and dropping the subscripts, Equation (35) is obtained:

$$Y = \frac{\alpha X}{1 + (\alpha - 1) X} \qquad (35)$$

allow $\beta = \alpha - 1$, thus $\alpha = \beta + 1$

$$Y = \frac{(\beta + 1) X}{1 + \beta X} \qquad (36)$$

$$\text{Area below isotherm (II)} = \int_0^1 Y \, dX \quad (37)$$

$$\text{Area above isotherm (I)} = \int_0^1 (1-Y) \, dX \qquad (38)$$

This reasoning can be seen in Figure (2).

The Substitution of (36) into (37) and (38) results in (39).

$$\text{Area (II)} = \int_0^1 \frac{(\beta + 1)\,X}{1 + \beta\,X}\,dX \qquad (39)$$

And

$$\text{Area (I)} = 1 - \int_0^1 \frac{(\beta + 1)}{1 + \beta\,X}\,dX \qquad (40)$$

The ratio of the two areas can be related to the separation factor by using an arbitrary variable (a).

$$\text{let } a = \int_0^1 \frac{(\beta + 1)}{1 + \beta\,X}\,dX \qquad (41)$$

then the ratio of the two areas can be related to (a) by Equation (42).

$$\frac{\text{Area (II)}}{\text{Area (I)}} = \frac{a}{1 - a} \qquad (42)$$

The integration of Equation (42) results in Equation (43).

$$a = (\beta + 1)\ \left[X/\beta\ - 1/\beta^2\ \ln(1 + \beta X)\right]_0^1 \qquad (43)$$

Evaluating Equation (43) at its limits and substituting α for $(\beta + 1)$ results in an equation exclusively in terms of α.

$$a = \frac{\alpha}{(\alpha - 1)} - \frac{\alpha}{(\alpha - 1)^2}\ln(\alpha) \qquad (44)$$

In terms of the ratio of the areas, $\frac{a}{1-a}$ is solved to result in the following relationship:

$$\frac{\text{Area(II)}}{\text{Area(I)}} = \frac{a}{1-a} = \frac{\dfrac{(\alpha^2 - \alpha - \alpha \ln \alpha)}{(\alpha - 1)^2}}{1 - \dfrac{(\alpha^2 - \alpha - \alpha \ln\alpha)}{(\alpha - 1)^2}} \qquad (45)$$

Equation (45) cannot be explicitly solved for α; however, it is quite simple to make use of root finding programs to solve for α by trial and error once the ratio of the areas above and below the isotherm is known experimentally. The process model in this study makes use of the separation factor rather than the selectivity coefficient and the following is a justification for the use of the separation factor.

Justification For Use of α Rather Than Selectivity

The separation factor α_B^A indicates directly the preference of a given phase, in this case the resin, for the superscript ion in question. It is the ratio of the distribution coefficient of ion A to that of ion B.

$$\alpha_B^A = \frac{\text{ratio of fractions of ion A between solid and liquid}}{\text{ratio of fractions of ion B between solid and liquid}}$$

Although the experimentally determined separation factors for many exchange processes are not constant, the ratio of the areas technique has provided a means by which a best fit factor can be determined. This then represents the preference the resin has for one ion over another over the entire range of equivalent fractions at some constant total concentration. This is true even for divalent/monovalent ion exchange.

The selectivity coefficient K_B^A at constant total concentration C_o is the ratio of the squared distribution of the monovalent species to the distribution of the divalent species; as such it is influenced by the units of the resin capacity and total concentration C_o. Consider the following example as demonstrated by Clifford[2].

$$A_y^{=} + 2\,B^- \rightleftharpoons 2\,B^- + A^{=} \qquad (46)$$

$$K_A^B = \frac{[B_y]^2\,[A_x]}{[B_x]^2\,[A_y]} \qquad (47)$$

$$K_A^B = \frac{C_o}{Q}\,\frac{Y_B^2\;X_A}{X_B^{\,2}\;Y_A} \qquad (48)$$

Assuming the resin has no preference for either ion, we can then write

$$Y_B = X_B \qquad (49)$$

$$Y_A = X_A \qquad (50)$$

$$\underline{K}_A^B = \frac{C_o}{Q} \qquad (51)$$

It is now clear that the value of the selectivity coefficient is dependent on the units of liquid and resin phase concentrations. For example if we allow the resin capacity to be 1 (eq/L) of resin and the total concentration of the liquid to be 0.005 eq/L of solution we get:

$$\underline{K}_A^B = 0.005$$

While choosing units of (meq/L) will result in the value of selectivity coefficient 1000 times larger.

$$\underline{K}_A^B = 5.0$$

Either of the above choices of units for C_o yields a selectivity coefficient which infers a large preference by the resin phase, first for ion A then for B. However, neither inference is correct, as the resin has an equal affinity for each ion. The separation factor being independent of C_o and Q correctly infers no preference with $\alpha_A^B = 1.0$. It should be noted that all ions in this study were monovalent and that based on this factor alone the selectivity coefficient can be used in the same sense as the separation factor. However, if this work were extended to the recovery of divalent or trivalent anions

such as citric acid, then the use of the separation factor can easily be justified.

SAMPLE CALCULATIONS

A. Equilibrium Isotherm Calculations

The calculations shown are from the acetate/butyrate equilibrium isotherm at pH = 7.5 shown in Figure (19). The liquid volume in each sample was 100 mL.

Table 5 . Equilibrium isotherm experimental data obtained for acetate and butyrate after shaking for 36 hours.

Sample	Initial Concentration AC (mM)	 BU (mM)	Final Concentration AC (mM)	 BU (mM)	Resin wt. (g)
1	273.0	0.0	240.74	30.39	3.00
2	273.0	0.0	213.85	53.16	6.00
3	0.0	278.0	110.88	157.14	7.25
4	0.0	278	39.12	200.09	3.36

Calculations carried out for sample #1.

$$X_{BU} = \frac{30.39}{30.39+240.74} = 0.1121$$

$$\text{Total acetate adsorbed} = (273 \times 10^{-3} - 240.74\times10^{-3})\frac{\text{mole}}{\text{L}}\ (0.1\ \text{L}) =$$

$$= 3.3\times10^{-3}\ \text{mole}$$

$$\text{Acetate concentration in resin} = \frac{3.3\times10^{-3}\ \text{eq}}{3.0\ \text{g}} = 1.1\times10^{-3}\ \frac{\text{eq}}{\text{g}} = 1.1\ \frac{\text{meq}}{\text{g}}$$

$$\text{Total butyrate in resin initially} = (2.4\ \frac{\text{meq}}{\text{g}})\times(3.0\ \text{g}) = 7.2\ \text{meq}$$

Total butyrate in solution at equilibrium $= (30.39 \mathrm{X} 10^{-3} \frac{\mathrm{mol}}{\mathrm{L}}) \mathrm{X} (0.1 \mathrm{~L}) =$

$$= 3.04 \mathrm{X} 10^{-3} \mathrm{mole} = 3.04 \mathrm{~meq}$$

Butyrate concentration in resin at equilibrium $= \frac{(7.2-3.04) \mathrm{~meq}}{3.0 \mathrm{~g}} =$

$$= 1.38 \mathrm{~meq/g}$$

$$Y_{BU} = \frac{q_{BU}}{Q} = \frac{1.38 \frac{\mathrm{meq}}{\mathrm{g}}}{2.4 \frac{\mathrm{meq}}{\mathrm{g}}} = 0.575$$

The resulting equilibrium liquid phase/resin phase dimensionless concentrations of butyrate are shown in Table 6.

Table 6. Equilibrium liquid phase-resin phase equivalent fractions of butyrate for the equilibrium isotherm of butyrate/acetate at T = 25°C, total concentration = 270 mM and pH = 7.5.

Sample	X_{BU}	Y_{BU}
1	0.1121	0.575
2	0.1990	0.6308
3	0.5863	0.6941
4	0.7379	0.8763

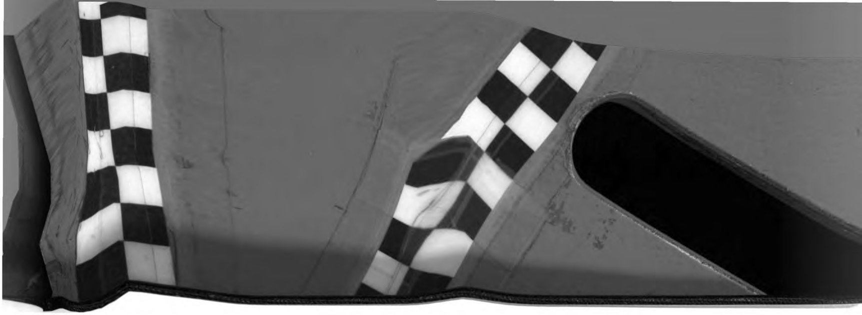

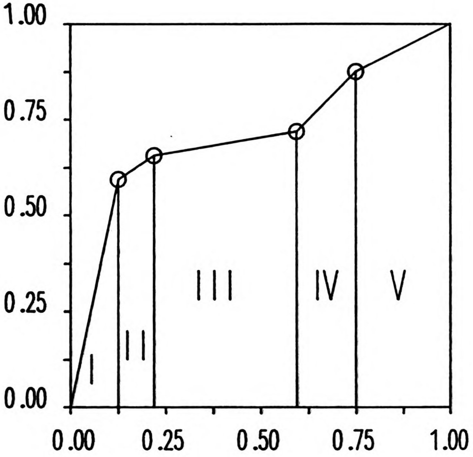

Figure 46. Equilibrium isotherm used for the calculation of average separation factors.

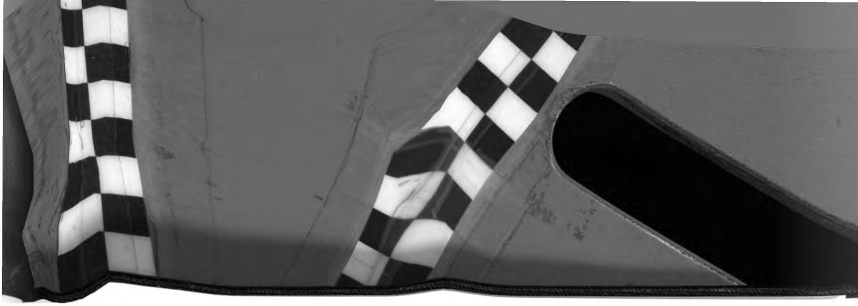

B. Calculation of Average Separation Factor by Ratio of Area's

Area below isotherm = Area I+Area II+Area III+Area IV+Area V

$$\text{Area I} = \frac{0.575 \times 0.1121}{2} = 0.03223$$

$$\text{Area II} = \frac{(0.575 + 0.6308)}{2} \times (0.199 - 0.1121) = 0.0524$$

$$\text{Area III} = \frac{(0.6308 + 0.6941)}{2} \times (0.5863 - 0.199) = 0.2566$$

$$\text{Area IV} = \frac{(0.6941 + 0.8763)}{2} \times (0.7397 - 0.5863) = 0.1204$$

$$\text{Area V} = \frac{(1.0 + 0.8763)}{2} \times (1.0 - 0.7397) = 0.2442$$

Total area below isotherm = 0.70583

Total area above isotherm = 1 - 0.70583 = 0.29417

$$\text{Ratio of areas} = \frac{\text{Area below}}{\text{Area above}} = 2.399$$

Then by trial and error α is calculated from the following equation:

$$\frac{\text{Area below}}{\text{Area above}} = \frac{\dfrac{(\alpha^2 - \alpha - \alpha \ln \alpha)}{(\alpha - 1)^2}}{1 - \dfrac{(\alpha^2 - \alpha - \alpha \ln\alpha)}{(\alpha - 1)^2}} \qquad (11)$$

$$\underline{\alpha_{AC}^{BU} \text{ (pH} = 7.5) \approx 4.0}$$

C. Calculations for Verification Of Differential Column

Experimental parameters and physical constants of the equipment and resin are listed below:

Column diameter = 10 mm
Particle diameter = 0.45 mm
Bed void fraction ≈ 0.35 (typical)
Density of dry resin = 0.34 (g/mL) measured
Resin capacity = 2.4 (meq/g dry)

The equipment layout for these experiments is shown in Figure (17). Since the column effluent was not recycled, the concentration of the effluent is a direct measure of concentration drop across the column. The results of one of the experiments for the differential column verification experiments are shown in Table 7. These experiments were carried out by first saturating the resin with acetate and then exchanging the acetate saturated resin with a solution of butyrate.

The concentration drop in Table 7 was calculated per cm of packed bed eventhough the column used was 1.9 cm long, this was done because the length of the column used in the subsequent rate experiments was 1 cm, and this type of calculation will allow direct comparison of the concentration drops. Experimental conditions were as follows:

Flow rate: 37 mL/min
Total Concentration: 102 mM
pH = 6.0
Resin weight: 0.50 g
Resin presaturant: Acetate

Table 7. Concentration drop across the differential column versus time. Concentration drop expressed per cm of packed bed because the column used for the subsequent rate experiments was 1 cm long.

Time (s)	[AC](mM)	[BU](mM)	ΔC(mM/cm)
5	13.63	73.29	12.12
15	9.67	88.42	6.79
25	9.59	91.78	5.11
35	8.14	91.73	5.14
45	7.47	95.22	3.39

The maximum concentration drop for butyrate is:

$$\Delta C^{Bu}\%(\max) = ((102 - 73.29)/102) \times 100 = 28\ \%$$

The maximum concentration rise for acetate is:

$$\Delta C^{Ac}\%(\max) = (13.63/102) \times 100 = 13\ \%$$

The difference between the two concentration drops could be due to non-ionic interactions of butyrate with the resin.

Since the concentration drops across the column are rather large, the length of the column was reduced from 1.9 cm to 0.95 cm for all of the rate experiments by reducing the quantity of the resin in the column from 0.5 g to 0.227 g. The dilution rate in all of the rate experiments was also increased. The experiment illustrated here was carried out at a dilution rate of (17.5 min^{-1}); The dilution rate in all of the rate experiments was maintained at a minimum of (40 min^{-1}), hence reducing the concentration drop across the column by a factor of ≈ 4.

D. Calculation of Overall Mass Transfer Coefficients from Experimental Data.

A component material balance written for the experimental apparatus shown in Figure 18 is shown in Equation (52).

$$V_T C_T \frac{dXi}{dt} = W_r Q \frac{dYi}{dt} \qquad (52)$$

The liquid phase concentration of i was measured directly as a function of time, and the initial presaturation condition of the resin was known. Variations in Yi as a function of time were calculated from variations in Xi. The rate of ion exchange was then modeled by the product of an overall mass transfer coefficient and an overall particle phase driving force.

$$\frac{d\underline{Y}i}{dt} = \underline{K}_{ij}(Yi^{*} - \underline{Y}i) \qquad (53)$$

The value of Yi^{*} was calculated by using the average separation factor for the binary system of i and j by Equation (28).

$$Yi^{*} = \frac{\alpha \, Xi}{1 + (\alpha - 1)\, Xi} \qquad (54)$$

Since the values of Yi^{*}, $\underline{Y}i$ and $\frac{d\underline{Y}i}{dt}$ could all be evaluated from experimental data, the overall mass transfer coefficient was calculated by Equation (55):

$$\underline{K}_{ij} = \frac{(dYi/dt)}{(Yi^{*} - Yi)} \qquad (55)$$

Any errors in the calculation of Yi^{*}, $\underline{Y}i$ or $d\underline{Y}i/dt$ result in errors in the calculated overall mass transfer coefficients. This error can be significant as Yi approaches the value of Yi^* and the denominator of Equation (55) approaches zero. The calculations shown here were performed using a spread sheet for every experiment. A sample of this spread sheet is shown on the next page.

The following Table is a sample of a spread sheet used to calculate mass transfer coefficients from experimental data.

W_r = 0.227 g V_T = 100 mL pH = 6.0 Flow rate = 20 mL/min

C_T = 20 mM butyrate presaturant = acetate

Subscript (s) : solution phase Subscript (p) : particle phase

All concentrations are in mM, all mass transfer coefficients in (s^{-1}).

Table 8. Spread sheet used for calculation of mass transfer coefficients.

Time(s)	[Ac]	[Bu]	[Total]	X(Ac)
0	0	20.56	20.56	0.0
30	0.563	21.77	22.33	0.0252
60	0.919	20.72	21.64	0.0425
120	1.342	20.96	22.30	0.0602
180	1.560	20.04	21.60	0.0722
240	1.855	19.89	21.75	0.0853
300	2.12	19.73	21.85	0.0970

Y^*(Ac)	dX(Ac)/dt	$V_T C_T / W_r Q$	dY(Ac)/dt	Y(Ac)
0	0.00000	4.0255	----	1.0000
0.1163	0.00084	4.3726	-0.0037	0.8898
0.0197	0.00058	4.2367	-0.0024	0.8166
0.0283	0.00030	4.3665	-0.0013	0.7393
0.0342	0.00020	4.2291	-0.0008	0.6884
0.0407	0.00022	4.2575	-0.0009	0.6327
0.0466	0.00020	4.2780	-0.0008	0.5825

Y^*- Y	$K_{Bu/Ac}$	$k_{Bu/Ac}$	$k_{Bu/Ac}$	$K'_{Bu/Ac}$	Y(Bu)
-1.0000	0.00000	0.00796	0.14662	0.007551	0.00000
-0.8781	0.00418	0.00423	0.14662	0.004110	0.11023
-0.7969	0.00306	0.00299	0.14662	0.002931	0.18335
-0.7110	0.00181	0.00224	0.14662	0.002206	0.26066
-0.6541	0.00129	0.00194	0.14662	0.001909	0.31161
-0.5920	0.00157	0.00171	0.14662	0.001690	0.36732
-0.5359	0.00156	0.00157	0.14662	0.001556	0.41745

$K_{Bu/Ac}$ = Experimental overall mass transfer coefficient.

$K'_{Bu/Ac}$ = Overall mass transfer coefficient from Eqn' (28).

Figure 47. Fortran code for the substrate shuttle program

```
C***********************************************************************)
C               ANION EXCHANGE SUBSTRATE SHUTTLE PROCESS                )
C       BY: ALI R. SIAHPUSH                                             )
C       AUGUST, 1988, MICHIGAN STATE UNIVERSITY, DEPARTMENT OF          )
C       CHEMICAL ENGINEERING                                            )
C***********************************************************************)

C       THIS PROGRAM WILL SIMULATE THREE COMPONENT ION EXCHANGE IN A    )
C       PACKED COLUMN FOR THE AQUEOUS SYSTEM OF ACETATE-1, BUTYRAE-2,   )
C       AND BICARBONATE-3. IT MODELS THE ION EXCHANGE COLUMN AS A SERIES)
C       OF STIRRED TANKS, THE NUMBER OF WHICH IS CONTROLLED BY THE      )
C       OPERATOR TO REPRESENT DIFFERENT DEGREE'S OF AXIAL MIXING IN THE )
C       COLUMN. THE SIX SIMULATNEOUS PARTIAL DIFFERENTIAL EQUATIONS ARE )
C       CONVERTED TO ORDINARY DIFFERENTIAL EQUATIONS BY THE METHOD OF   )
C       CHARACTERISTICS AND THEN SOLVED BY A THIRD ORDER RUNGE-KUTTA    )
C       TECHNIQUE WITH A BUILT IN PREDICTOR CORECTOR.                   )
C***********************************************************************)

C***********************************************************************)
C                         VARIABLE DEFINITIONS                          )
C
C       ACP,BUP,BIP - PRESATURATION CONDITION OF THE RESIN              )
C       ALP21,ALP13,ALP23 - SEPARATION FACTORS FOR BINARY SYSTEMS       )
C               ALP21-(Y2*X1/X2*Y1)
C       ACETAX,BUTYRAX,BICX - CHARACTER NAMES FOR THE FILES IN WHICH THE)
C               COMPOSITIONS MUST BE STORED. IT SHOULD BE NOTED THAT    )
C               THESE FILES ARE DEFINED WITH THE STATUS-'OLD' AND MUST  )
C               THEREFORE EXIST IN THE USER DIRECTORY                   )
C       B - LOOP VARIABLE INDICATING HOW MANY TIME STEPS OF SIZE DELT   )
C               NEED TO BE TAKEN TO COVER A PROCESS PRL LONG.
C       C - DISCHARGING SOLUTION INDIVIDUAL CONCENTRATIONS OF ACETATE   )
C               ,BUTYRATE, AND BICARBONATE (mM)                         )
C       C1MX,C1MN - THE MAXIMUM AND MINIMUM CONCENTRATIONS OF ACETATE   )
C               ALLOWED IN THE EFFLUENT DURING A CYCLICAL OPERATION     )
C       C2MX,C2MN - SAME AS C1MX AND MN BUT FOR BUTYRATE                )
C       CD - DISCHARGING SOLUTION TOTAL CONCENTRATION (mM)              )
C       CT - CHARGING SOLUTION TOTAL CONCENTRATION (mM)                 )
C       D - COLUMN DIAMETER (CM)                                        )
C       DELT - TIME STEP SIZE FOR SOLVING THE SIX DIFFERENTIAL EQUATIONS)
C              IN UNITS OF SECONDS. THE OPTIMAL TIME STEP HAS BEEN FOUND)
C              TO BE BETWEEN ONE AND FIVE SECONDS, ALTHOUGH STEP SIZES  )
C               AS LARGE AS TEN SECONDS WERE FOUND TO WORK FOR MANY     )
C               CASES                                                   )
C       DENOM1 - DENOMINATOR OF TERNARY MASS TRANSFER COEFFICIENT       )
C               EQUATION, USED TO INCREASE COMPUTATIONAL SPEED          )
```

```
C               REACTOR                                                )
C       XSIN - INLET COMPOSITION OF THE COLUMN, REGARDLESS OF THE STATE )
C               OF THE OPERATION, WHETHER CHARGING OR DISCHARGING      )
C       XXIN - CHARGING INLET COMPOSITION FOR THE COLUMN               )
C       XXSIN - DISCHARGING INLET COMPOSITION FOR THE COLUMN           )
C       YAVG - AVERAGE SOLID PHASE COMPOSTION OF EACH COMPONENT IN THE )
C               ENTIRE COLUMN. THIS IS AN INTEGRAL POSITION AVERAGE    )
C               EQUAL TO THE INTEGRAL(Yi)dN/INTEGRAL(dN)               )
C       YN - NEW CORRECTED ESTIMATE OF SOLID PHASE COMPOSITIONS        )
C       YO - FIRST ESTIMATE OF SOLID PHASE COMPOSITIONS                )
C       YSTR - SOLID PHASE COMPOSITION IN EQUILIBRIUM WITH THE LIQUID  )
C               PHASE COMPOSITION                                      )
C***********************************************************************)

        INTEGER I,J,K,L,N,SPC,M,B

        CHARACTER*15  ACETAX,BUTYRX,BICX,INPUT
        CHARACTER*1 PAR1,PAR2,PAR3,PAR4
        INTRINSIC FLOAT
        DOUBLE PRECISION T,TOL,XO(3,50),YO(3,50),XSIN(3)
      1 ,PRL,DELT,WT,WR,WTW,VC,PB,F,QEFF,Q,QES,XN(3,50),YN(3,50)
      1 ,EP,XIN(3),VT,D,S,K12,K13,K23,KK12,KK13,ALP13,ALP23
      1 ,KK23,YSTR(3,50),YAVG(3),E(3),CT,ACP,BUP,BIP,ALP21
      1 ,XAC,XBU,XBI,KK21,YIN(2),XAVG(3),CD,C(3),XXIN(3),XXSIN(3)
      1 ,DENOM1,DENOM2,X1MN,X2MN,X1MX,X2MX,C1MN,C2MN,C1MX,C2MX
        COMMON/B1/F,VC

C       PROMPT USER FOR NAME OF FOLES TO STORE THE OUTPUT IN

        WRITE(*,'(A:)') ' NAME OF OUTPUT FILE TO STORE X OR Y(ACETATE)'
        WRITE(*,'(A:)') ' VS. TIME. TO STORE ON DISK: A:FILENAME'
        READ(*,'(A:)') ACETAX

        OPEN(1,FILE-ACETAX,ACCESS-'SEQUENTIAL',STATUS-'OLD')

        WRITE(*,'(A:)') ' NAME OF OUTPUT FILE TO STORE X OR Y(BUTYRATE)'
        WRITE(*,'(A:)') ' VS. TIME. TO STORE ON DISK: A:FILENAME'
        READ(*,'(A:)') BUTYRX

        OPEN(2,FILE-BUTYRX,ACCESS-'SEQUENTIAL',STATUS-'OLD')

        WRITE(*,'(A:)') ' NAME OF OUTPUT FILE TO STORE'
        WRITE(*,'(A:)')' X OR Y(BICARBONATE) VS. TIME'
        WRITE(*,'(A:)') ' TO STORE ON DISK: A:FILENAME'
        READ(*,'(A:)') BICX
        OPEN(3,FILE-BICX,ACCESS-'SEQUENTIAL',STATUS-'OLD')

C       PROMPT USER, ASK IF INPUT IS INTERACTIVE OR VIA DISK FILE
```

```
C        DENOM2 - DENOMINATOR OF EQUILIBRIUM SOLID PHASE CONCENTRATION   )
C                EQUATION, USED TO INCREASE COMPUTATIONAL SPEED           )
C        E - CHARGING SOLUTION INDIVIDUAL CONCENTRATIONS OF ACETATE,      )
C                BUTYRATE, AND BICARBONATE (mM)                           )
C        EP - BED POROSITY OF VOID FRACTION, NOT DIRECTLY USED IN THE     )
C                PROGRAM                                                  )
C        F - SOLUTION FLOW RATE (ml/sec)                                  )
C        I,J,K,L,M - LOOP COUNTING VARIABLES                              )
C                K IS ALSO USED AS A COUNTER TO INDICATE WHEN IT IS TIME  )
C                TO SAVE THE COMPOSITIONS ONCE AGAIN                      )
C        N - NUMBER OF CSTR'S (INPUT BY USER)                      -1     )
C        K12,K13,K23 - BINARY OVERALL MASS TRANSFER COEFFICIENTS (S  )    )
C        KK12,KK21,KK13,KK23 - TERNARY OVERALL MASS TRANSFER COEFFICIENTS)
C        PAR1 - DETERMINES IF THE INPUT IS BY DISK FILE OR INTERACTIVE    )
C        PAR2 - DETERMINES WHETHER THE STORED DATA IS THE LIQUID PHASE    )
C                COMPOSITION (X) OR THE SOLID PHASE (Y)                   )
C        PAR3 - DETERMINES IF COMPOSITIONS ARE TO BE MONITORED AS A       )
C                FUNCTION OF TIME OR SOLUTION VOLUME PUMPED THROUGH       )
C                THE COLUMN, (BED VOLUMES)                                )
C        PAR4 - DETERMINES WHETHER THE SIMULATION WILL BE SINGLE PASS     )
C                OR A CYCLIC OPERATION     2                              )
C        S - COLUMN CROSSECTIONAL AREA (CM )                              )
C        SPC - VARIABLE INPUT SPACING OF SAVED COMPOSITIONS. THE MAIN     )
C                PURPOSE OF THIS VARIABLE IS TO SAVE MEMORY SPACE AND     )
C                TO INCREASE COMPUTATIONAL SPEED                          )
C        T - VARIABLE SET EQUAL TO TIME OR BED VOLUMES. THIS IS THE       )
C                INDEPENDENT VARIABLE AS A FUNCTION OF WHICH THE          )
C                COMPOSITIONS ARE CALCULATED                              )
C        VC - TOTAL VOLUME TAKEN UP BY WETTED RESIN IN THE COLUMN (ml)    )
C        VT - RESIN VOLUME IN EACH REACTOR (ml)                           )
C        WR - RESIN WEGHT IN EACH REACTOR (gm) DRY RESIN                  )
C        WT - TOTAL WEIGHT OF RESIN IN COLUMN (gm) WET                    )
C        WTW - PERCENTAGE WATER OF WET RESIN (%)                          )
C        XAC,XBI,XBU - LIQUID PHASE COMPOSITION OF THE THREE COMPONENTS   )
C                IN EQUILIBRIUM WITH THE INITIAL  CONDITION OF THE RESIN  )
C                CALCULATED FROM EQUILIBRIUM THEORY                       )
C        XAVG - AVERAGE LIQUID PHASE COMPOSITION CALCULATED FROM A FIRST  )
C                ESTIMATE TO CALCULATE A FIRST ESTIMATE OF THE SOLID      )
C                PHASE COMPOSITION                                        )
C        X1MX,X1MN,X2MX,X2MN - SAME AS C1MX AND MN'S BUT IN EQUIVALENT    )
C                FRATCTION BASIS                                          )
C        XN - CORRECTED ESTIMATE OF LIQUID PHASE COMPOSITIONS (EQUIVALENT)
C                FRACTION BASIS)                                          )
C                                                                         )
C                ALL X'S AND Y'S HAVE NO UNITS AND ARE ON EQUIVALENT      )
C                FRACTION BASIS. Xi - Ci/CT                               )
C        XO - FIRST ESTIMATE OF LIQUID PHASE COMPOSITIONS                 )
C        XIN - INLET COMPOSITION OF THE COMPONENTS FOR EACH INDIVIDUAL    )
```

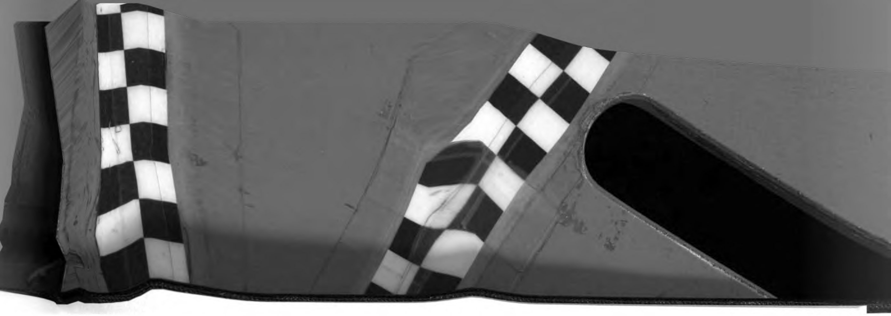

```
      WRITE(*,'(A:)')' INPUT VIA DATA FILE - (F)'
      WRITE(*,'(A:)')' INTERACTIVE         - (I)'
      READ(*,'(A:)') PAR1

      IF(PAR1.EQ.'F')THEN

      WRITE(*,'(A:)')' NAME OF INPUT DATA FILE'
      READ(*,'(A:)') INPUT
      OPEN(7,FILE-INPUT,ACCESS-'SEQUENTIAL',STATUS-'OLD')
      READ(7,*)WT,WTW,E(1),E(2),E(3),ACP,BUP,PRL,DELT
     1 ,Q,N,F,D,VC,ALP23,ALP13,SPC,PAR2,PAR3,PAR4,C1MX
     1 ,C1MN,C2MX,C2MN,C(1),C(2),C(3)
      GOTO 51
      ENDIF


      WRITE(*,'(A:)')' TOTAL RESIN WET WEIGHT(gm)?'
      READ(*,'(A:)') WT
      WRITE(*,'(A:)')' WEIGHT PERCENT WATER IN RESIN'
      WRITE(*,'(A:)')' AS FRACTION OF 100%?'
      READ(*,'(A:)') WTW
      WRITE(*,'(A:)')' INLET CONCENTRATIONS IN (mMOL/LITER) OF '
      WRITE(*,'(A:)')' ACETATE, BUTYRATE, BICARBONATE ?'
      READ(*,'(A:)') E(1),E(2),E(3)
      WRITE(*,'(A:)')' PRESATURATION CONDITION OF RESIN INPUT AS'
      WRITE(*,'(A:)')' EQUIVALENT BED CAPACITY OCCUPIED BY THE '
      WRITE(*,'(A:)')' THREE COMPONENTS IN SAME ORDER, A NUMBER'
      WRITE(*,'(A:)')' FROM ZERO TO ONE IN EACH CASE'
      READ(*,'(A:)')ACP,BUP
      WRITE(*,'(A:)')' PROCESS LENGTH(SECONDS)?'
      READ(*,'(A:)') PRL
      WRITE(*,'(A:)')' TIME STEP(SECONDS)?'
      READ(*,'(A:)')  DELT
      WRITE(*,'(A:)')' RESIN CAPACITY(meq/gm dry)?'
      READ(*,'(A:)') Q
      WRITE(*,'(A:)')' HOW MANY TANKS IN SERIES?'
      READ(*,'(A:)') N
      WRITE(*,'(A:)')' FLOW RATE (ml/SEC)?'
      READ(*,'(A:)') F
      WRITE(*,'(A:)')' COLUMN DIAMETER(CM)?'
      READ(*,'(A:)')D
      WRITE(*,'(A:)')' COLUMN VOLUME (ml)?'
      READ(*,'(A:)') VC
      WRITE(*,'(A:)')' ALPHA (BU/HCO3)?'
      READ(*,'(A:)')ALP23
      WRITE(*,'(A:)')' ALPHA (AC/HCO3)?'
      READ(*,'(A:)')ALP13
      WRITE(*,'(A:)')' ENTER THE STEP INCRIMENTS THAT OUTPUT IS'
      WRITE(*,'(A:)')' DESIREL (SECONDS):'
      READ(*,'(A:)')SPC
      WRITE(*,'(A:)')' DESIRED OUTPUT:LIQUID PHASE COMPOSITION-(X)'
      WRITE(*,'(A:)')'               SOLID  PHASE COMPOSITION-(Y)'
      READ(*,'(A:)')PAR2
      WRITE(*,'(A:)')' COMPOSITION VS. TIME (T), OR BED VOL. (B)?'
      READ(*,'(A:)')PAR3
      WRITE(*,'(A:)')' CYCLICAL OPERATION    -(C)'
      WRITE(*,'(A:)')' SINGLE PASS OPERATION -(S)'
      READ(*,'(A:)') PAR4

      IF(PAR4.EQ.'S')THEN
      GOTO 51
      ENDIF

      WRITE(*,'(A:)')' ENTER MAXIMUM AND MINIMUM CONCENTRATION'
      WRITE(*,'(A:)')' OF ACETATE ALLOWED IN EFFLUENT(mM):'
      READ(*,'(A:)') C1MX,C1MN
      WRITE(*,'(A:)')' ENTER MAXIMUM AND MINIMUM CONCENTRATION'
      WRITE(*,'(A:)')' OF BUTYRATE ALLOWED IN EFFLUENT(mM):'
      READ(*,'(A:)') C2MX,C2MN
      WRITE(*,'(A:)')' COMPOSITION OF DISCHARGING SOLUTION,'
      WRITE(*,'(A:)')' ACETATE,BUTYRATE, AND BICARBONATE(mM):'
      READ(*,'(A:)') C(1),C(2),C(3)


51    CONTINUE

C     CALCULATE THE THIRD NEEDED SEPARATION FACTOR

      ALP21 - ALP23*(1.0D00/ALP13)

      B-INT(PRL/DELT)

C     CALCULATE LIQUID PHASE COMPOSITIONS THAT BRING ABOUT THE
C     SOLID PHASE COMPOSTIONS PRESATURATION CONDITION AND ASSUME
C     THAT A LIQUID PHASE OF THIS COMPOSITION HAS BEEN FLOWING
C     THROUGH THE BED LONG ENOUGH FOR EQUILIBRIUM TO EXIST


      AA - ACP/(1.0D00-ACP)
      BB - BUP*(1.0D00+AA)/(1.0D00-BUP*(1.0D00+AA))
      XBU-BB*(1.0D00-AA*(AA+ALP13))/(ALP23-((AA*BB/
     1 (AA+ALP13))*(1.0D00-ALP23)-BB))

      XAC - AA*(1.0D00-XBU*(1.0D00-ALP23))/(ALP13+AA)
      XBI - 1.0D00-XBU-XAC
```

```
        BIP - 1.0D00-ACP-BUP

C       SET INITIAL CONDITIONS OF THE BED

        DO 2 I-1,N

        XO(1,I)-XAC
        XO(2,I)-XBU
        XO(3,I)-XBI
        YO(1,I)-ACP
        YO(2,I)-BUP
        YO(3,I)-BIP

2       CONTINUE


C       CALCULATE INDIVIDUAL CSTR CHARACTERISTICS AND CONVERT SOLUTION
C       CONCENTRATIONS TO TOTAL CONCENTRATION AND EQUIVALENT FRACTIONS

        VT - VC/FLOAT(N)
        WR - (WT*(1-WTW/100.0D00))/FLOAT(N)
        CD - C(1)+C(2)+C(3)
        CT - E(1)+E(2)+E(3)
        Z - (WR*Q)/(VT*CT)
        S - 3.1415926536*(D/2.0D00)**2

C       SET INLET CONDITIONS

        DO 4 I-1,3
        XIN(I)-E(I)/CT
        XSIN(I)-XIN(I)
        XXIN(I)-XIN(I)
        XXSIN(I)-C(I)/CD
4       CONTINUE

C       CALCULATE THE MINIMUM AND MAXIMUM COMPOSITIONS FOR CYCLICAL
C       OPERATION

        X1MN - C1MN/CD
        X1MX - C1MX/CT
        X2MN - C2MN/CD
        X2MX - C2MX/CT

        K - 1

C***********************************************************************)
C       MAIN LOOPS FOR THE CALCULATION OF VARIABLE COMPOSITIONS         )
C***********************************************************************)
```

```
      DO 100 I=1,B
C     FOR A SMALL TIME STEP CALCULATE THE COMPOSITIONS IN THE  N       )
C     REACTORS AND CORRECT THEM WITH NEW ESTIMATES                     )
      DO 5 J=1,N

      XN(1,J)= DELT*((F/VT)*(XIN(1)-XO(1,J)))+ XO(1,J)

      XN(2,J)= DELT*((F/VT)*(XIN(2)-XO(2,J)))+ XO(2,J)

      XN(3,J)= 1.0D00-XN(1,J)-XN(2,J)

      XAVG(1)=(XN(1,J)+XO(1,J))/2.0D00
      XAVG(2)=(XN(2,J)+XO(2,J))/2.0D00
      XAVG(3)=1.0D00-XAVG(1)-XAVG(2)

      CALL KBA(K12,F,XAVG(2),YO(2,J),S,ALP21,CT)
      CALL KAH(K13,F,XAVG(1),YO(3,J),S,ALP13,CT)
      CALL KBH(K23,F,XAVG(2),YO(3,J),S,ALP23,CT)

      DENOM1 = XAVG(1)*K23+XAVG(2)*K13+XAVG(3)*K12

      KK12 = K12*((XAVG(2)+XAVG(3))*K13+XAVG(1)*K23)/DENOM1

      KK13 = K13*((XAVG(3)+XAVG(2))*K12+XAVG(1)*K23)/DENOM1

      KK23 = K23*((XAVG(3)+XAVG(1))*K12+XAVG(2)*K13)/DENOM1

      KK21 = K12*((XAVG(1)+XAVG(3))*K23+XAVG(2)*K13)/DENOM1

      DENOM2 = XAVG(3)+ALP23*XAVG(2)+ALP13*XAVG(1)

      YSTR(1,J) = ALP13*XAVG(1)/DENOM2

      YSTR(2,J) = ALP23*XAVG(2)/DENOM2

      YSTR(3,J) = XAVG(3)/DENOM2


      YN(1,J)=DELT*(KK12*(YO(2,J)-YSTR(2,J))+
     + KK13*(YO(3,J)-YSTR(3,J)))+ YO(1,J)

      YN(2,J)=DELT*(KK21*(YO(1,J)-YSTR(1,J))+
     + KK23*(YO(3,J)-YSTR(3,J)))+YO(2,J)

      YN(3,J)=1.0D00-YN(1,J)-YN(2,J)
```

```
   XN(1,J)= DELT*((F/VT)*(XIN(1)-XO(1,J))) -
+  Z*(YN(1,J)-YO(1,J))+XO(1,J)

   XN(2,J)= DELT*((F/VT)*(XIN(2)-XO(2,J))) -
+  Z*(YN(2,J)-YO(2,J))+XO(2,J)

   XN(3,J)= 1.0D00-XN(1,J)-XN(2,J)


   XAVG(1)=(XN(1,J)+XO(1,J))/2.0D00
   XAVG(2)=(XN(2,J)+XO(2,J))/2.0D00
   XAVG(3)=1.0D00-XAVG(1)-XAVG(2)

   CALL KBA(K12,F,XAVG(2),YN(2,J),S,ALP21,CT)
   CALL KAH(K13,F,XAVG(1),YN(3,J),S,ALP13,CT)
   CALL KBH(K23,F,XAVG(2),YN(3,J),S,ALP23,CT)



   KK12 = K12*((XAVG(2)+XAVG(3))*K13+XAVG(1)*K23)/DENOM1

   KK13 = K13*((XAVG(3)+XAVG(2))*K12+XAVG(1)*K23)/DENOM1

   KK23 = K23*((XAVG(3)+XAVG(1))*K12+XAVG(2)*K13)/DENOM1

   KK21 = K12*((XAVG(1)+XAVG(3))*K23+XAVG(2)*K13)/DENOM1

   YSTR(1,J) = ALP13*XAVG(1)/DENOM2

   YSTR(2,J) = ALP23*XAVG(2)/DENOM2

   YSTR(3,J) = XAVG(3)/DENOM2


   YN(1,J)=DELT*(KK12*(YO(2,J)-YSTR(2,J))+
+  KK13*(YO(3,J)-YSTR(3,J)))+ YO(1,J)

   YN(2,J)=DELT*(KK21*(YO(1,J)-YSTR(1,J))+
+  KK23*(YO(3,J)-YSTR(3,J)))+YO(2,J)

   YN(3,J)=1.0D00-YN(1,J)-YN(2,J)


   XN(1,J)= DELT*((F/VT)*(XIN(1)-XO(1,J))) -
+  Z*(YN(1,J)-YO(1,J))+XO(1,J)

   XN(2,J)= DELT*((F/VT)*(XIN(2)-XO(2,J))) -
```

```
     +  Z*(YN(2,J)-YO(2,J))+XO(2,J)

        XN(3,J)= 1.0D00-XN(1,J)-XN(2,J)

C       INLET CONCENTRATION OF NEXT REACTOR IS THE OUTLET OF THE
C       REACTOR JUST CONSIDERED

        XIN(1)= XN(1,J)
        XIN(2)= XN(2,J)
5       CONTINUE


C       CHECK OUTLET CONCENTRATION OF LAST REACTOR, WHEN IN CHARGING
C       MODE, DON'T ALLOW THE CONCENTRATIONS TO RISE ABOVE THE
C       MAXIMUM ALLOWABLE CONCENTRATIONS SET BY USER, AND WHEN IN
C       DISCHARGING MODE, DON'T ALLOW THE CONCENTRATIONS TO DROP BELOW
C       THE MINIMUM ALLOWABLE CONCENTRATIONS SET BY USER

        IF(PAR4.EQ.'C')THEN

          IF(XSIN(1).EQ.XXIN(1))THEN
            IF(XSIN(2).EQ.XXIN(2))THEN

              IF(XN(1,N).GE.X1MX)THEN
                XSIN(1) = XXSIN(1)
                XSIN(2) = XXSIN(2)

C**********************************************************************)
C       SEND SIGNAL THE THE PROCESS CONTROL VALVE TO REDIRECT FLOW     )
C       AND BEGIN DISCHARGING COLUMN                                   )
C**********************************************************************)

                GOTO 53
              ENDIF
              IF(XN(2,N).GE.X2MX)THEN
                XSIN(1) = XXSIN(1)
                XSIN(2) = XXSIN(2)
C**********************************************************************)
C       SEND SIGNAL THE THE PROCESS CONTROL VALVE TO REDIRECT FLOW     )
C       AND BEGIN DISCHARGING COLUMN                                   )
C**********************************************************************)
                GOTO 53
              ENDIF
            ENDIF
          ENDIF

          IF(XSIN(1).EQ.XXSIN(1))THEN
            IF(XSIN(2).EQ.XXSIN(2))THEN
```

```
              IF(XN(1,N).LE.X1MN)THEN
                IF(XN(2,N).LE.X2MN)THEN
                  XSIN(1) - XXIN(1)
                  XSIN(2) - XXIN(2)
C**********************************************************************)
C       SEND SIGNAL THE THE PROCESS CONTROL VALVE TO REDIRECT FLOW     )
C       AND BEGIN    CHARGING COLUMN                                   )
C**********************************************************************)
                  GOTO 53
                ENDIF
              ENDIF
            ENDIF
          ENDIF

        ENDIF

53      CONTINUE

C       RESET CONDITIONS TO THAT OF THE INLET OF THE COLUMN

        XIN(1)- XSIN(1)
        XIN(2)- XSIN(2)

        DO 150 L-1,3
                DO 151 M-1,N
                XO(L,M)-XN(L,M)
                YO(L,M)-YN(L,M)
151             CONTINUE
150     CONTINUE


C       SAVE EVERY SPC'TH DATA POINT

        IF(I/(SPC*(K-1)+1).EQ.1)THEN
          IF(PAR2.EQ.'Y')THEN
          CALL RITE(I,N,K,DELT,PAR3,YN)
          GOTO 101
          ENDIF

          CALL RITEX(I,N,K,DELT,XN,PAR3,CT)
101       CONTINUE

        ENDIF

100     CONTINUE
300     CONTINUE
        END
```

```
C***********************************************************************)
C       SUBROUTINES FOR THE CALCULATION OF THE MASS TRANSFER-          )
C       COEFFICIENTS                                                     )
C***********************************************************************)

        SUBROUTINE KBA(K12,F,X2,Y2,S,ALP21,CT)
        DOUBLE PRECISION K1,K2,K12.F,X2,Y2,S,BO,B1,B2,KP,M
     1 ,ALP21,CT

        IF (CT.LE.200)THEN
          B1 = 3.5056E-05*CT +0.0059973D00
          GOTO 3
        ENDIF
        B1=0.013005
3       CONTINUE
        IF (CT.LE.220) THEN
          B2 = 0.0329875*CT - 8.107066
          GOTO 4
        ENDIF
        B2 = -0.83373
 4      CONTINUE
        B3 = 0.11876E-03+0.68252E-04*CT-0.542619E-06*CT**2+
     1  0.93642E-09*CT**3

        IF(X2.EQ.0.0)THEN
        X2 = 1.0E-15
        ENDIF
        IF(Y2.LT.0.013)THEN
        K2 = 0.50D00
        GOTO 1
        ENDIF
        K2 = B1*EXP(B2*(1.0D00-Y2))+B3
1       CONTINUE

        K1 = 0.10902*(F/60.0)**2.2

C       M=ALP21*(1.0D00-X2)/(1.0D00+(ALP21-1.0D00)*X2)**2
        M = 1.00D00-0.3208*Y2
        K12 = K1*K2/(K1+M*K2)
        RETURN
        END

        SUBROUTINE KAH(K13,F,X1,Y3,S,ALP13,CT)
        DOUBLE PRECISION K1,K2,K13,F,X1,Y3,S,BO,B1,B2,KP,M
     1 ,ALP13,CT


        IF(X1.EQ.0.0)THEN
        X1 - 1.0E-15
        ENDIF
        K2 - 0.02203527-0.06116024*Y3+0.06392725*Y3**2
        IF(X1.EQ.0.0)THEN
        X1 - 1.0E-15
        ENDIF
1       CONTINUE
        K1 - 0.10902*(F/60.0)**2.2

C       M-ALP13*(1.0D00-X1)/(1.0D00+(ALP13-1.0D00)*X1)**2
        M-1.0D00+0.3208D00*(Y3)
        K13- K1*K2/(K1+M*K2)
        RETURN
        END

        SUBROUTINE KBH(K23,F,X2,Y3,S,ALP23,CT)
        DOUBLE PRECISION K1,K2,K23,F,X2,Y3,S,B0,B1,B2,KP,M
     1 ,ALP23,CT

        IF(X2.EQ.0.0)THEN
        X2 - 1.0E-15
        ENDIF
        K2 - 0.01202947-0.02408781*Y3+0.0240139*Y3**2
        K1 - 0.10902*(F/60.0D00)**2.2

C       M-ALP23*(1.0D00-X2)/(1.0D00+(ALP23-1.0D00)*X2)**2
        M - 1.0D00+0.3208*Y3
        K23 - K1*K2/(K1+M*K2)
        RETURN
        END

C***********************************************************************)
C       SUBROUTINES THAT SAVE DATA EVERY SPC'TH POINT                   )
C***********************************************************************)

        SUBROUTINE RITE(I,N,M,DELT,PAR3,YN)
        CHARACTER*1 PAR3
        INTEGER I,N,M
        DOUBLE PRECISION DELT,YAVG(3),YN(3,N),T,F,VC
        COMMON/B1/F,VC

C       LOOP TO CALCULATE THE AVERAGE SOLID PHASE COMPOSITION OF THE
C       COLUMN

        YAVG(1)-0.0D00
        YAVG(2)-0.0D00
        YAVG(3)-0.0D00
        IF(PAR3.EQ.'T')THEN
```

```
         T = I*DELT
         GOTO 50
        ENDIF
        T = F*I*DELT/VC
50      CONTINUE

        DO 200 K=1,N

        YAVG(1)=YAVG(1)+YN(1,K)
        YAVG(2)=YAVG(2)+YN(2,K)
        YAVG(3)=YAVG(3)+YN(3,K)
200     CONTINUE

        YAVG(1)=YAVG(1)/FLOAT(N)
        YAVG(2)=YAVG(2)/FLOAT(N)
        YAVG(3)=YAVG(3)/FLOAT(N)

        WRITE(1,152) T,YAVG(1)
152     FORMAT(F10.4,F15.9)
        WRITE(2,153) T,YAVG(2)
153     FORMAT(F10.4,F15.9)
        WRITE(3,154) T,YAVG(3)
154     FORMAT(F10.4,F15.9)

        M=M+1
        RETURN
        END

        SUBROUTINE RITEX(I,N,M,DELT,XN,PAR3,CT)
        CHARACTER*1 PAR3
        INTEGER I,N,M
        DOUBLE PRECISION DELT,XN(3,N),T,F,VC,CT
        COMMON/B1/F,VC

        IF(PAR3.EQ.'T')THEN
         T = I*DELT
         GOTO 50
        ENDIF
        T = F*I*DELT/VC
50      CONTINUE



        WRITE(1,152) T,XN(1,N)*CT
152     FORMAT(F10.4,F15.9)
        WRITE(2,153) T,XN(2,N)*CT
153     FORMAT(F10.4,F15.9)
```

```
      WRITE(3,154) T,XN(3,N)*CT
154   FORMAT(F10.4,F15.9)

      M=M+1
      RETURN
      END
```

REFERENCES

REFERENCES

1. Marinski, Jacob A., Ion Exchange. A Series of Advances, V. 1, Marcel Dekker Inc., NY. 1966.

2. Clifford, D. A., and W. J. Beber Jr., "Nitrate Removal from Water Supplies by Ion Exchange", EPA-600/2-78-052, U.S. Environmental Protection Agency (1978).

3. Clifford, D. A., "Multicomponent Ion Exchange Calculations for Selected Ion Separations", Industrial and Engineering Chemistry Fundamentals, No. 21, p. 141 (1982).

4. Belter, P. A., F. L. Cunningham and J. W. Chen, "Development Of A Recovery Process For Novobiocin", Biotechnology and Bioengineering, V. 15, pp. 533-49, (1973).

5. Thomas, H. C., "Heterogeneous Ion Exchange in a Flowing System", Journal of The American Chemical Society, V. 66, pp. 1664-66, (1944).

6. Sherwood, T. K., Rovert L. Pigford, and C. R. Wilkie, Mass Transfer, McGraw and Hill, (1975).

7. Pietrzyk, D. J., Zaid Iskandariani, and G. L. Schmitt, "Anion Exchange Adsorption on Low Capacity Anion Exchangers: Separation of Organic Acids, Amino Acids, and Small Chain Peptides", Journal of Liquid Chromatography , V. 9 , No. 12, pp. 2633-59, (1986).

8. Dechow, F. J., "Ion Exchange", Fermentation and Biochemical Engineering, Chapter 7, pp. 202-226, (1982).

9. Bradley, W. G., and N. H. Sweed, "Rate Controlled Constant Pattern Fixed-Bed Sorption with Axial Dispersion and Nonlinear Multi-component Equilibria", AICHE Symposium Series NO. 152, 71, 59 (1975).

10. Krishnamurthy, R., and R. Taylor, "A non-equilibrium Stage model for MUlticomponent Separation processes. Part 2: Comparison with Experiment", AICHE Journal. 31 (3) p. 456, (1985).

11. Omatete O. O., R. N. Clazie, and T. Vermeulen, "Column Dynamics of Ternary Ion Exchange. Part 2: Solution Mass Transfer Controlling", Chem. Engr. Jour., No. 19, p. 241, (1980).

12. Krishna, R., and R. Taylor, "Multicomponent Mass Transfer: Theory and Application", Handbook of Heat and Mass Transfer Operations, N. P. Cheremisinoff (ed.) (1985).

13. Smith, T. G., and J. S. Dranoff, "Film Diffusion Controlled Kinetics in Binary Ion Exchange", Industrial and Engineering Chemistry Fundamentals, V. 3, p. 195 (1964).

14. Frey, D. D., "Prediction of Liquid Phase Mass Transfer Coefficients in Multicomponent Ion Exchange: Comparison of Matrix Film Model and Effective Diffusivity Model", Chemical Engineering Communication, V. 47, pp. 273-93 (1986).

15. Horng, L. L., "Modeling of Ion Exchange Process", Journal of The Chinese Institute of Chemical Engineers, V. 16, No. 2, pp. 91-101 (1985).

16. Dranoff, J. S., and L. Lapidus, "Ion Exchange in Ternary Systems", Industrial and Engineering Chemistry, V. 53, No. 1, (1961).

17. Barba, D., Giovanni Del Re, and Pier Ugo Foscolo, "Numerical Simulation of Multicomponent Ion Exchange Operations", The Chemical Engineering Journal, V. 26, pp. 33-39, (1983).

18. Klein, G.. D. Tondeur, and T. Vermeulen, Industrial and Engineering Chemistry Fundamentals, V. 6, pp. 339, (1967).

19. Clazie, R., G. Klein, T. Vermeulen, University of California Sea Water Conversion Report, pp. 67-74 (1967).

20. Vermeulen, T., N. K. Diester, and B. Klein, "Chemical Engineers Handbook", 6th ed. John H. Perry, (ed.), McGraw-Hill Book co. Inc., NY.

21. Vermeulen, T. , and R. E. Quilici, Industrial and Engineering Fundamentals, No. 1, p. 179 (1970).

22. Fujine, S., Keiichirō Saito, and K. Shiba, "Radial Dispersion of A Solute in a Bed Packed With Ion Exchange Resin", Journal of The Japanees Institute of Chemical Engineers, V. 17, No. 3, pp. 327-29 (1984).

23. Boyd, G. E., A. W. Adamson, and C. S. Myers Jr., Journal of the American Chemical Society, V. 69, p. 2836 (1947).

24. Omatete O. O., "Column Dynamics of Ternary Ion Exchange", PhD. Dissertation, University of California at Berkely, Dept. of Chemical Engineering, (1978).

25. Bird, R. B., W. E. Stewart, and E. N. Lightfoot, "Transport Phenomena", John Wiley and Sons, Inc. NY. New York, (1960).

26. Viswanthan, S., D. R. Rao, S. Y. Kekre and M. Gopala Rao, "Ion Exchange in the Process Industries", Soc. Chem. Ind. London, pp. 281-4, (1970).

27. Helfferich, F., and G. Klein, "Multicomponent Chromatography", Marcel Dekker Inc., NY. (1970).

28. Rhee, H. K., R. Aris, and N. R. Amundson, Phil. Trans. Royal Soc. London, A267, No. 1182, 419 (1970).

29. Dranoff, J. S., L. Lapidus, "Multicomponent Ion Exchange Column Calculations", *Industrial and Eng. Chem.*, V. 50, No. 11, pp. 1648-53 (1958).

30. Sanders, S. J., M. Rafal, D. M. Clark, R. D. Young, N. C. Scrivner, R. A. Pease, S. L. Grise, and R. B. Diemer, "Modeling The Separation of Amino Acids be Ion Exchange Chromatography", *Chem. Engr. Prog.*, pp. 47-54, Aug (1988).

31. Vermeulen, T., and R. N. Clazie, *Office of Saline Water Report*, No. 326 (1968).

32. Rohm and Haas Co., *The Rohm and Haas Catalog for Amberlite Ion Exchange Resins*, Rohm and Haas Fluid Process Chemicals Div., Phil., Pennsylvania. (1987).

33. Gaw, Charles, *The Rohm and Haas Company*, Technical Sales Representative, Industrial Fluid Processing Division, (personal communication per phone).

34. Treybal, R. E., *Mass Transfer Operations*, third ed., McGraw-Hill Book Co., N.Y.

35. Perry, R. H., and Don Green, *Chemical Engineer's Handbook*, sixth ed., McGraw-Hill Book Co., N.Y.

36. Voigtlander, Felix, *Zeitschrift Fur Physikalische Chemie*, V. 3, p. 316, (1892).